NAVAL POSTGRADUATE SCHOOL
Monterey, California

THESIS

DETIDING SHIPBOARD-MOUNTED ADCP DATA: AN ANALYSIS OF MODEL DATA AND OBSERVATIONS USING A POLYNOMIAL INTERPOLATION METHOD

by

Marc Thomas Steiner

December, 1994

Thesis Advisor: Newell Garfield
Co-Advisor: Franklin B. Schwing

REPORT DOCUMENTATION PAGE

Form Approved OMB No. 0704

1. AGENCY USE ONLY *(Leave blank)*	2. REPORT DATE December, 1994	3. REPORT TYPE AND DATES COVERED Master's Thesis

4. TITLE AND SUBTITLE Detiding Shipboard-mounted ADCP Data: An Analysis of Model Data and Observations Using a Polynomial Interpolation Method

5. FUNDING NUMBERS

6. AUTHOR(S) Steiner, Marc T.

7. PERFORMING ORGANIZATION NAME(S) AND ADDRESS(ES)
Naval Postgraduate School
Monterey CA 93943-5000

8. PERFORMING ORGANIZATION REPORT NUMBER

9. SPONSORING/MONITORING AGENCY NAME(S) AND ADDRESS(ES)

10. SPONSORING/MONITORING AGENCY REPORT NUMBER

11. SUPPLEMENTARY NOTES The views expressed in this thesis are those of the author and do not reflect the official policy or position of the Department of Defense or the U.S. Government.

12a. DISTRIBUTION/AVAILABILITY STATEMENT
Approved for public release; distribution is unlimited.

12b. DISTRIBUTION CODE

13. ABSTRACT *(maximum 200 words)*

A method for determining the net non-tidal flow from shipboard-mounted acoustic Doppler current profiler (ADCP) data is applied to observations from the Gulf of the Farallones in 1991-2. Tidal currents represent a significant portion of the total flow in the region. Both the tidal and non-tidal current fields are characterized by spatial and temporal variability on small scales. The detiding method performs a least-squares fit to determine the spatial structure of both the amplitudes of the major tidal constituents and the magnitude of the non-tidal flow. Synthetic data is used to examine the requirements and constraints in choosing the best polynomial fitting function for each of the field's components. Arbitrarily choosing a higher-order polynomial to represent these fields may result in misrepresentation of the true flow. Results of applying this technique to vertically-averaged ADCP data from five seasonal surveys of approximately five-day duration are presented.

14. SUBJECT TERMS Oceanography, Tides, Detiding, Coastal Processes, Eastern Boundary Currents

15. NUMBER OF PAGES 97

16. PRICE CODE

17. SECURITY CLASSIFICATION OF REPORT	18. SECURITY CLASSIFICATION OF THIS PAGE	19. SECURITY CLASSIFICATION OF ABSTRACT	20. LIMITATION OF ABSTRACT
Unclassified	Unclassified	Unclassified	UL

NSN 7540-01-280-5500

Standard Form 298 (Rev. 2-89)

Approved for public release; distribution is unlimited.

DETIDING SHIPBOARD-MOUNTED ADCP DATA: AN ANALYSIS OF MODEL DATA AND OBSERVATIONS USING A POLYNOMIAL INTERPOLATION METHOD

by

Marc Thomas Steiner
Lieutenant, United States Navy
B.A., Virginia Polytechnic Institute and State University, 1988

Submitted in partial fulfillment of the
requirements for the degree of

MASTER OF SCIENCE IN METEOROLOGY AND PHYSICAL OCEANOGRAPHY

from the

NAVAL POSTGRADUATE SCHOOL
December, 1994

Author: 
Marc T. Steiner

Approved By: 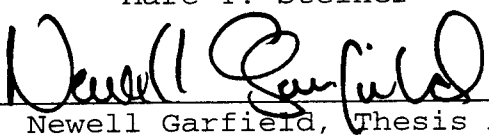
Newell Garfield, Thesis Advisor

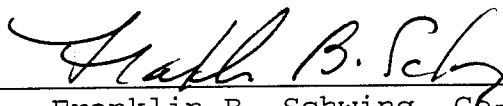
Franklin B. Schwing, Co-Advisor


Robert H. Bourke, Chairman,
Department of Oceanography

ABSTRACT

A method for determining the net non-tidal flow from shipboard-mounted acoustic Doppler current profiler (ADCP) data is applied to observations from the Gulf of the Farallones in 1991-2. Tidal currents represent a significant portion of the total flow in the region. Both the tidal and non-tidal current fields are characterized by spatial and temporal variability on small scales. The detiding method performs a least-squares polynomial fit to determine the spatial structure of both the amplitudes of the major tidal constituents and the magnitude of the non-tidal flow. Synthetic data is used to examine the requirements and constraints in choosing the best polynomial fitting function for each of the field's components. Arbitrarily choosing a higher-order polynomial to represent these fields may result in misrepresentation of the true flow. Results of applying this technique to vertically-averaged ADCP data from five seasonal surveys of approximately five-day duration are presented.

TABLE OF CONTENTS

ACKNOWLEDGEMENT

I am deeply indebted to the many people who have helped me to prepare this thesis. My advisors, Frank Schwing and Toby Garfield spent many a long Friday afternoon when I felt totally baffled by the project. Their enthusiasm and professionalism were inspirational. John Locke, a local high school teacher and summer employee, did an incredible job with the numerous programs that had to be written and modified to make this research possible. Mike Cook, the MATLAB guru, and fellow students Emil Petruncio and Rost Parsons always had helpful hints. Julie McClean and Tarry Rago were always willing to listen and contribute. Most of all, the love and support of my wife, Deanna, and our children, Jimmy and Elizabeth, kept me on the right track.

I. INTRODUCTION

Determining the net sub-tidal circulation in a coastal region is a complex problem. It requires removal of the tidal circulation from the total flow, both of which may vary temporally and spatially on varying scales. Two sources of data commonly used for determining this circulation are shipboard-mounted Acoustic Doppler Current Profilers (ADCP) and moored current meters. Current meter records are collected at a single point which allows the use of time series analysis to separate the tidal and non-tidal components of the flow. Unfortunately, removing the tidal flow from ADCP data can be complicated by temporal and spatial variability in the tidal constituents, and influenced by other physical processes and by topographic irregularities. Accurate estimations of the tidal and non-tidal components of the velocity field are vital to ensure the best possible representation of a region's circulation. The results of these calculations can be used to characterize the physical properties of an estuary or region with some computational tools such as salt and heat budgets.

The Gulf of the Farallones is one such region where the circulation is spatially and temporally complex. In addition, the tides have large amplitudes compared with the mean flow and exhibit a spatially heterogeneous structure. Periodic tidal effects are nearly averaged out over a tidal cycle; however, non-periodic effects such as bottom friction and changing topography can generate Stokes drift which leads to net motion over one cycle (Officer, 1976). The velocity field used in this study will be characterized largely through the analysis of data collected from a shipboard-mounted ADCP. Observations were collected from various cruises of four to five day duration in the Gulf of the Farallones and thus constitute records longer than one cycle for each of the dominant tidal constituents. Additionally, measurements from current meters moored in the region and geostrophic velocities calculated from Conductivity-Temperature-Depth (CTD) measurements will be used to compare different depictions of the velocity field.

Standard time-series analysis cannot be applied to the ADCP data since each

observation is collected at a unique position in space and time. Possible techniques to remove the tidal signal from the data would be to apply simultaneous analysis of tidal constituents from current meter records (Gezgin, 1991), apply a tidal numerical model designed for the region (Foreman and Freeland, 1991), or to use arbitrary interpolation functions to represent spatial variations (Candela et al., 1990; Munchow et al., 1992). The latter method is relatively simple but requires some understanding of the behavior of these functions when applied to the presumed geometries in a region. The importance of this will be demonstrated with the use of synthetic velocities created using known functions.

Much of the current interest in the Gulf of the Farallones region is related to a study jointly funded by the U.S. Environmental Protection Agency (EPA), Region 9, San Francisco, CA and the U.S. Navy (Ramp et al., 1992). Results from this research will help researchers to understand the important processes in the Gulf including: seasonal circulation patterns; residence time; and effects on pollutant dispersion. These results will be instrumental in selecting a dredge spoil dump site and scheduling and monitoring dumping activity.

This report will be presented in the following order: Summaries of the current meter studies conducted primarily by the United States Geological Survey and a detailed description of the Gulf of the Farallones will be given in Chapter II. Chapter III will show details of the model applied to the ADCP data to separate tidal and non-tidal portions of the flow. Observations during the five cruises will be discussed in Chapter IV. A description of the resulting flow field and transports will be given in Chapter V followed by a discussion of their implications in Chapter VI.

II. DESCRIBING THE REGION

A. SITE DESCRIPTION

The Gulf of the Farallones is an exposed region overlying the continental margin off the mouth of San Francisco Bay. Water depths range from an average of about 60 m over the continental shelf to depths of greater than 3000 m over the outer continental slope. The continental shelf is narrow compared to many parts of the world but is relatively wide when compared to most areas off of the western United States. An average width is about 80 km although the width varies significantly from north to south. Sharp bathymetry gradients near the shelf break create shelf-slope dynamics that differ from adjacent areas. Figure 1 illustrates the bathymetric contours and the CTD and ADCP survey plan used during the 1991 and 1992 ***R/V Pt. Sur*** cruises during which the observations analyzed here were collected. The study area features a complex circulation dominated by wind-forced synoptic scale events interacting with the offshore California Current System (CCS).

Physical processes affecting the circulation include wind forcing, tides, large-scale circulation, bathymetric influences, and buoyancy effects from boundary layer interactions and fresh water exchange (Schwing et al., 1991). Additionally, mesoscale features such as the offshore eddy field will affect the flow. The area is influenced by moderate to strong upwelling from local wind forcing and larger scale remote forcing throughout much of the year. Sub-tidal flow is masked by strong tidal currents that exhibit apparent spatial variation of the amplitude and phase of diurnal and semi-diurnal tidal constituents over relatively small distances (Noble and Gelfenbaum, 1990).

1. Influence of Large Scale Currents

The CCS is the southward flowing extension of the North Pacific Gyre. Equatorward surface currents referred to as the California Current (CC) are considered to be offshore of the study region. The core of this flow is 100-200 km offshore at Point Sur

to the south (Chelton, 1984). There is also poleward flow associated in the boundary region of the CCS. These are identified as the California Undercurrent (CUC) and the Davidson Current (Hickey, 1979). CUC velocities are concentrated in a region 50-100 km offshore at Point Sur (Chelton, 1984) and have been observed in hydrographic surveys in the Farallones region (Ramp et al., 1992). Surfacing of the poleward flow occurring in fall and winter seasons is referred to as the Davidson Current (Huyer, 1983).

2. Bathymetry

Isobaths are generally aligned parallel to the coastline at an angle oriented northwest to southeast. The positive along-shore axis is defined at 328 degrees with the across-shore axis at 058 degrees true. Gradients in the bathymetry over the slope are greater in the northern portions of the survey region. This strong slope may have a significant impact on the magnitude and phase of the diurnal tidal constituents and is an area where internal tidal energy may become more important (Noble, personnel communication). The detiding method applied to the ADCP data will be unable to differentiate these internal features because the velocities will be vertically averaged yielding a barotropic flow field.

3. Complex Circulation

Although there has not been a comprehensive study of the region prior to this EPA/Navy study, some presumptions can be made about the constitution of the flow field. First, tidal signals represent a significant part of the total signal. This is an area that is characterized as one with mixed tides (Pond and Pickard, 1983). Current meter records show spatial variability over extraordinarily short distances in both the principal lunar (M2) and principal solar (K1) bands. Additionally, the K1 component's magnitude nearly doubles from the slope to the shelf (Kinoshita et al., 1992).

Tides have a significant impact on the structure of the current field in a region such as the Gulf of the Farallones because they constitute a large portion of the total flow. Results of current meter data analysis show significant variation in the relative importance of each tidal constituent between moorings, particularly between the continental slope and

shelf. This variation invalidates the application of tidal constituents derived from one current meter station to a broader region, such as a data set collected from a hull-mounted ADCP survey. Careful examination of the existing current data is necessary to produce the best estimation of the magnitude and spatial structure of the tidal constituents.

B. RECENT STUDIES AND DATA

1. Historical Observations from the 1980's

Current measurements in the Gulf are sparse. One continental shelf mooring from the Super CODE experiment (37.4N, 122.6W) measured currents in 80 m of water from April 1981 through August 1982 (Strub et al., 1987). Chelton et al. (1988) analyzed measurements at 70 m depth from moorings located at the 100 m and 500 m isobaths during February 1984 through July 1985. Two moorings were maintained by the United States Geological Survey (USGS) during May through October 1989 (Noble and Gelfenbaum, 1990). Two important results are common to these studies. First, the records are dominated by the principal semi-diurnal and diurnal frequency bands. Second, the sub-tidal energy has greater influence from synoptic-scale features than seasonal dependence. Details of representative tidal ellipses in the Gulf are discussed later in this paper.

2. Detailed Survey of 1990

A five-day cruise in the Gulf was conducted by the ***R/V Point Sur*** from August 5-10, 1990. The survey included ADCP and CTD data collected continuously along four transections; two parallel (alongshore) and two perpendicular (cross-shore) to the local bathymetry. The velocity data were detided and analyzed in a report on the hydrographic conditions, including volume and salt budget calculations for the period (Gezgin, 1991). Details on the calibration and processing of these data are available in that report.

Tidal characteristics from the USGS slope current meter records (July 7 to August 21, 1990) were determined using a standard stationary detiding program (Foreman, 1978) and used to represent all locations deeper than the 200 m isobath. Tidal currents over the

continental slope were represented by data from 285 m and 485 m in 2525 m of water. Resulting magnitudes and phases for the dominant tidal constituents were depth-averaged and converted to an hourly predicted tide that was removed from the three-minute averaged ADCP record to produce the detided velocities.

Essentially the same technique was applied to the shelf ADCP data using the two USGS shelf moorings located at 37-41.18N, 122-47.78W and 37-47.03N, 122-56W. Results from the detiding analysis were averaged together, although there was some significant spatial variation in the magnitude of some of the components between these observation points. The most notable difference was in the magnitude and phase of the principal lunar (M2) constituent. The semi-major axis reflected a velocity of 6.2 cm s^{-1} at one mooring and only 3.4 cm s^{-1} at the other with a 54 degree difference in the phase orientation. This spatial variation was ignored when detiding that data set but serves as an argument for consideration of a more complex detiding method.

3. Current Meter Observations During the 1991-2 Farallones Study

A comprehensive study of the circulation and physical processes of the Gulf over the period February 1991 - March 1992 included six current meter moorings (Kinoshita et al., 1992) and five hydrographic and vessel-mounted ADCP surveys on the ***R/V Pt. Sur*** (Ramp et al., 1992). Five of the sites were located over the slope region, since there were few measurements in this area prior to this project. Three proposed EPA dredge spoil dump sites are located in the slope region. Details of the analysis of the data records are given in Kinoshita et al. (1992) and a series of data reports published by the Naval Postgraduate School (Jessen et al., 1992 a-d; Rago et al., 1992).

To observe the spatial variability, one can examine the calculated tidal ellipses from the current meter records. Figure 2 a,b displays the calculated tidal ellipses for the two major tidal constituents at depths in the middle of the water column (e.g. 75 m for slope moorings). These meters do not have the same record length and were not necessarily deployed for the same time period. Spatial variation is apparent mainly in the magnitude and inclination (with respect to due east) of the K1 frequency. Moorings labeled A-F were

from the Farallones study of 1991-2 (Kinoshita et al., 1992). Temporal variability of the tidal phase and amplitude are evident in several current meter records but will not be addressed in this paper.

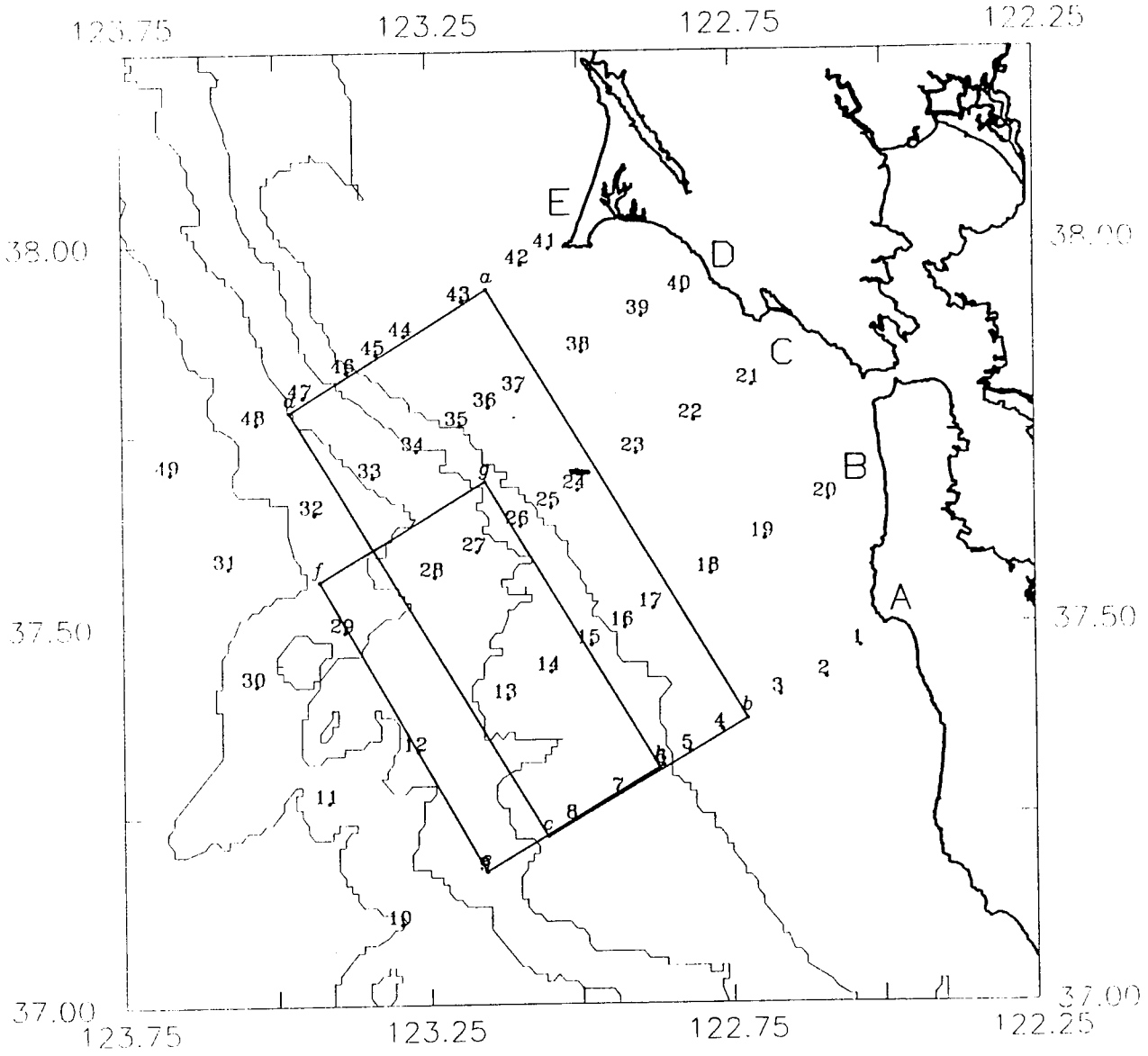

Figure 1. CTD sampling grid station numbers and ADCP uninterrupted sampling lines for the Gulf of the Farallones circulation study cruises (1991-92). Bathymetry contours are shown for the 200, 1000, 2000, and 3000 m isobaths. The uppercase letters indicate the five across-shore transects and lowercase letters are turning points for the ADCP grid.

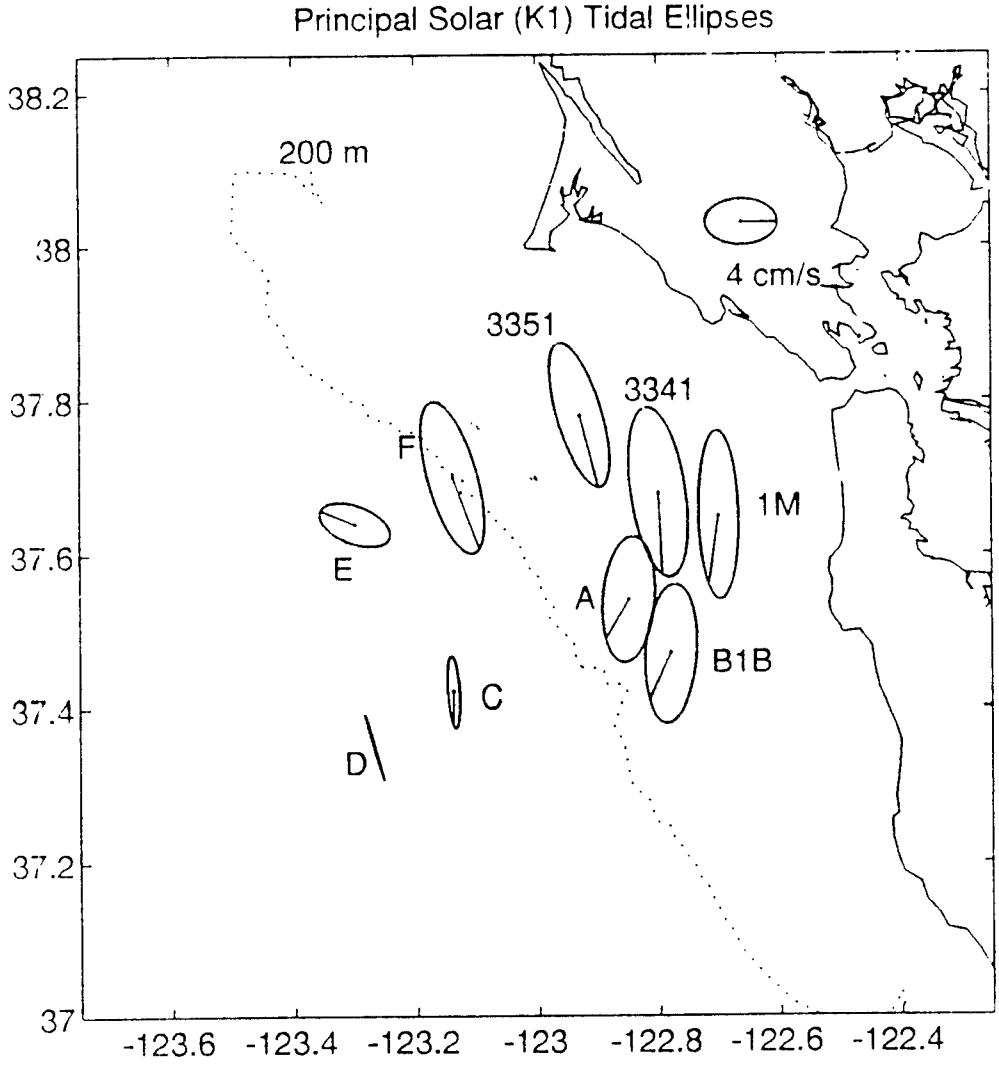

Figure 2a. Representative tidal ellipses for the K1 tidal constituent from current meter records. Phase is illustrated by line segment within each ellipse. Data were collected during separate studies: 3341, 3351 (1988); B1B, 1M (1989); A,C,D,E,F (1991). Slope moorings were from 75 m instruments. Shelf data were collected at representative middle depths.

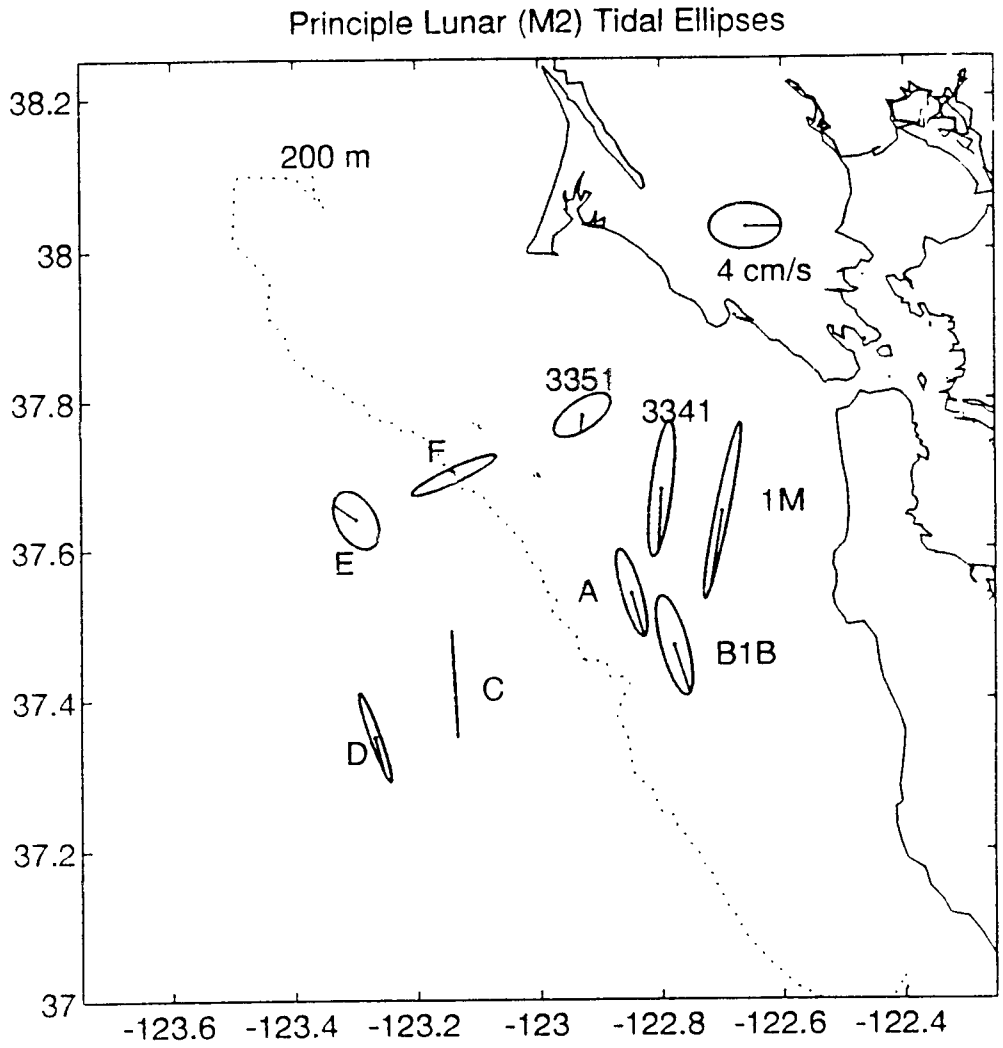

Figure 2b. Representative tidal ellipses for the M2 tidal constituent from current meter records. Phase is illustrated by line segment within each ellipse. Data were collected during separate studies: 3341, 3351 (1988); B1B, 1M (1989); A,C,D,E,F (1991). Slope moorings were from 75 m instruments. Shelf data were collected at representative middle depths.

III. DISCUSSION OF DETIDING MODEL

A. BACKGROUND

Candela (1990) designed a method for removing tidal variability from shipboard-collected ADCP data using several choices for basis functions. These functions are arbitrarily chosen interpolating functions. A rough approximation can be made using polynomials that depend on spatial position. This can be poorly behaved at the edges of the observational region when there are rapid changes in the magnitude of a given constituent. This effectively creates a discontinuity in the interpolating function. Candela also applied a Green's function solution to the biharmonic equation that was originally introduced by Sandwell (1987) as an interpolation scheme for irregularly spaced satellite altimeter data.

Constructing a series of polynomial functions to represent each tidal constituent and a residual flow is relatively simple. The main challenge is to choose the proper order of these polynomials. As a minimum, there must be a reasonable knowledge of the spatial structure of each constituent to make an accurate choice. These functions are put into a large matrix (using the matrix language MATLAB) along with the observed data. The coefficients are recovered using a matrix inversion technique (Candela, 1990). The result is a least squares fit for these coefficients with linearly independent basis functions. Since the data that this technique is applied to are not exact, one must be cognizant of the error tolerance value for the solved matrix. A measure of this is the condition number that Candela (1992) stated should be less than 10^4. Another indicator of matrix stability is given by the value of the smallest singular value (Foreman and Freeland, 1991).

B. VALIDATION OF MODEL FOR FARALLONES DATA SET

A series of synthetic data sets were created to simulate Gulf of the Farallones data

and sampling conditions. These sets consisted of transport values along seven east-west tracks running from 122.8W to 123.5W, separated by one tenth of one degree increments between 37.3N and 37.8N. This latitudinal and longitudinal information is not real but is used for ease of comparison with real data. The observational period covers 56 hours or slightly more than four cycles of the M2 tide. Due to the length of the record and their relatively large amplitudes, only the principal diurnal and semi-diurnal (K1 and M2, respectively) tidal frequencies are considered. This is shorter than the data collected during actual cruises assuming that the model can properly handle resolution of the tidal frequencies if the data set were to be longer. Various cases of vertically averaged transports (units:m^3s^{-1}) were run through the program to illustrate the effect of spatial variability in the tides, mean flow, and choice of polynomial basis function. All of these synthetic sets include one-dimensional (east-west) dependence on the constituents with a north-south oriented shelf break. Actual cruise legs were generally oriented in the cross-shelf and along-shelf directions.

1. Case 1: Constant Tides, Constant Mean Flow

The first case assumed a flat bottom with no spatial variance in the tidal constituents or the mean flow. The magnitude of both the K1 and M2 species were 4 cm s^{-1} with no phase variation over the region and a constant northward 10 cm s^{-1} background mean flow. Since the simulated ship track follows a series of straight lines, linear first-order dependence of the basis functions between data points is introduced to the matrix resulting in a large condition number for these cases. However, the tidal variance and the mean current signal are still accurately estimated. This is consistent with Candela's findings using a similar case for a rectangular flat bottom gulf.

A sharp continental shelf break was added to this case at 122.85W. All points to the east are considered to be on a flat shelf in 100 m of water and points to the west in 400 m. No immediate modification was made to the observed velocities but the input transports were changed accordingly. This demonstrated the models ability to handle data points in variable water depths while still properly extracting the components of the flow

correctly. It is important to note that the bottom depth or maximum depth reached buy the ADCP is included in the data input. Based on this depth, the observed transport is converted to a barotropic velocity at that point.

2. Case 2: Linearly Varying Mean Flow

A next logical step was to add a variable mean flow. The northward current was varied linearly from a 10 cm s^{-1} northward velocity at the western edge of the data region deceasing to a maximum of 10 cm s^{-1} southward current at the eastern edge. As expected, the model was able to resolve this using a first-order polynomial basis function.

3. Case 3: Variable Diurnal Tidal Constituent

Moored current meter observations suggest a sudden increase in the amplitude of the K1 tidal constituent over the continental shelf (Noble and Gelfenbaum, 1991). Several substitutions for the function were attempted to simulate the sharp increase in the magnitude of this constituent over the shelf break.

a. Step Function at the Shelf Break

First the K1 tide was broken into two regions; a 3 cm s^{-1} amplitude over the slope and 6 cm s^{-1} on the shelf. This discontinuity was difficult for any polynomial function to fit. Second-order polynomial functions are particularly poor in this situation and amplify the value of the tidal constituent to such a great degree that the residual results are completely unusable. One possible solution to this problem would involve breaking the domain into a shelf and slope region. This effectively makes the function piecewise continuous. However, in the ocean it may be extremely arbitrary where to define the discontinuity points, and the amplitude of the tide would change over some finite distance.

b. Sharp Linear Change at Shelf Break

This represents a more realistic view of what may occur in the region of the shelf break. The magnitude of the K1 constituent was increased linearly over a scaled cross-shelf (x) distance equivalent to approximately 20 km. The result of running a linear fit to the tidal constituent was that all values to the east and west of this transition region

were overestimated. Residual flow was poorly modeled. A third-order fit was significantly better.

c. Fitting a Third-Order Curve for the K1

A third-order input function was created by specifying values for the magnitude of the tidal constituent at small increments in the cross-shelf direction. The third-order input for the K1 constituent was calculated to be : $-26642.36\ x^3 + 4302.74\ x^2 - 1.5748\ x + 0.0472$ where x represents the scaled distance increasing in the onshore direction. The resulting curve yields the input field of tidal ellipses for K1 shown in Figure 3a. This input was combined with a constant 4 cm s^{-1} M2 tide (Figure 3b) and a variable mean flow represented by a first order polynomial decreasing from 10 cm s^{-1} to -10 cm s^{-1} in the onshore direction (Figure 3c). The sum of these inputs is the total input velocity field in Figure 3d. Figure 4 a-c shows the model values on the corresponding input curves for the proper polynomial fit. Each component of the field has a one-dimensional (longitudinal) dependence. This figure gives the range of values in the appropriate scale range. There are 56 observed modeled values plotted. Since this choice of fitting polynomials was exactly correct, all of the model values lie on the curve. Figure 4d explains how well the model reproduces the total velocity field. There is one-to-one correlation for this case (corr = 1).

Several combinations of curve fits were used to demonstrate the effects of choosing the correct fit to the designed input. Ideally, these functions should be represented by a first-order polynomial for the mean flow, a constant M2 component, and a third-order curve for the K1. Using this as an input data set, the curves for the mean flow and the K1 component were represented using first, second and third order functions while the M2 was modeled as a constant or as linear. The results of these sub-cases demonstrated the sensitivity of the model to changes in the arbitrary fitting function choice. Although each of the cases shows nearly perfect correlation of the input and modeled undetided vectors (sum of the tides and mean flow), the results of the tides and residual flow vary greatly. Thus the correlation specified by the model may be misleading. A more

sophisticated measure of how well the model is performing is needed.

Table 1 demonstrates the correlations between the input and modeled velocities for the tidal constituents, the calculated mean flow, and the modeled total field with their corresponding input values. The degree of the fitting polynomial is listed as *pm* for the total and residual flow fields and *pt* for the M2 and K1 constituents. It shows that an improper choice in the fitting function can lead to reduced correlations and an unrealistic representation of the field being modeled.

pm	pt (M2,K1)	M2 cor	K1 cor	resid cor	corr
1	1,1	0.9996	0.9898	1.0000	0.9999
1	1,2	0.9987	0.9885	1.0000	0.9999
1	1,3	1.0000	1.0000	1.0000	1.0000
2	1,1	0.9990	0.9898	0.9999	0.9999
2	1,2	0.9974	0.9963	0.9975	1.0000
2	1,3	1.0000	1.0000	1.0000	1.0000
3	1,1	0.9990	0.9894	0.9999	0.9999
3	1,2	0.9980	0.5109	0.9108	1.0000
3	1,3	1.0000	1.0000	1.0000	1.0000
1	2,3	1.0000	1.0000	1.0000	1.0000
1	2,2	0.9987	0.9872	0.9999	1.0000
3	2,2	0.9647	0.2317	0.9741	1.0000

Table 1. Calculated correlation coefficients for model fit to the M2 and K1 tidal ellipses, residual field, and the undetided velocity field for the synthetic data set.

The input data vary only as a function of longitude. However, there is apparently an error introduced in the north-south direction introduced because the technique uses the same degree fit in both directions. The values along all transects should be identical for all cases with this data set.

Improperly setting the polynomial degree leads to poor estimates of the tidal and mean contributions to the circulation. For example, when the choice of polynomial fit was third-order for the mean flow and input current field, first-order for M2, and second order for K1, the model created unrealistic results.In comparison with the results shown in Figure 3, spurious results are apparent in the ellipses of the K1 constituent (Figure 5a), M2 constituent (Figure 5b), and the calculated residual velocity field (Figure 5c). Figure 5d verifies that the total input field was the same as with the perfect fit (Figure 3d). The spurious placement of energy in the modeled K1 values (Figure 6a) occurs in both the cross-shore (x) direction and the alongshore direction. The latter condition is true because different values for the magnitude are calculated in the along-shore (y) direction which was prescribed to be constant (Figure 3a). Overfitting the polynomial choice for the constant M2 constituent yields improper calculations by the model in both dimensions (Figure 6b). Most importantly, the steady flow is not properly fit (Figure 6c) although the least-squares correlation (resid cor) is relatively high (0.9108). In a real world data set with two-dimensional variation, one would assume that this north-south variation is real since the correlation for the observed to modeled nondetided velocities was one-to-one. The resulting magnitude range was not extraordinarily large which could also be misleading. Additionally, only the correlation between the modeled vectors and the observation vectors of the total field (Figure 6d) can be calculated when working with actual data. This implies that total field may be accurately represented, but each of the constituents of the field is incorrectly represented. Using this as a criterion for model performance would be erroneous. These results also indicate that lower order fits to the tidal constituents should be applied.

d. Random Noise Effects

Ideally, the model will correctly identify energy in the specified tidal frequencies and consider the remainder to be part of the residual (detided) flow. Random noise was added to the previous cases. In general, the input versus modeled correlation was somewhat reduced depending on the magnitude of the noise relative to the true mean and tidal flows as well as the length of the data set. Overall, the model did a good job of properly accounting for the mean flow. Some energy did appear erroneously in the tidal frequencies. Random noise was added to a longer data set representing nearly a four-day period. As expected, the tides were more accurately represented and the noise appeared in the residual flow. This is a desirable finding which reinforces the idea that this method improves by increasing the length of the data set.

4. Case 4: Higher Order Residual Flow

Complete flow patterns in the study region may require a higher-order fit to best represent the total structure of the field. A third-order polynomial equation ($889.3404\ x^3 - 140.8715\ x^2 + 5.0152\ x + 0.0970$) replaced the linearly varying background flow discussed in Case 3. The magnitude of the northward velocities ranged from a maximum of 14.86 cms^{-1} over the outer slope to a minimum of 5.14 cms^{-1} on the shelf. The corresponding tidal ellipses (Figure 7a,b), steady flow (Figure 7c), and total velocities (Figure 7d) were used to further investigate the effects of polynomial choice. The ideal fit to the composite field would be a third order mean flow fit (*pm*) with constant (zero-order) M2 and third order for the K1 component (*pt*=0,3). Correlations for each component of this perfect fit is illustrated in Figure 8 a-d.

Several combinations of fitting polynomials were applied to this input case. Resulting correlation coefficients are given in Table 2. It is apparent that an improper fit for the mean flow can give a poor representation of the flow field if too large a polynomial fitting function is chosen. This is most obvious in the case with a fifth order fit applied to the total and residual velocity fields.

Based on the results of the Case 3, one would first choose a linear fit for all

polynomials if the exact input were not known. Figure 9 a-d illustrates the resulting model fields when first-order polynomials were chosen for the mean flow and K1 with a constant M2. A corresponding plot of the model correlation values is given in Figure 10 a-d. There is some north-south variation introduced even though there is no dependence in that direction in the input constituents but the overall fit is good.

Using the assumption about overfitting the tidal constituents shown in Case 3, linear fits were applied to both the K1 (Figure 11a) and M2 (Figure 11b) components with the mean flow modeled as a linear polynomial (Figure 11c). The fit to the total field (Figure 11d) is still nearly perfect but the correlation of the individual components (Figure 12) is slightly worse than when the M2 component was held constant. North-south variability is illustrated by the modeled values (circles) differing magnitudes at constant scaled longitude (x) values.

pm	pt	M2 cor	K1 cor	resid cor	corr
3	1,3	1.0000	0.9999	1.0000	1.0000
1	1,1	0.9995	0.9875	0.9894	0.9984
2	1,1	0.9991	0.9871	0.9890	0.9984
3	1,1	0.9990	0.9894	0.9996	1.0000
4	1,1	0.9984	0.9783	0.9980	1.0000
5	1,1	0.9979	0.6297	0.8787	1.0000
1	0,1	1.0000	0.9898	0.9896	0.9983
4	0,1	1.0000	0.9881	0.9992	0.9999

Table 2. Calculated correlation coefficients for the model fit to the M2 and K1 tidal ellipses, residual field, and the undetided velocity field for the synthetic data set. Actual input field is pm = 3, pt = 0,3.

Fourth-order fits may be a realistic representation of the total flow field in the study region and were applied to this case. The fields are modeled with a first-order K1 tide (Figure 13a), constant M2 tide (Figure 13 b), and fourth-order background and total flow (Figure 13c,d). This yields a higher correlation to each of the tidal constituents and residual flow (Figure 14) than does the comparable linear fit to the mean flow. There is slight degradation of the model of the fields (Figure 15a-d) when the M2 tidal fit is increased to a linear function. The correlation values decrease (Figure 16 a-d) and reinforce the consequence of overfitting the tides.

C. SUMMARY OF MODEL'S USEFULNESS

Candela's model provides a method to estimate the net flow pattern using spatially and temporally varying data. Estimates of the magnitude of individual tidal constituents may be poorer than the estimate of the residual (mean) flow field. Higher order functions can slightly improve the estimate of the flow field but can be ill-behaved if they are not the proper fit for the region of interest. A lower-order fit is the best alternative if sufficient information about the spatial variability in an area can not be determined. As a result of these findings, first-order polynomials will be applied to both the M2 and K1 constituents since they are known to be spatially varying but can be reasonably represented using the linear least-squares fit. The mean flow apparently is best fit by a third-order polynomial or higher. Both fourth-order and first-order fits will be applied to the real data to illustrate the structure of the flow. Results of the application of these functions will be discussed in the next chapter.

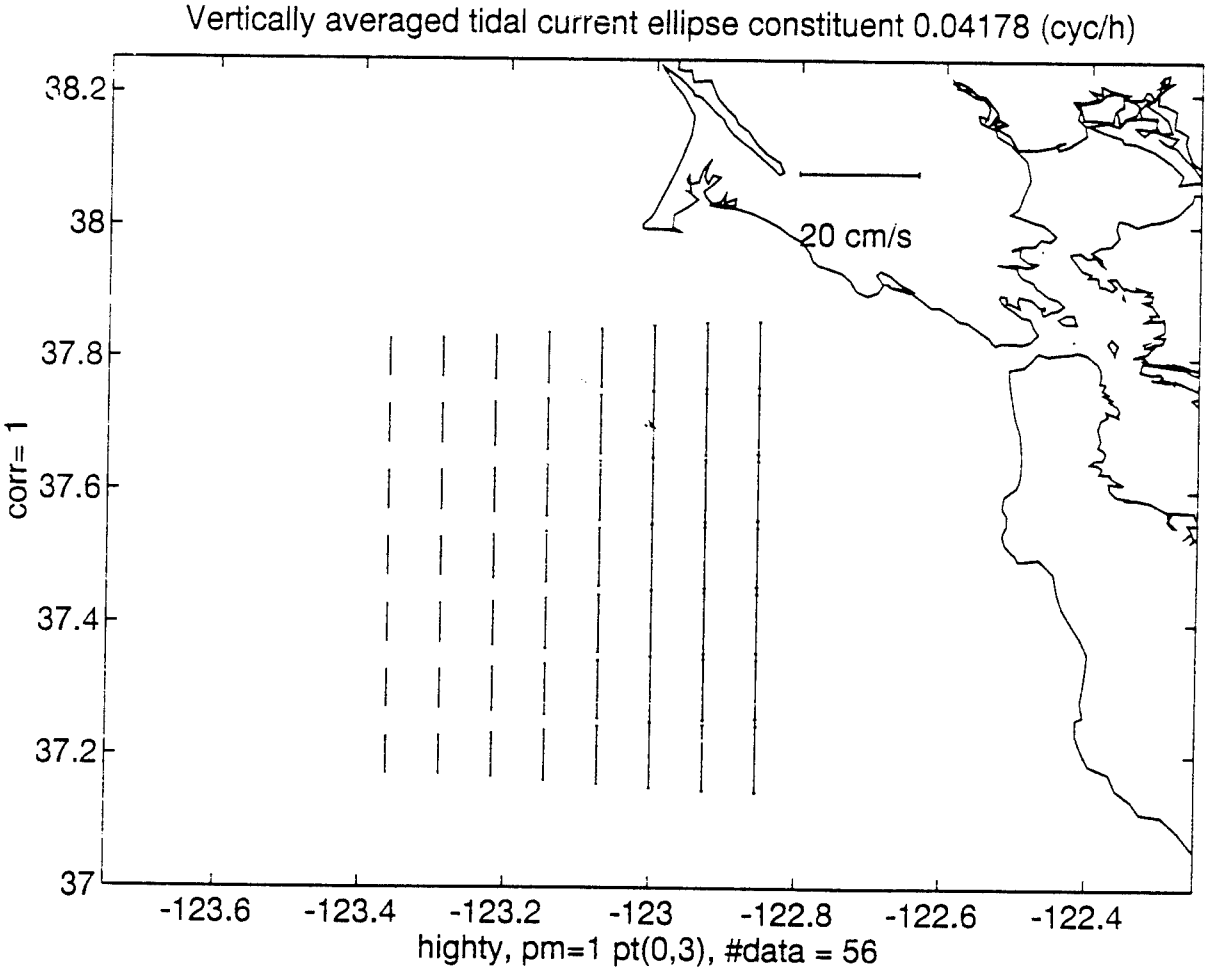

Figure 3a. K1 Tidal ellipse axes for third-order input flow. Flow is north-south with east-west variation increasing from approximately 3 cm s^{-1} to 6 cm s^{-1} in the onshore direction. Phase is assumed to be constant.

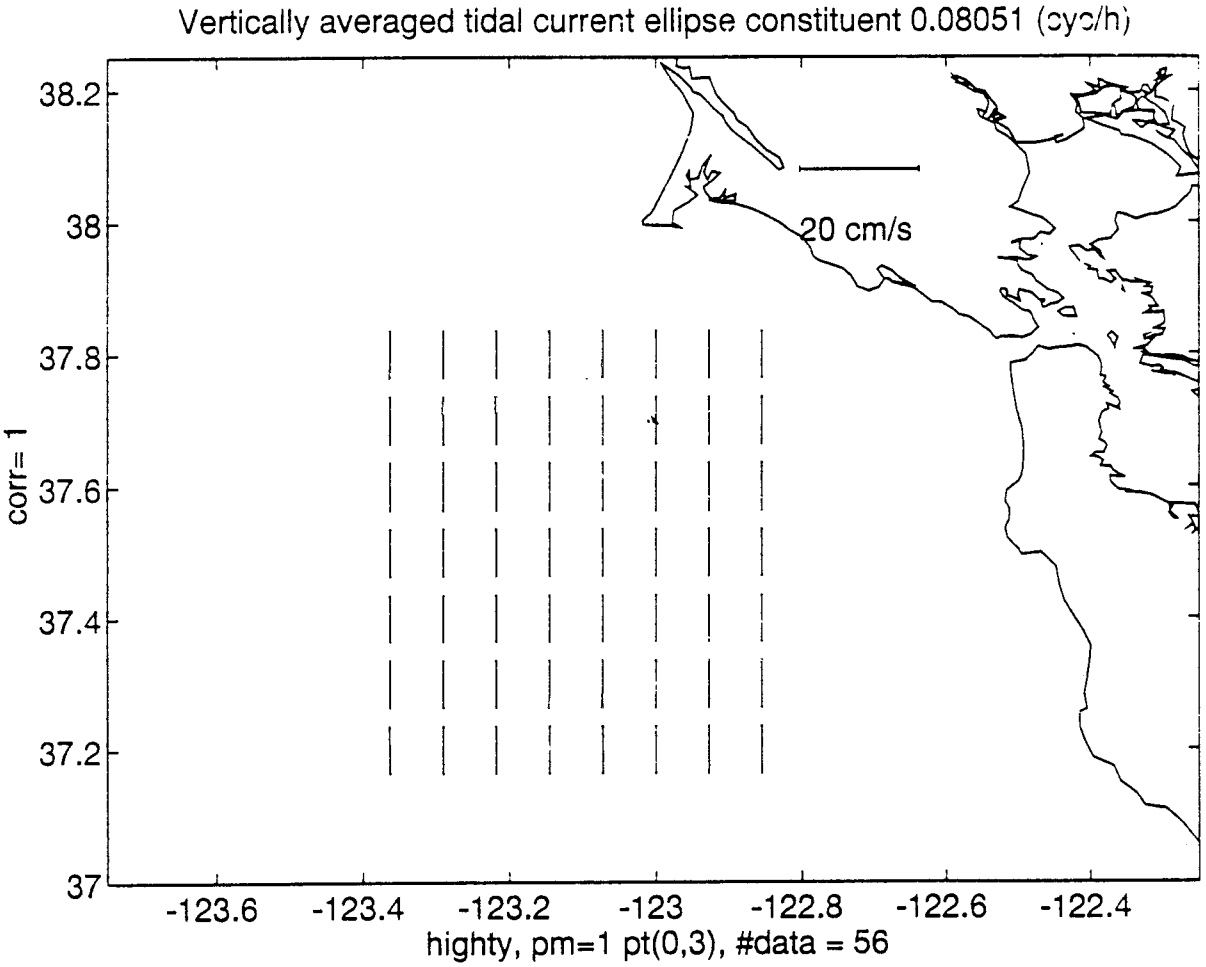

Figure 3b. M2 Tidal ellipse axes for constant (4 cm s^{-1}) input flow. Flow is north-south. Phase is assumed to be constant.

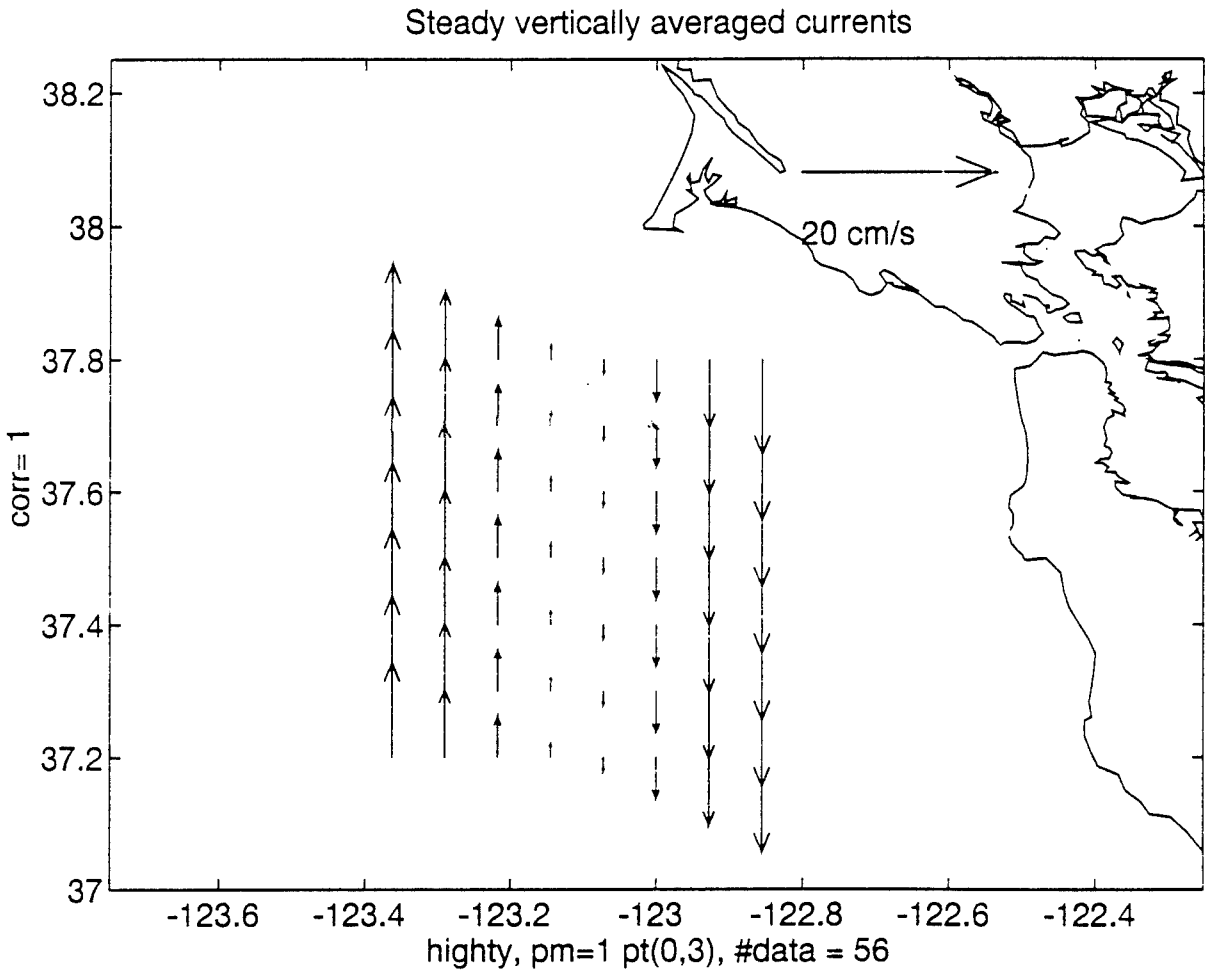

Figure 3c. Vertically averaged current vectors for linearly varying steady input flow. Flow is north-south with east-west variation. Maximum northward flow is 10 cm s^{-1} decreasing to southward maximum flow (-10 cm s^{-1}) onshore.

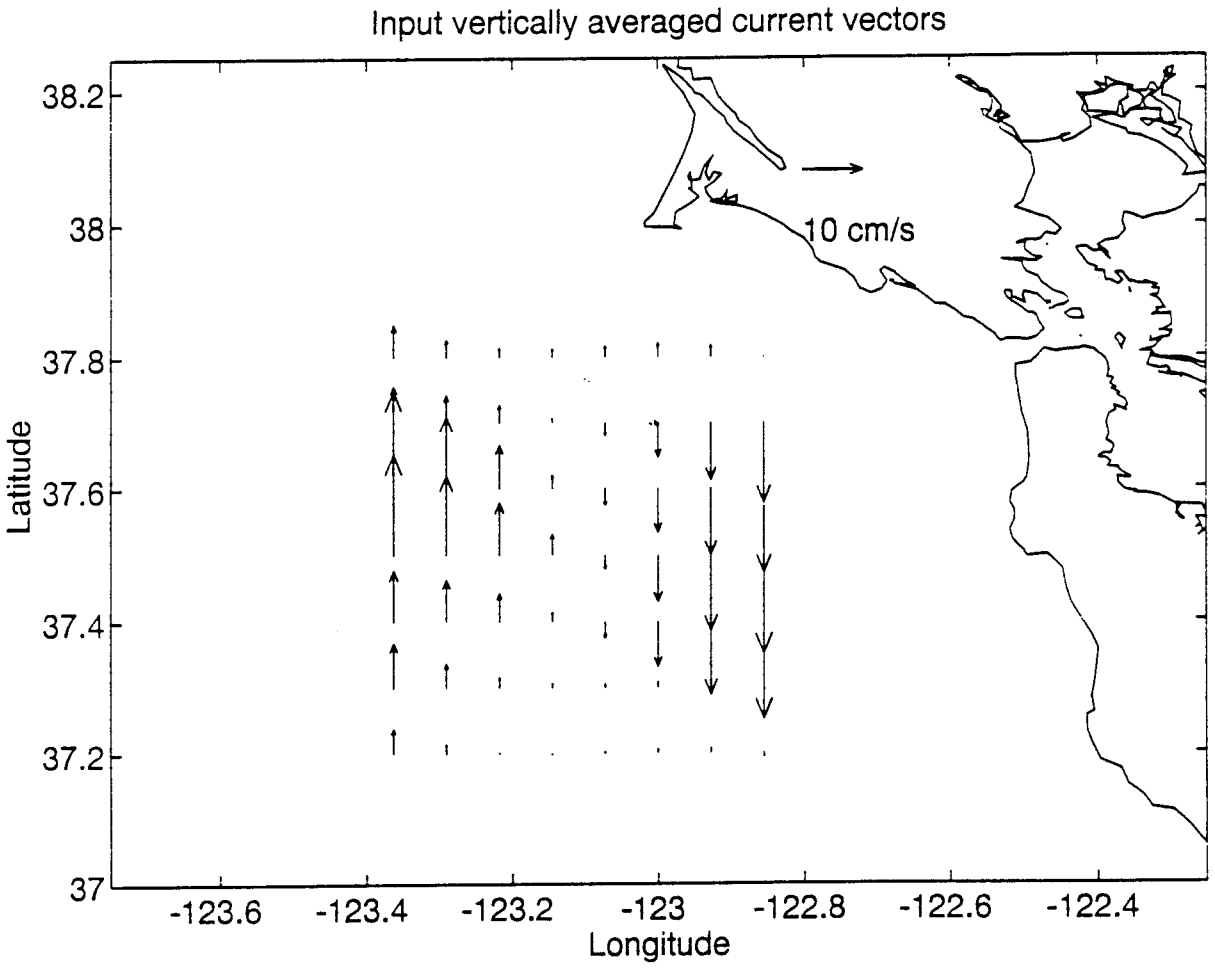

Figure 3d. Total input flow field. Represents the sum of linearly varying steady flow (pm=1), constant M2 and third-order varying K1 tidal constituents (pt=0,3). Flow is north-south with variability in the east-west direction.

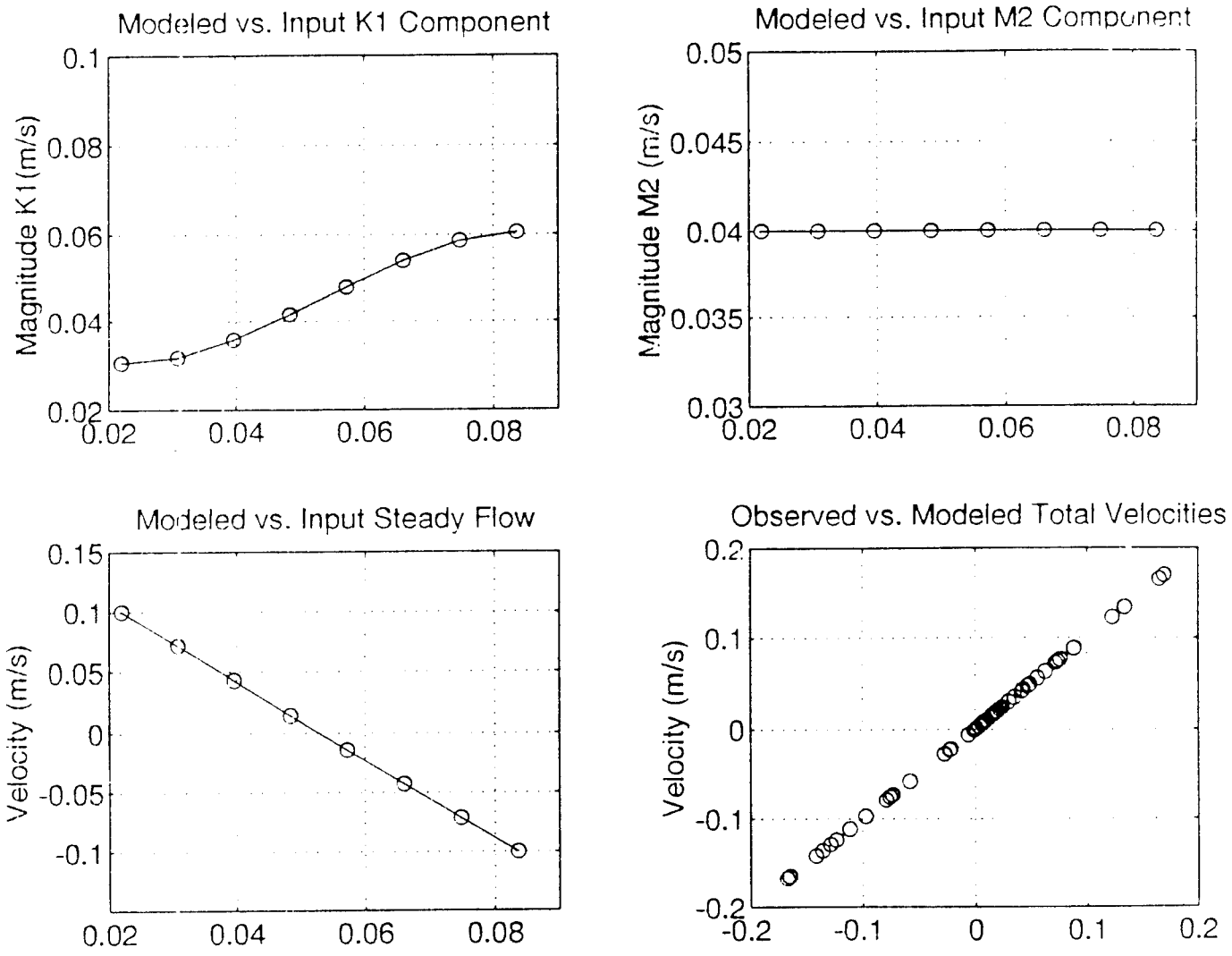

Figure 4. Modeled versus input correlation for proper fit to input fields (pm=1, pt=0.3). (a) Magnitude of K1 component versus a scaled longitudinal component increasing in the onshore direction. Solid line represents third-order input function with circles illustrating the modeled value. All 56 points are plotted with 7 circles for each value of the scaled longitude coincident. (b) Perfect fit for the M2 component magnitude versus scaled longitude. (c) Perfect fit for steady flow field. (d) Input vs. modeled velocities. A straight line indicates that each value has been properly modeled.

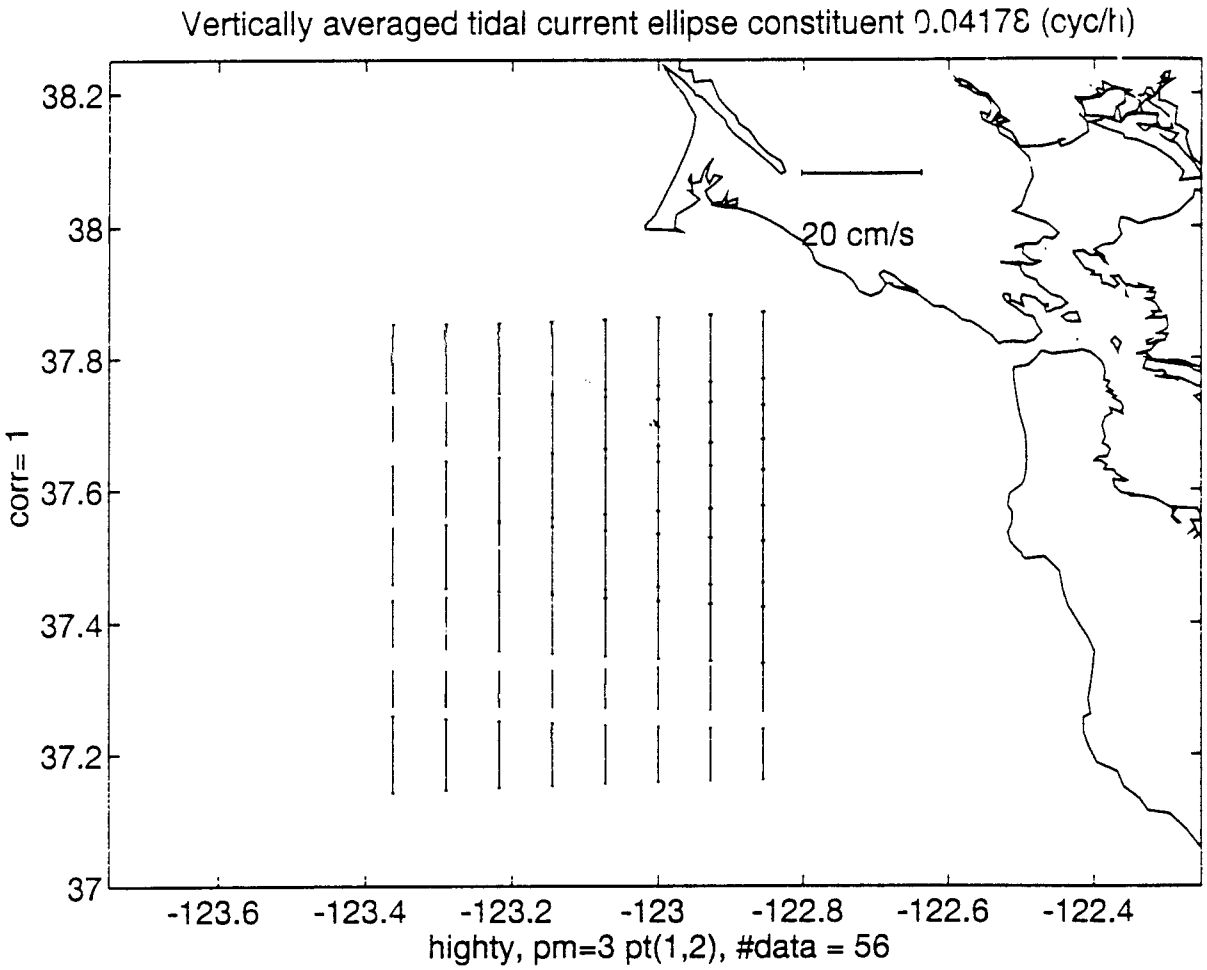

Figure 5a. K1 Tidal ellipse axes for improper choice of polynomial fitting function. Input flow varies north-south. Model introduces incorrect variability in both the north-south and east-west directions.

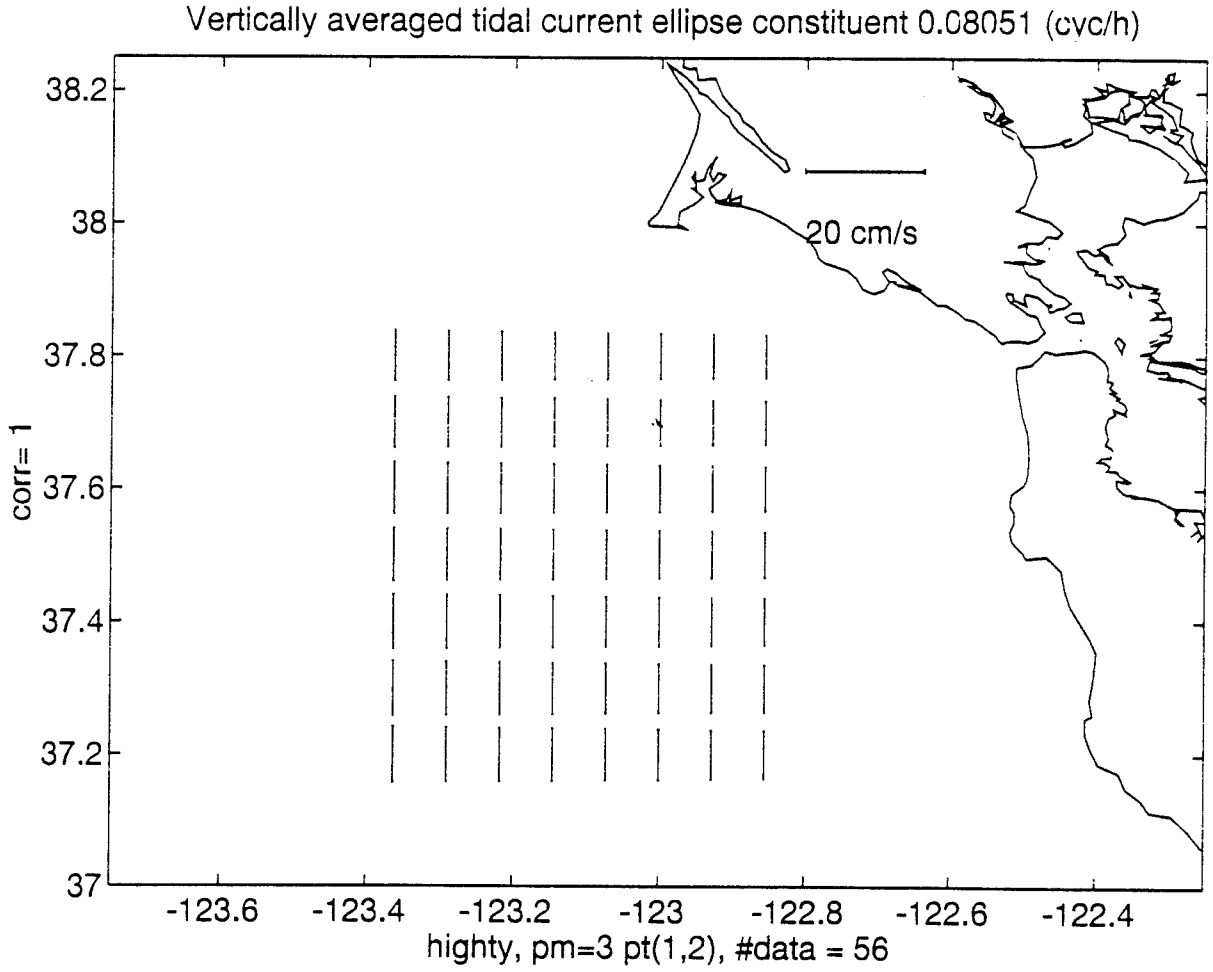

Figure 5b. M2 Tidal ellipse axes for improper choice of polynomial fitting function. Input flow is constant. Model introduces incorrect variability in both the north-south and east-west directions.

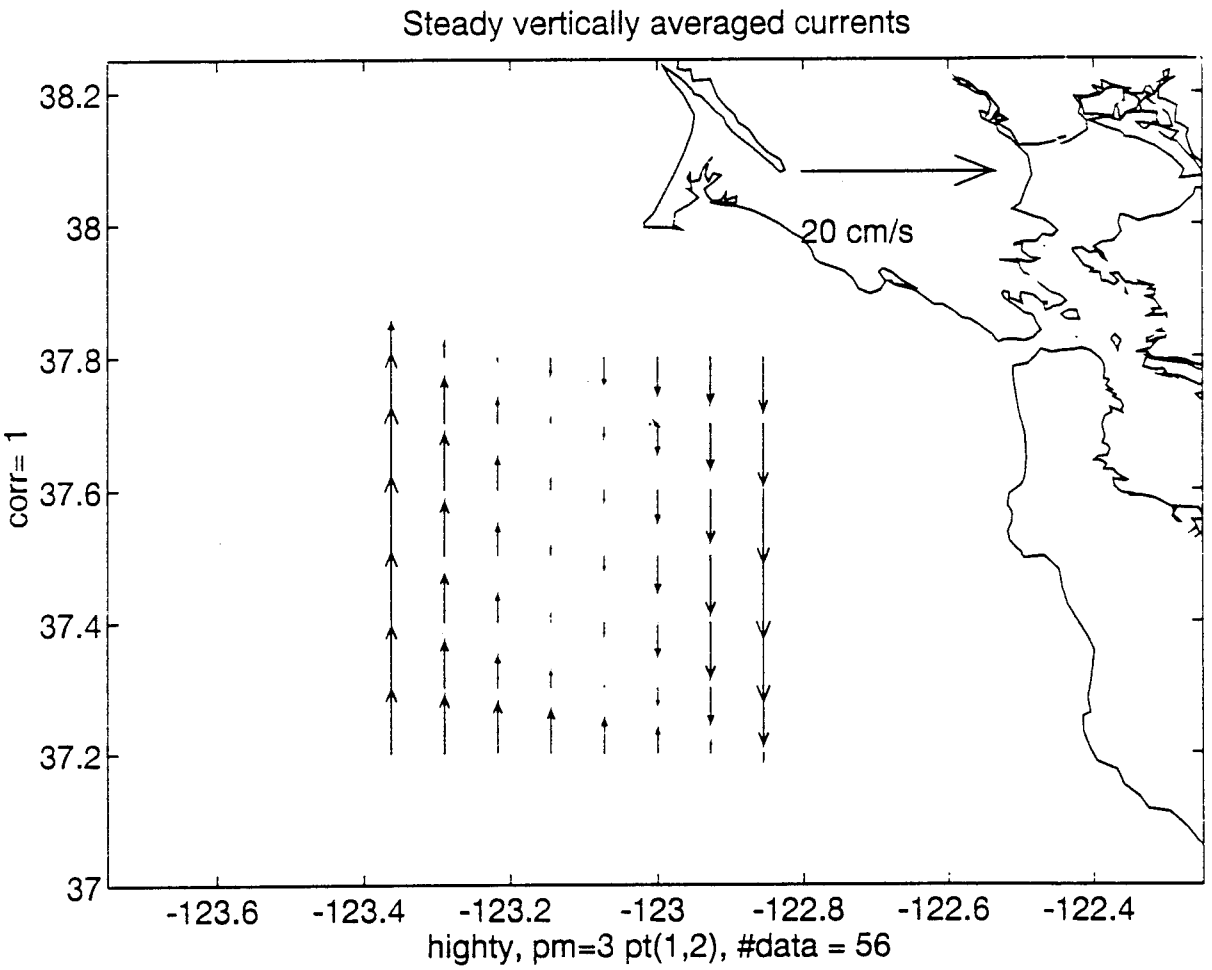

Figure 5c. Steady flow field for improper choice of polynomial fitting function. Input flow is north-south with east-west variation. Model incorrectly calculated velocities in both the north-south and east-west directions.

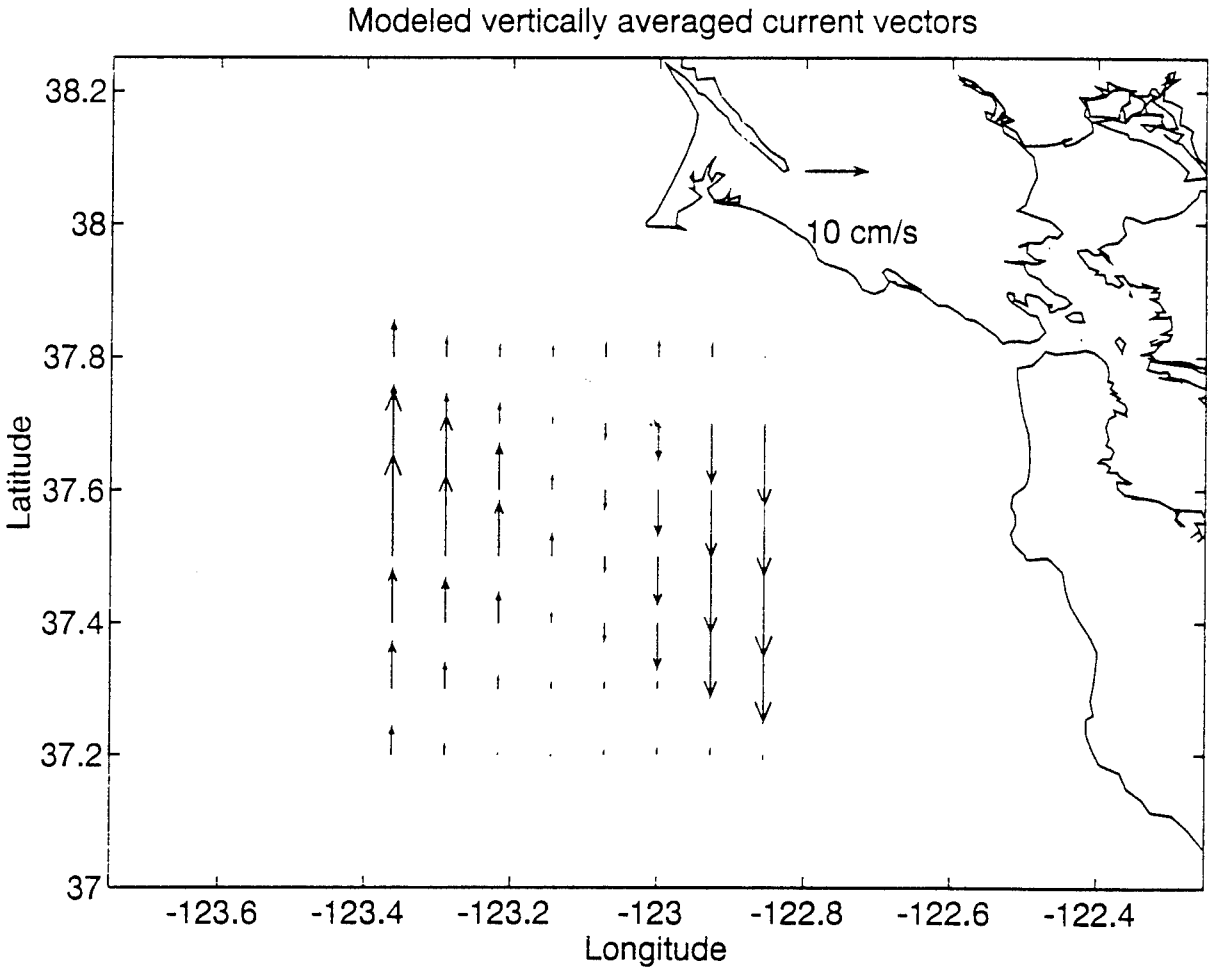

Figure 5d. Modeled total flow field for improper choice of polynomial fitting function. Velocities are perfectly correlated with the total input flow field. (corr=1)

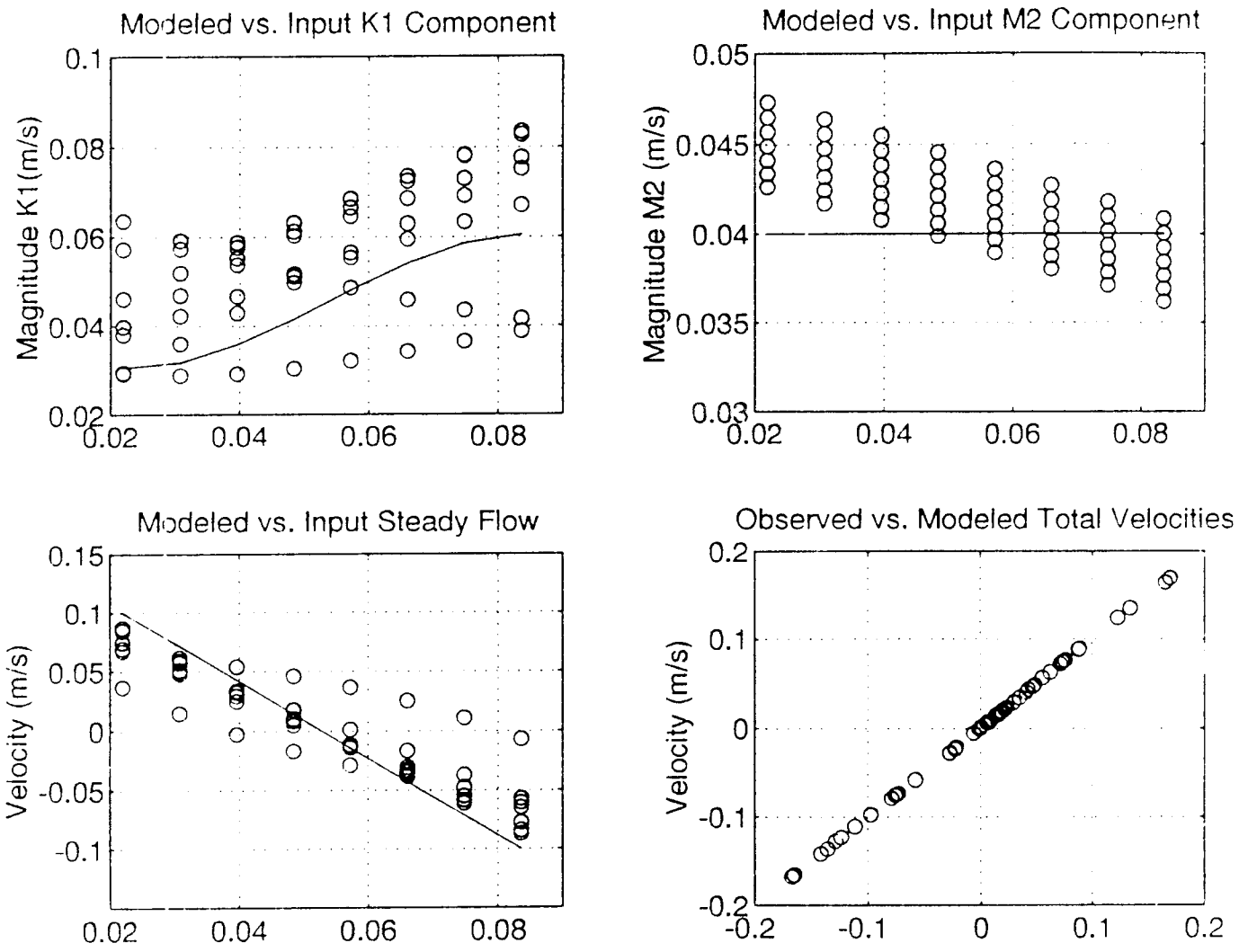

Figure 6. Correlation for improper choice of polynomial fitting functions. (a) K1 magnitudes are generally overestimated. Model values (circles) should vary only in the east-west (x) direction. Improper north-south variations are apparent because constant magnitudes should be calculated for a constant east-west (x) value. (b) Similar variability is apparent in the M2 component. (c) Modeled steady flow is underestimated offshore and overestimated onshore. (d) Total field is correctly modeled.

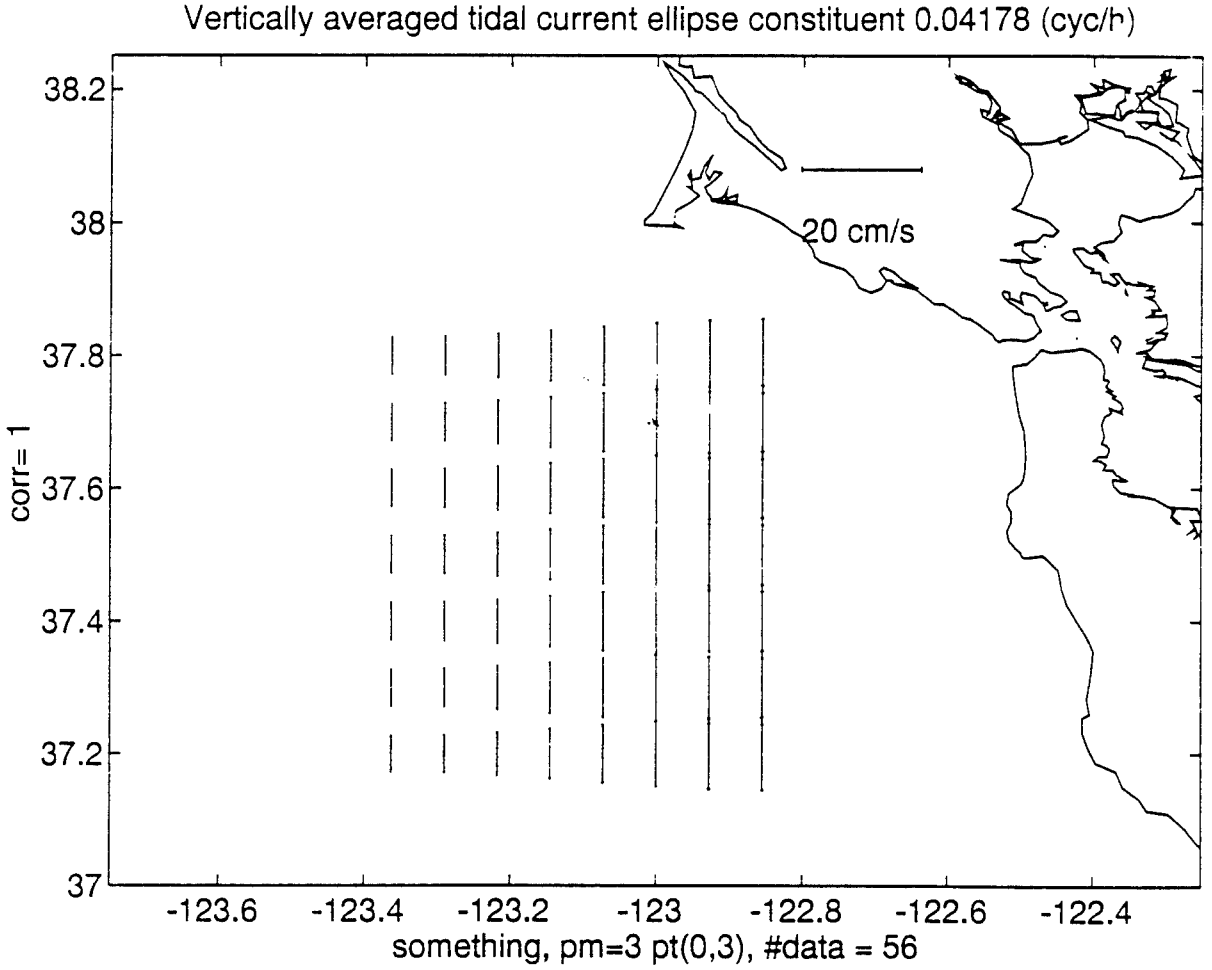

Figure 7a. K1 Tidal ellipse axes for third-order input flow used with Higher Order Residual Flow (Case 4).

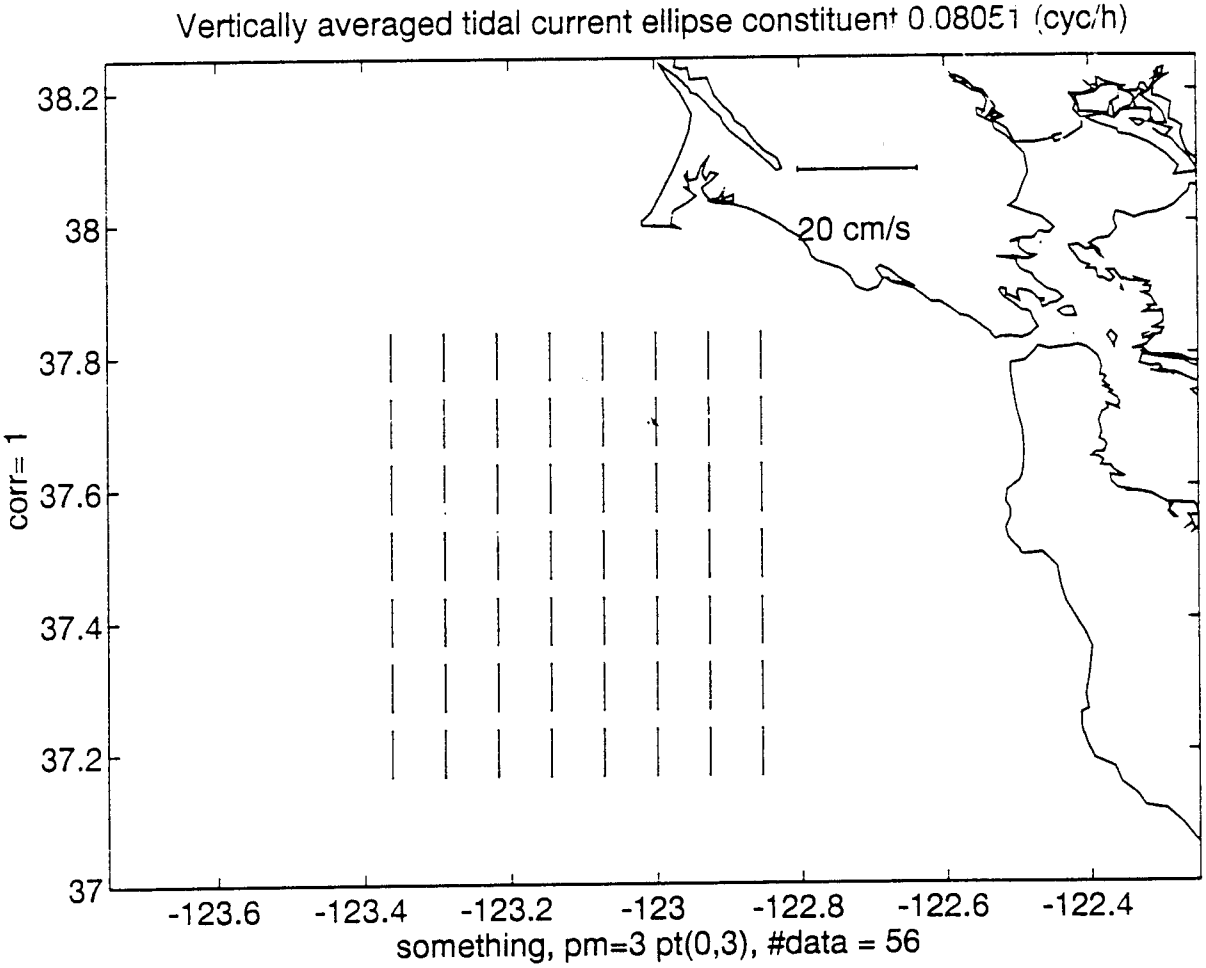

Figure 7b. M2 Tidal ellipse axes with constant magnitude used with Case 4.

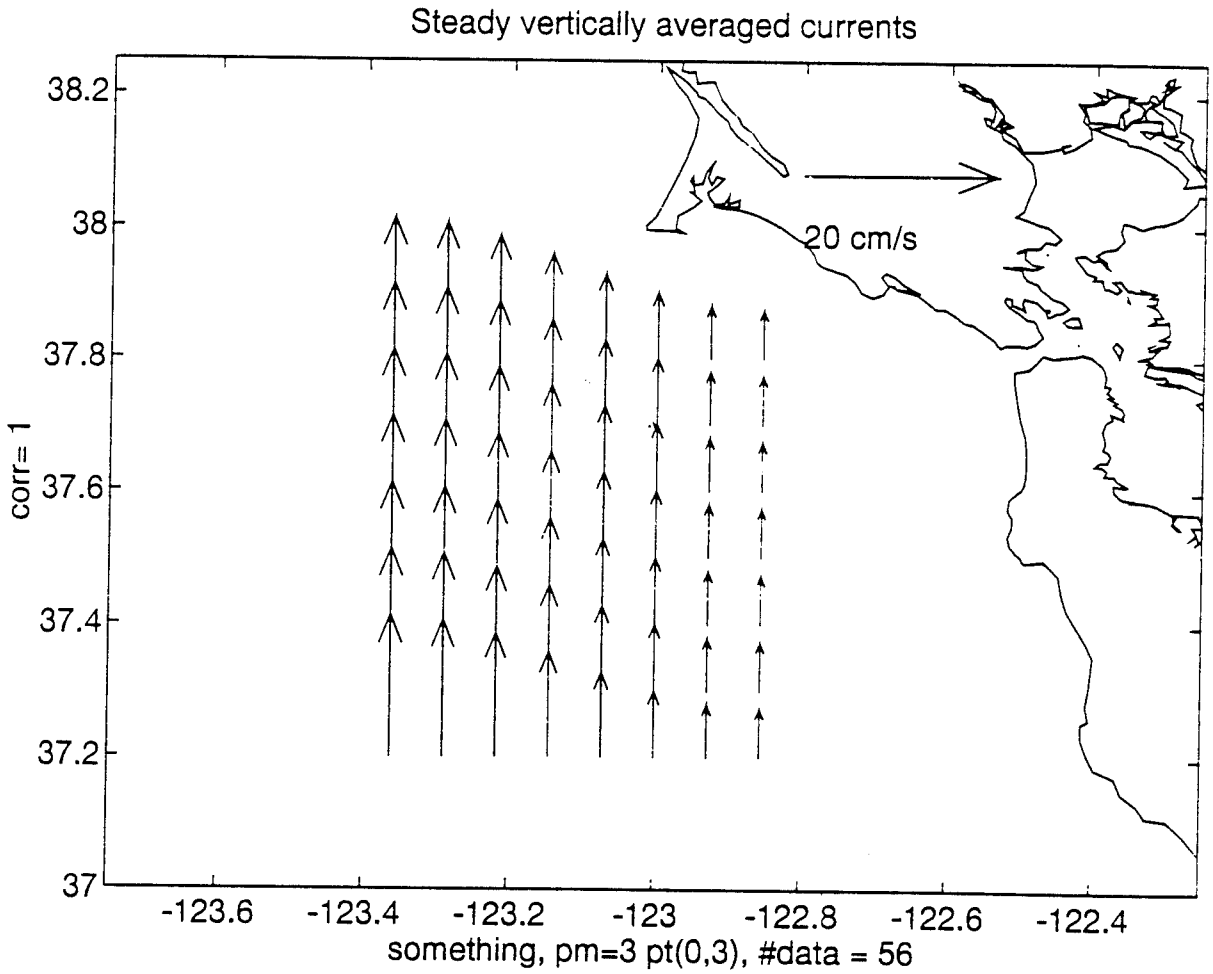

Figure 7c. Third-order input steady flow used for Case 4. Velocities decrease from 14.86 cm s^{-1} to 5.14 cm s^{-1} in the onshore direction.

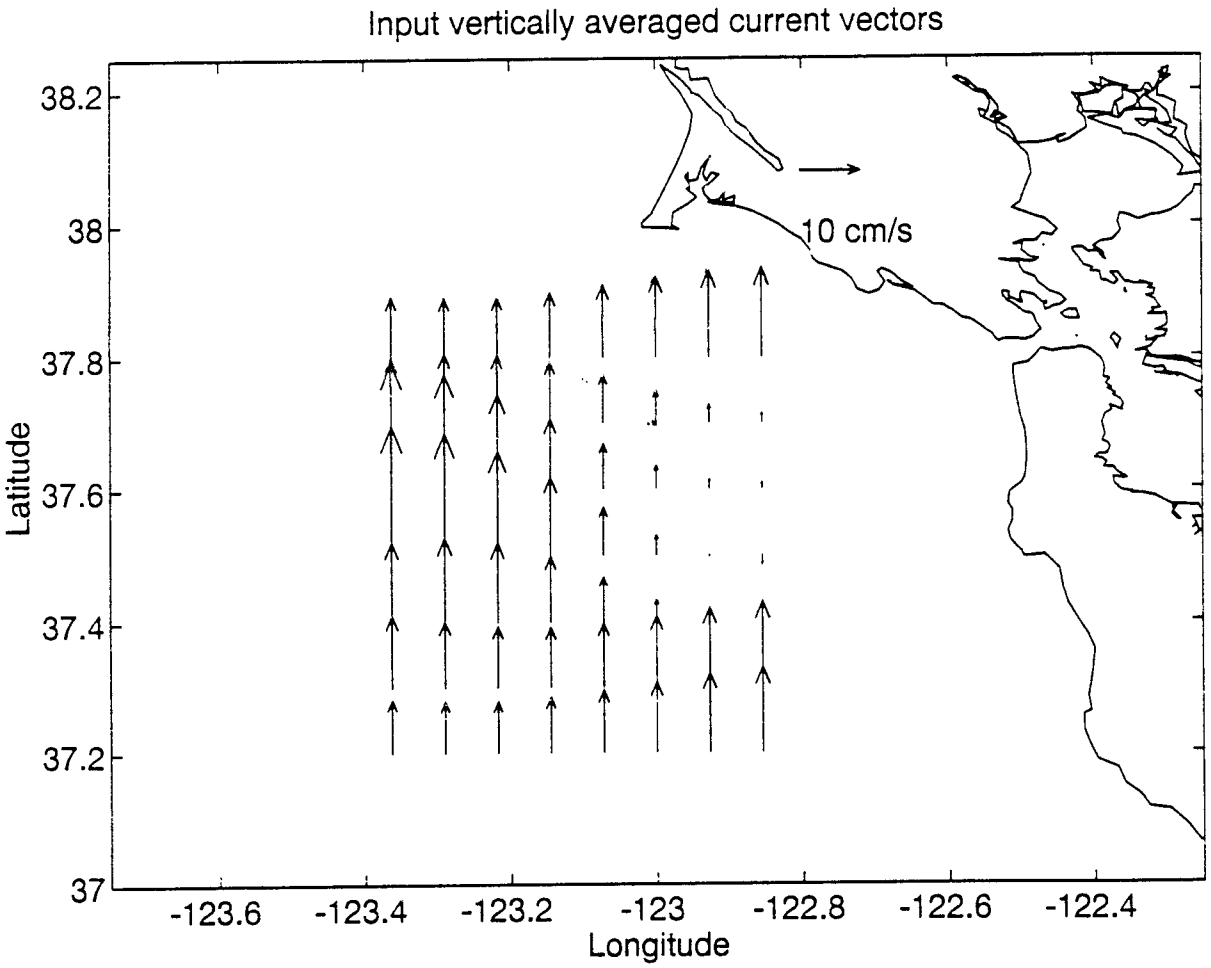

Figure 7d. Total input flow field for Case 4. Represents the sum of a third-order steady flow (pm=3), constant M2 and third-order varying K1 tidal constituents (pt=0,3).

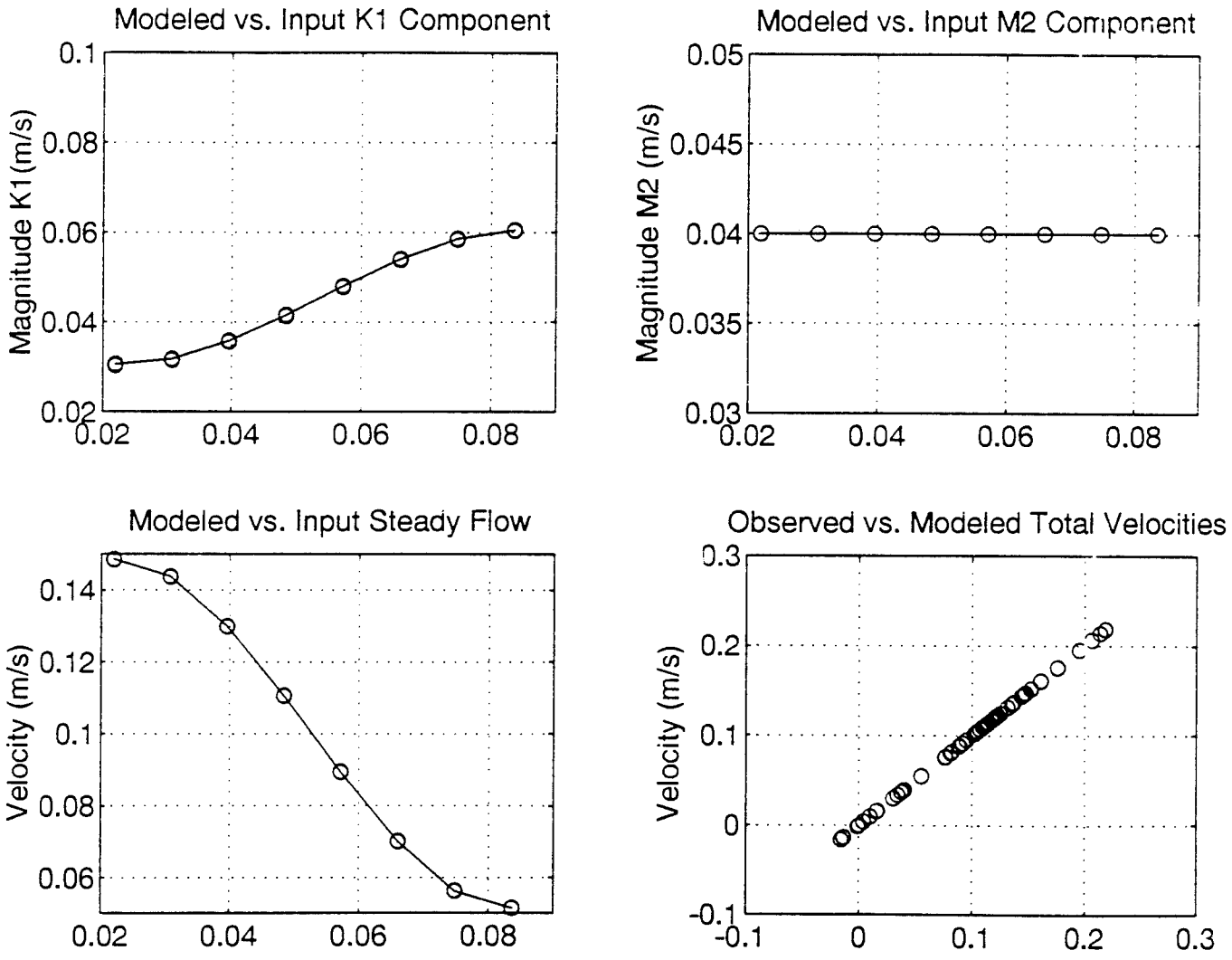

Figure 8. Correlation for proper fit to input fields for Case 4 (pm=3, pt=0,3). (a) K1 Tidal constituent. (b) M2 Tidal constituent. (c) Steady flow field. (d) Total flow field.

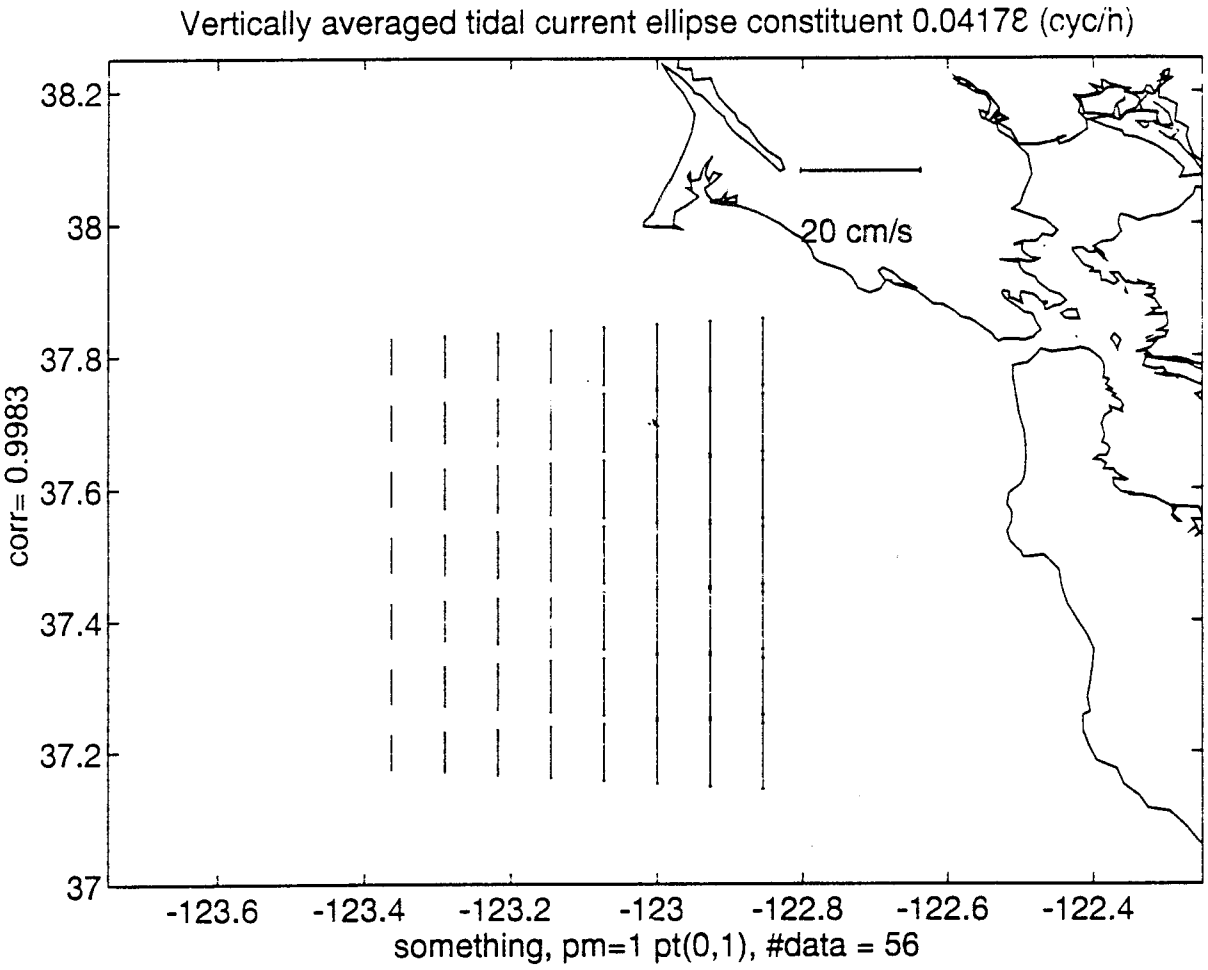

Figure 9a. K1 Tidal ellipse axes for specified polynomial fit (pm=1, pt=0,1) to Case 4.

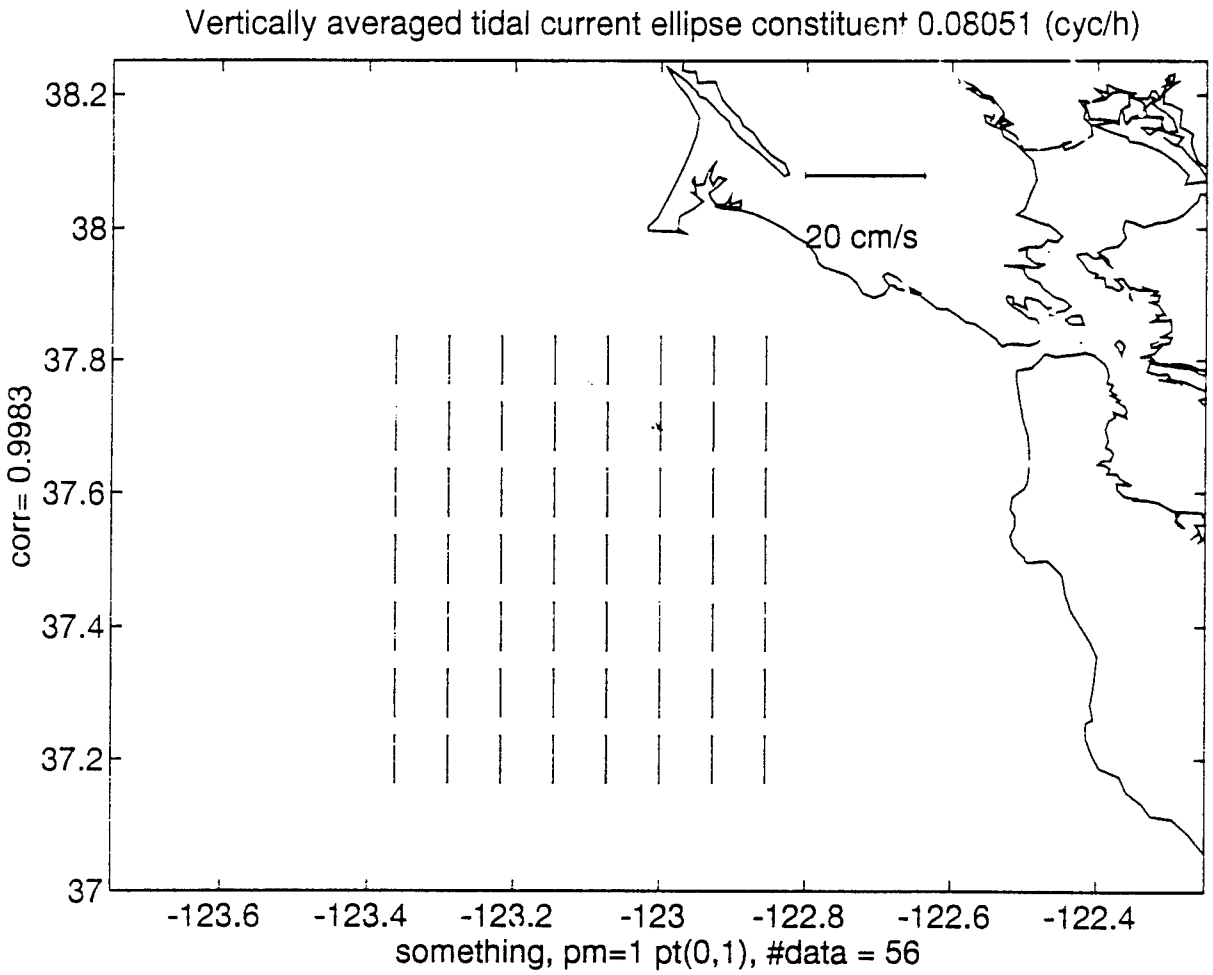

Figure 9b. M2 tidal ellipse axes for specified polynomial fit (pm=1, pt=0,1) to Case 4.

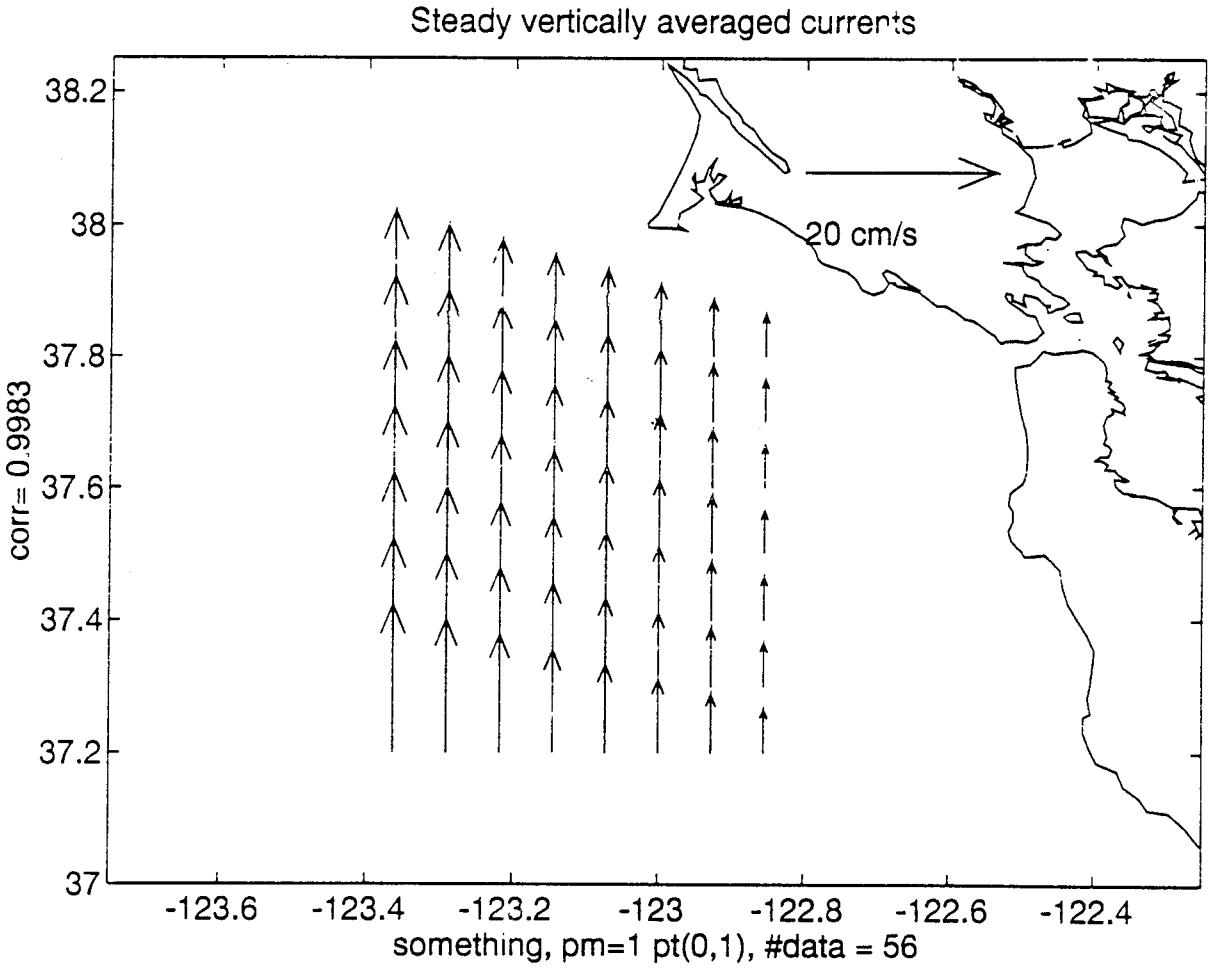

Figure 9c. Steady flow field for specified polynomial fit (pm=1, pt=0,1) to Case 4.

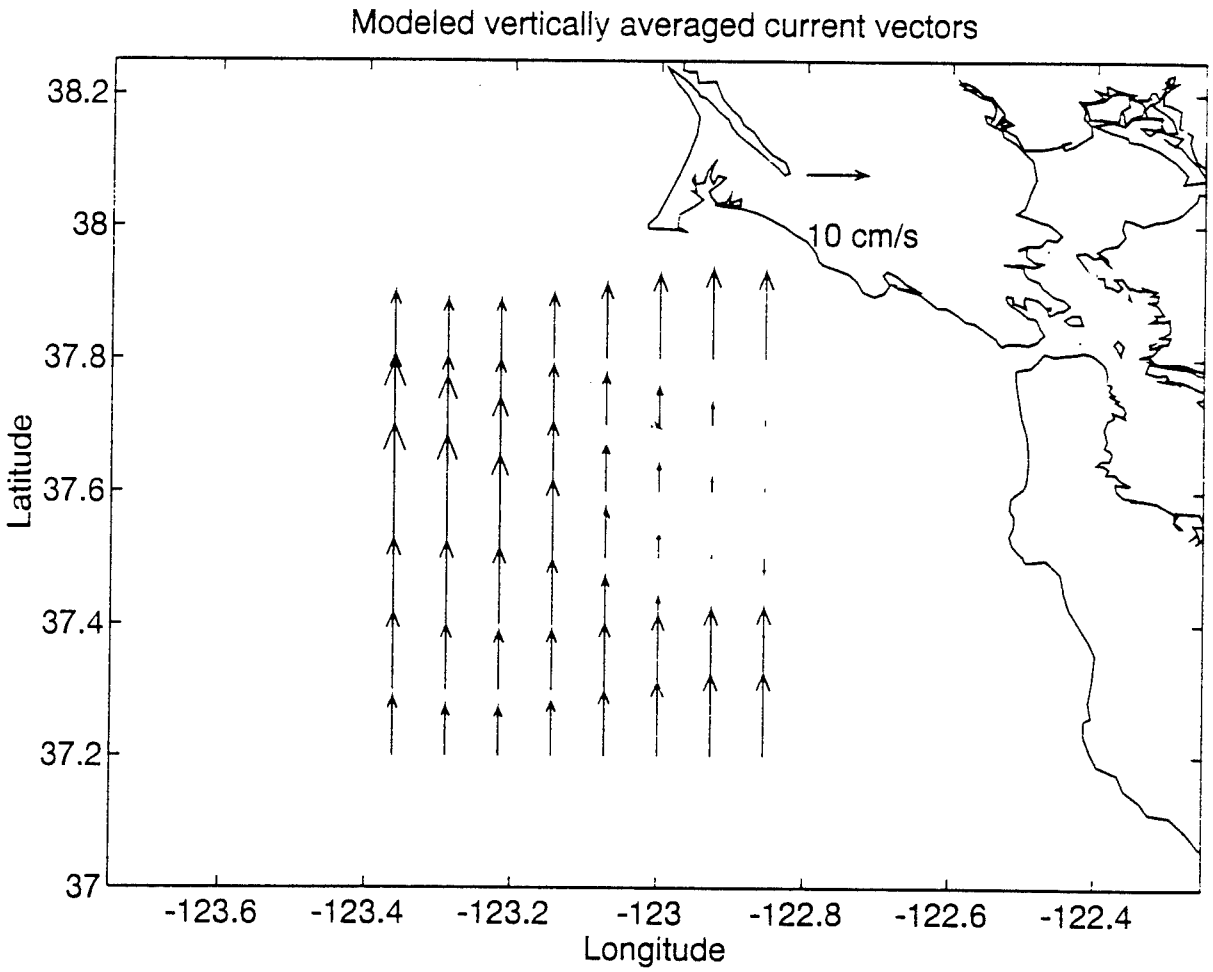

Figure 9d. Modeled total flow field for polynomial fit (pm=1, pt=0,1) to Case 4.

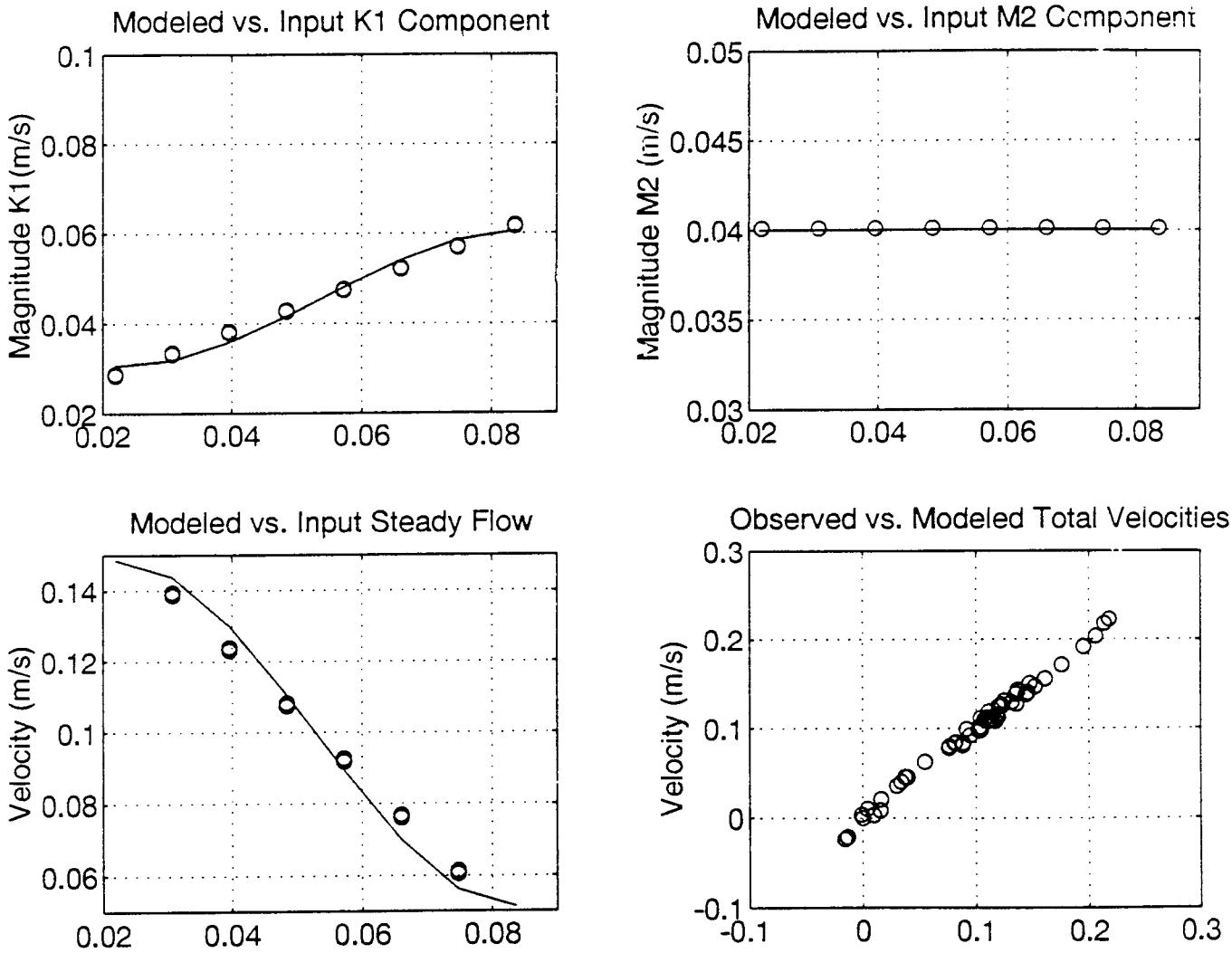

Figure 10. Correlation for specified fit (pm=1, pt=0,1) to Case 4. (a) K1 magnitudes fit nearly perfectly. Little incorrect north-south variation is modeled. (b) M2 magnitudes are properly modeled. (c) Steady flow is well modeled with some slight north-south variation erroneously depicted. (d) Total field is nearly perfectly modeled.

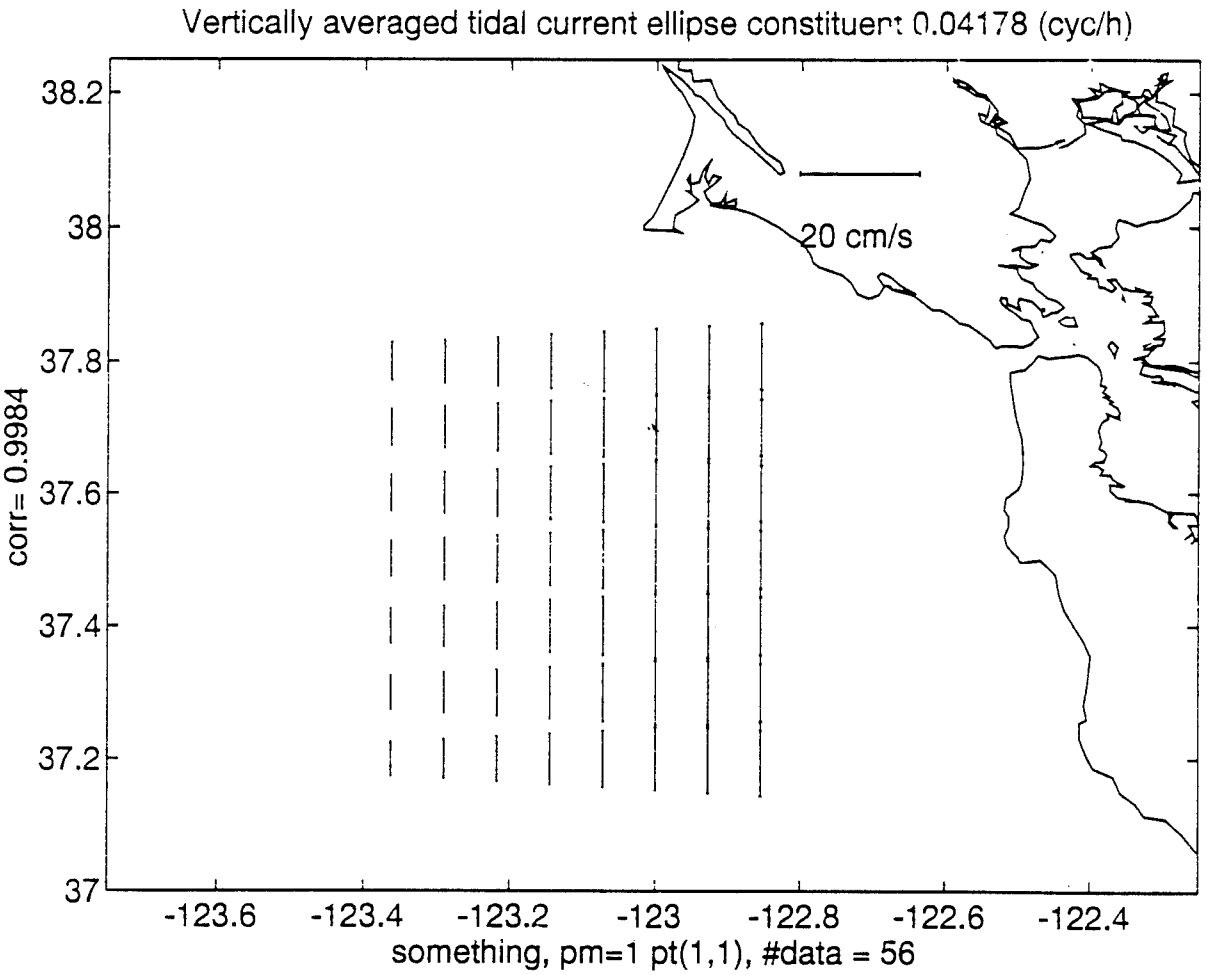

Figure 11a. K1 Tidal ellipse axes for specified polynomial fit (pm=1, pt=1,1) to Case 4.

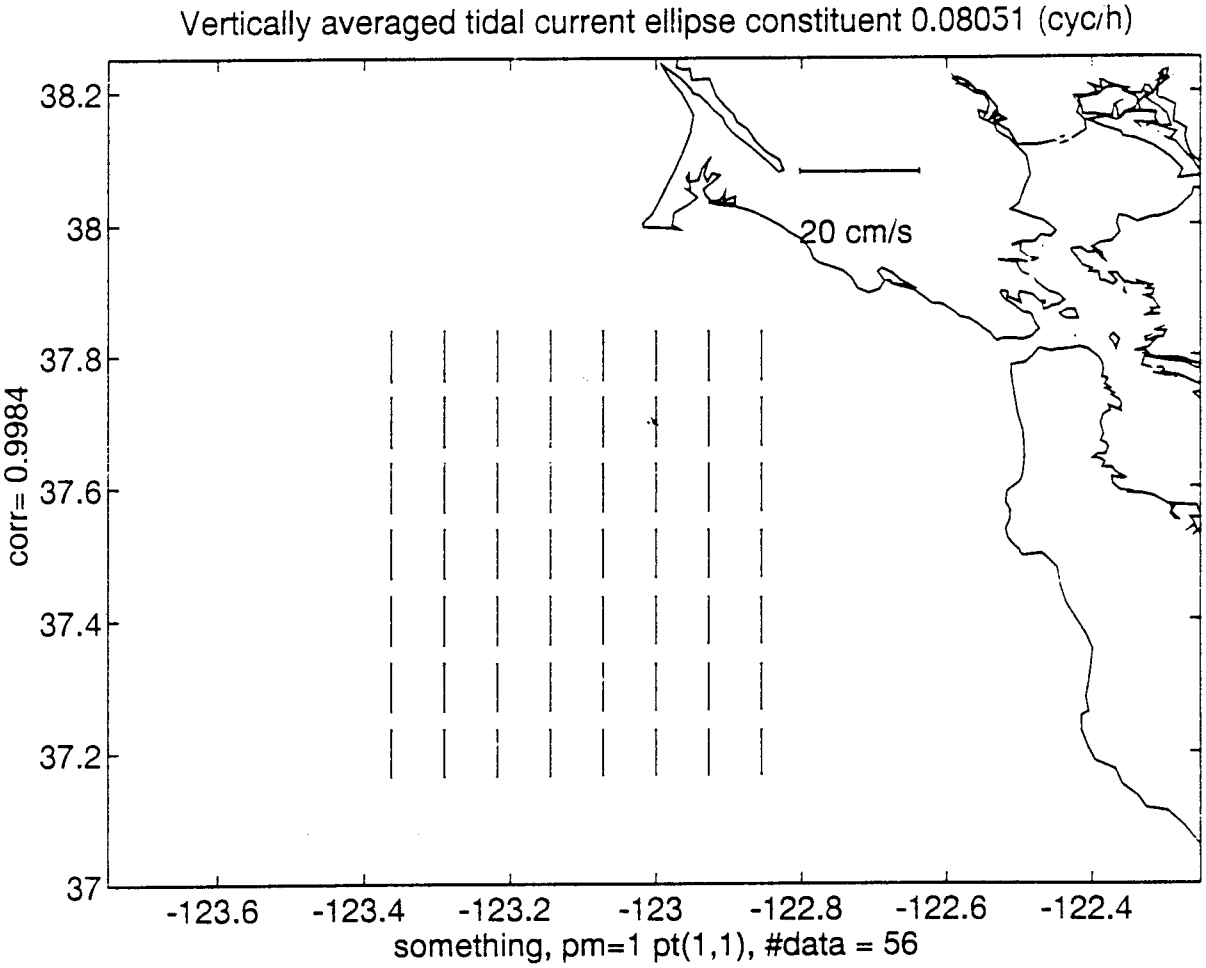

Figure 11b. M2 Tidal ellipse axes for specified polynomial fit (pm=1, pt=1,1) to Case 4.

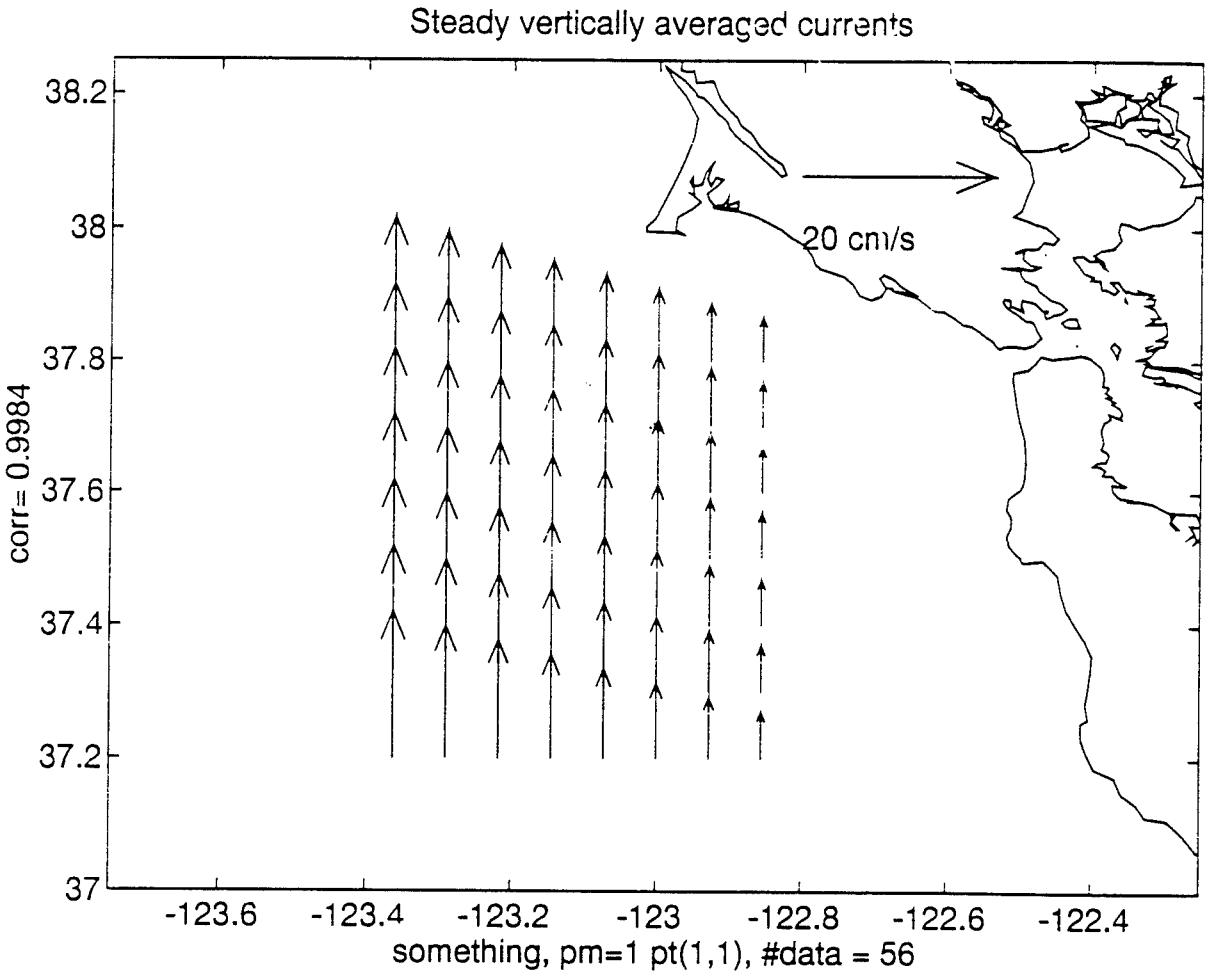

Figure 11c. Steady flow field for specified polynomial fit (pm=1, pt=1,1) for Case 4.

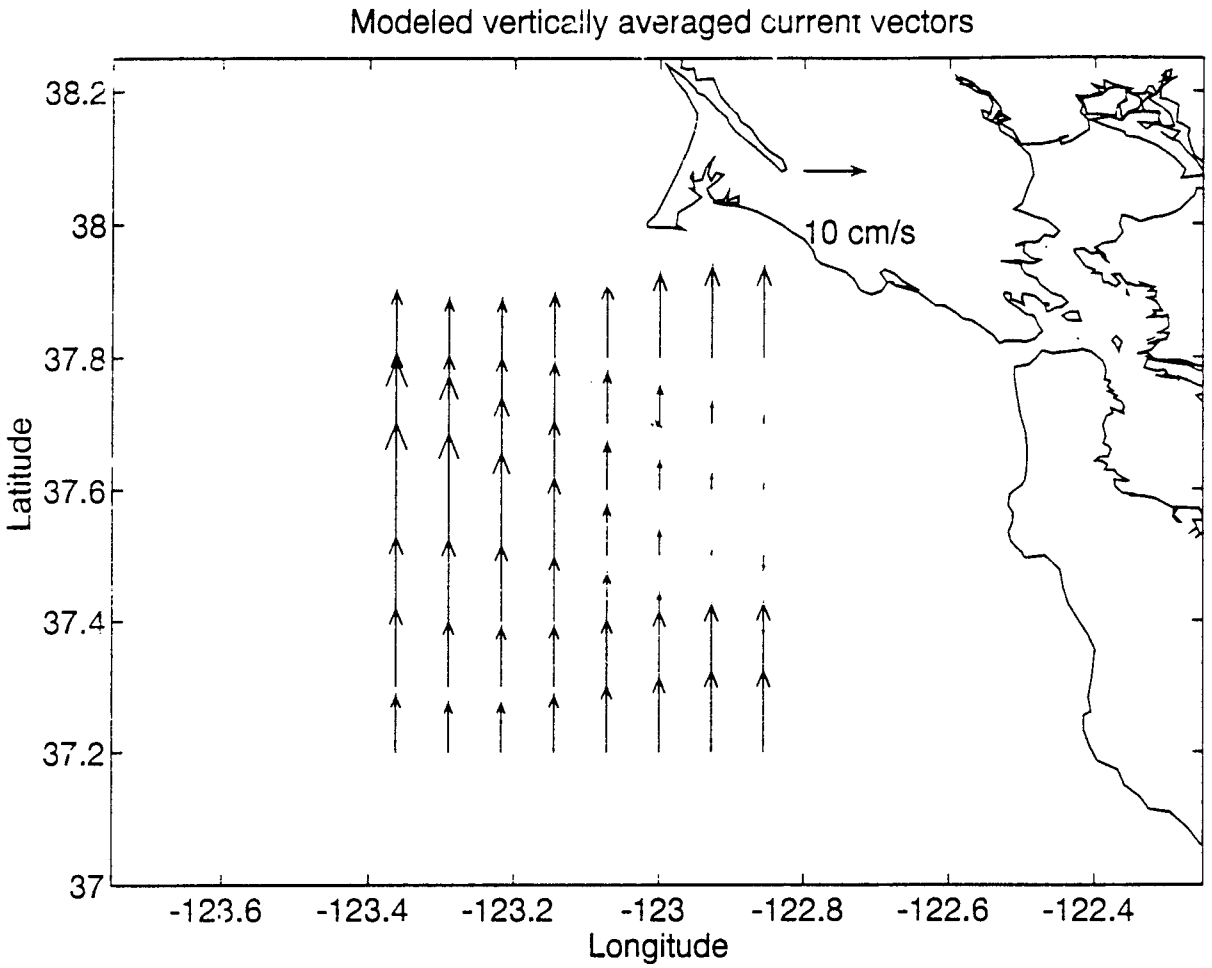

Figure 11d. Modeled total flow field for polymonial fit (pm=1, pt=1,1) for Case 4.

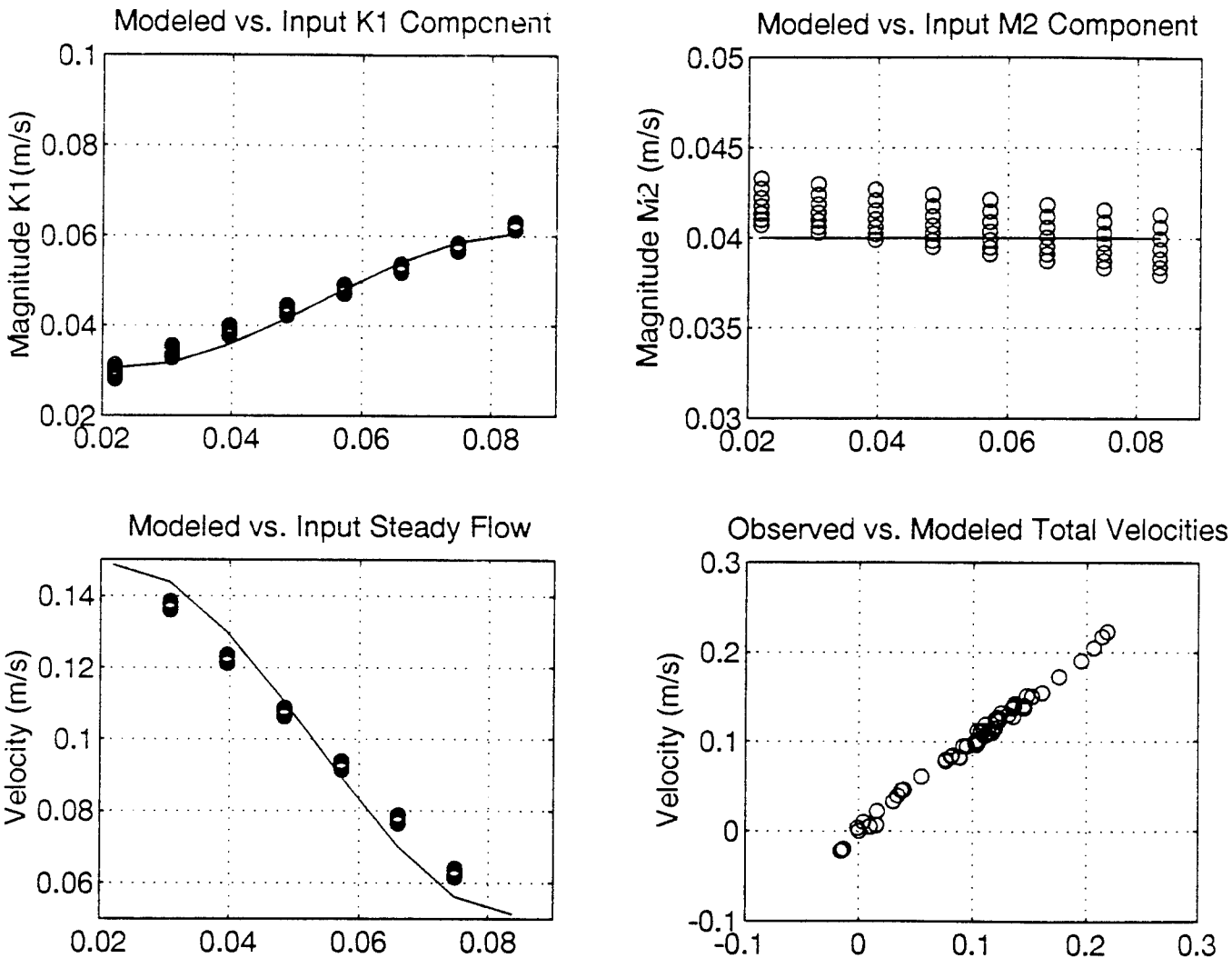

Figure 12. Correlation for specified fit (pm=1, pt=1,1) for Case 4. (a) K1 magnitude. (b) M2 magnitude. (c) Steady flow. (d) Total flow field.

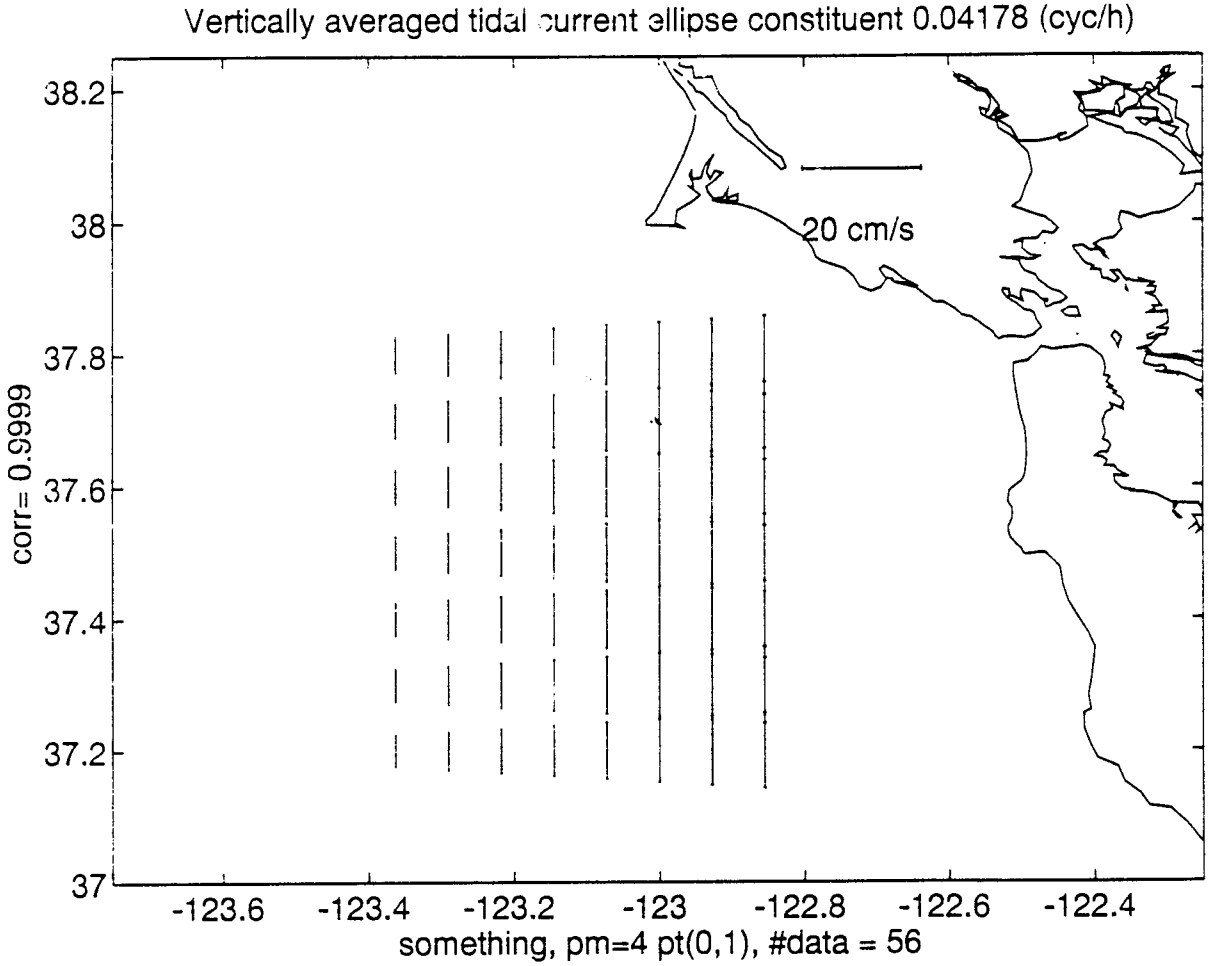

Figure 13a. K1 Tidal ellipse axes for specified polynomial fit (pm=4, pt=0,1) to Case 4.

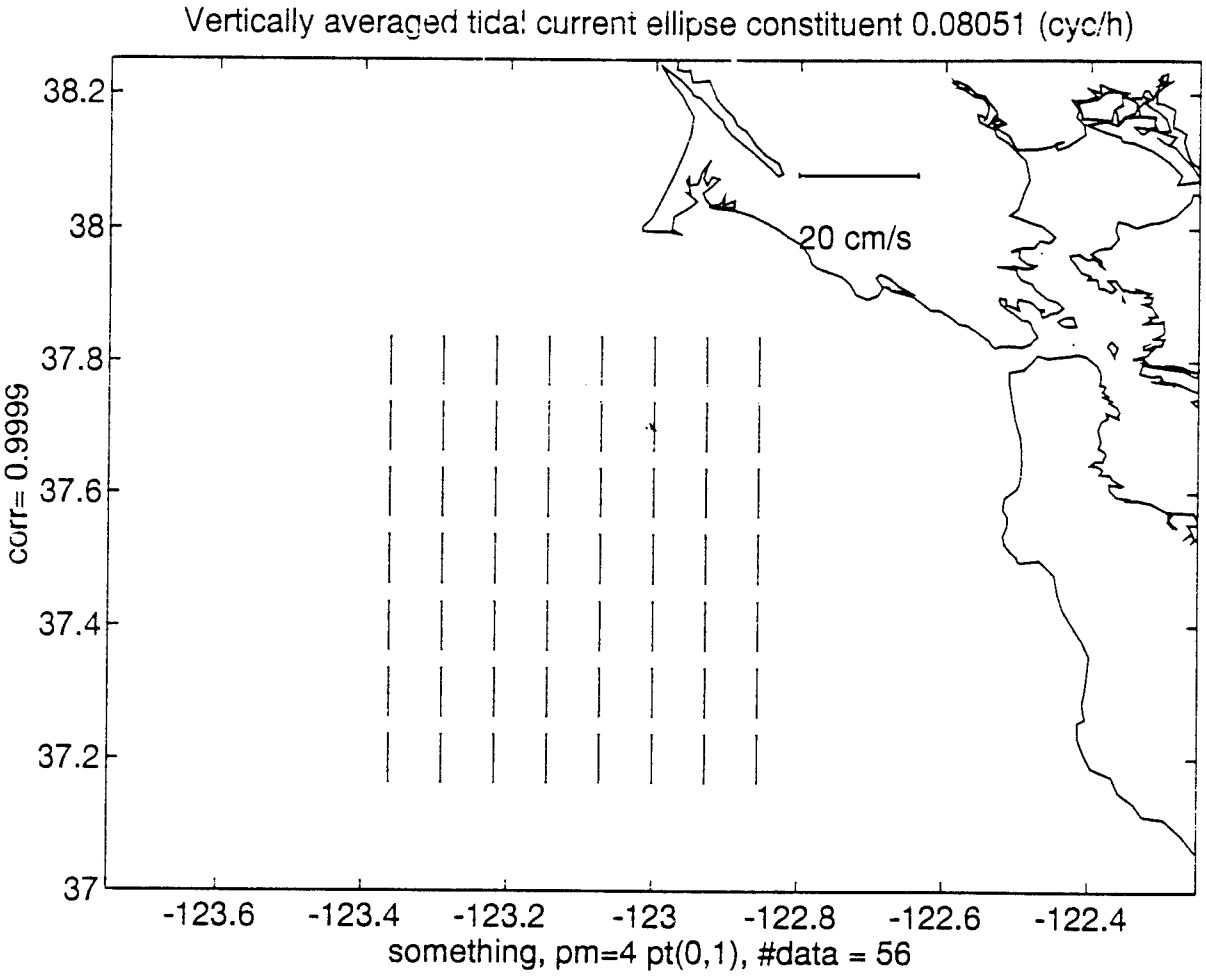

Figure 13b. M2 Tidal ellipse axes for specified polynomial fit (pm=4, pt=0,1) to Case 4.

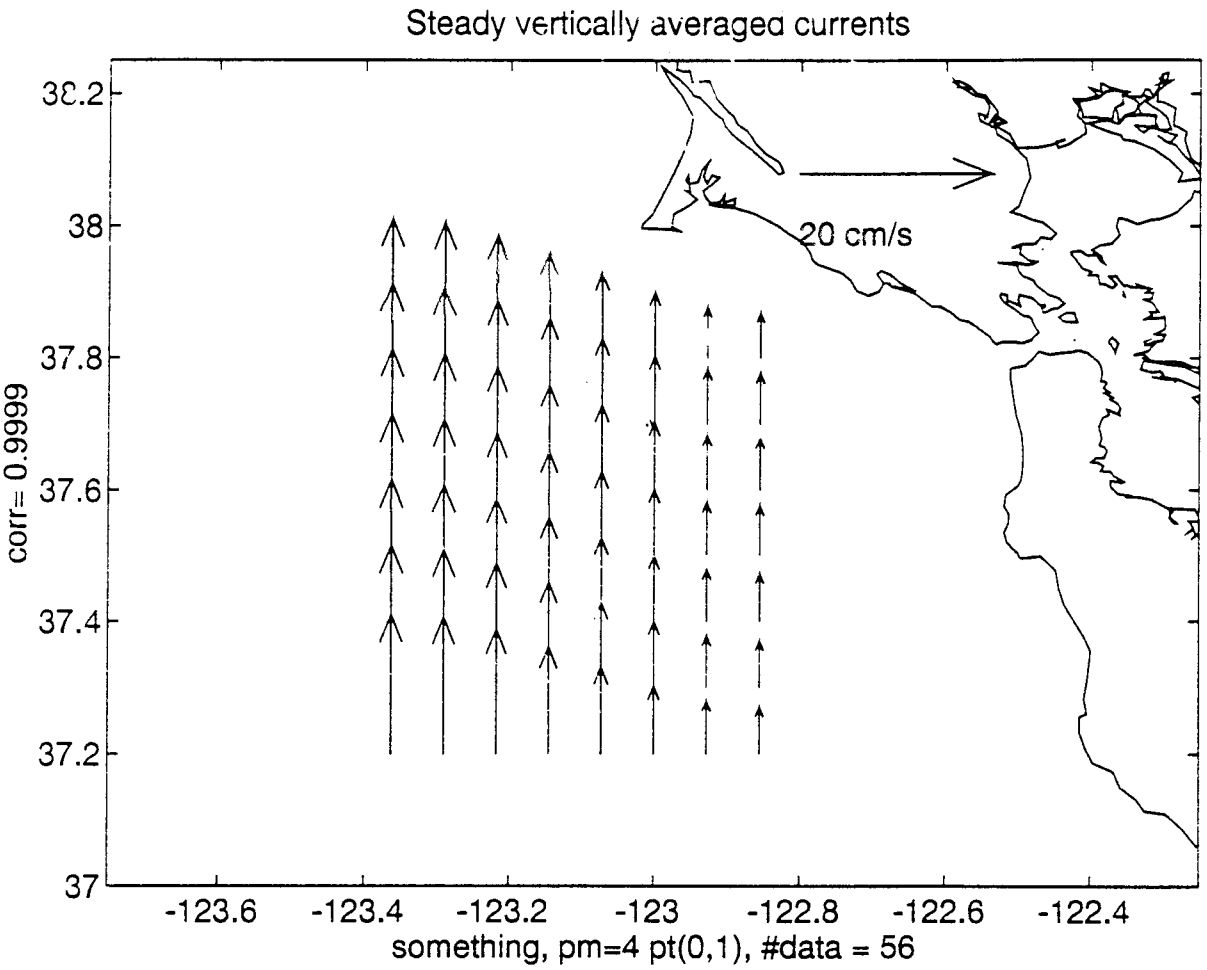

Figure 13c. Steady flow field for specified polynomial fit (pm=4, pt=0,1) to Case 4.

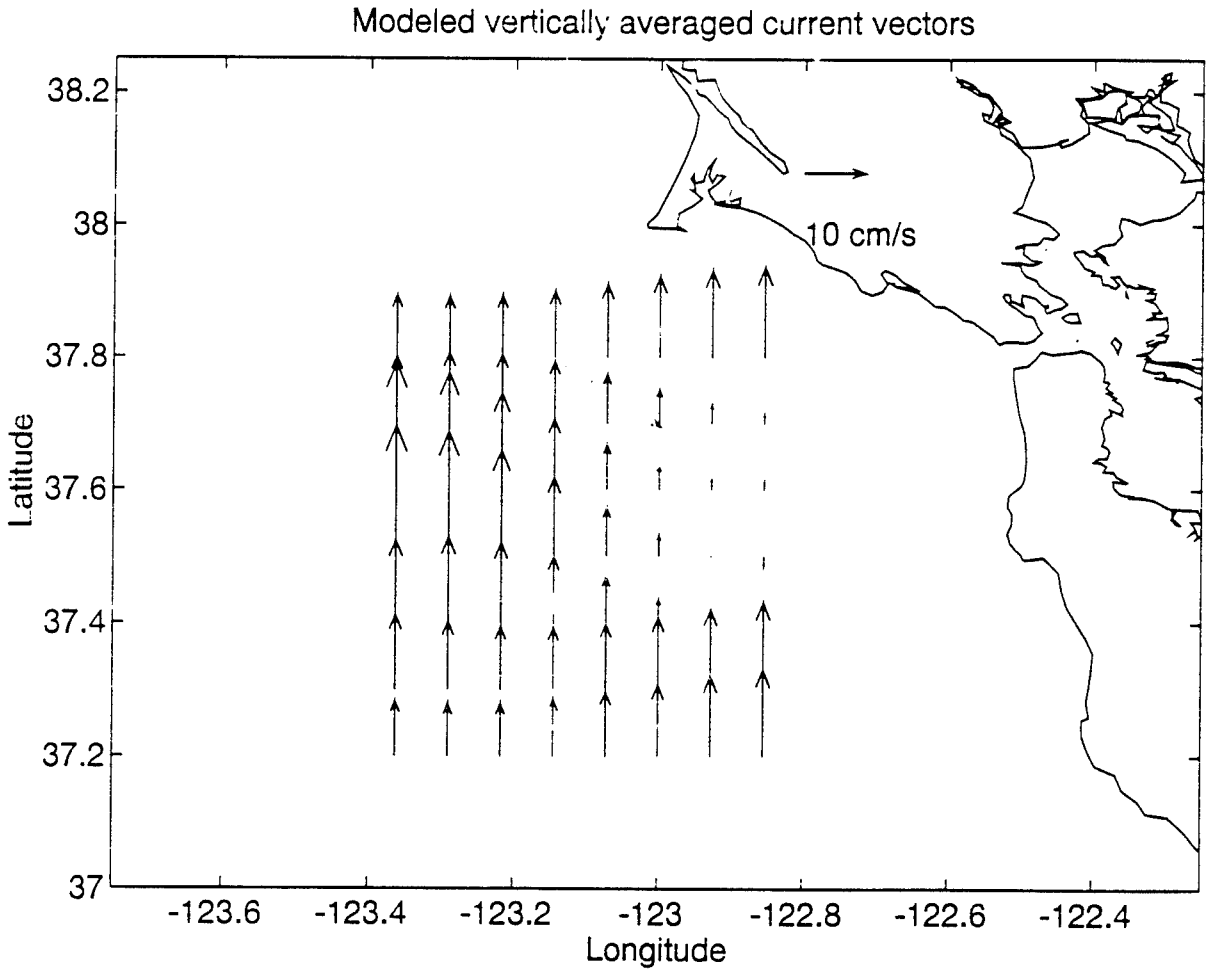

Figure 13d. Modeled total flow field for polynomial fit (pm=4, pt=0,1) to Case 4.

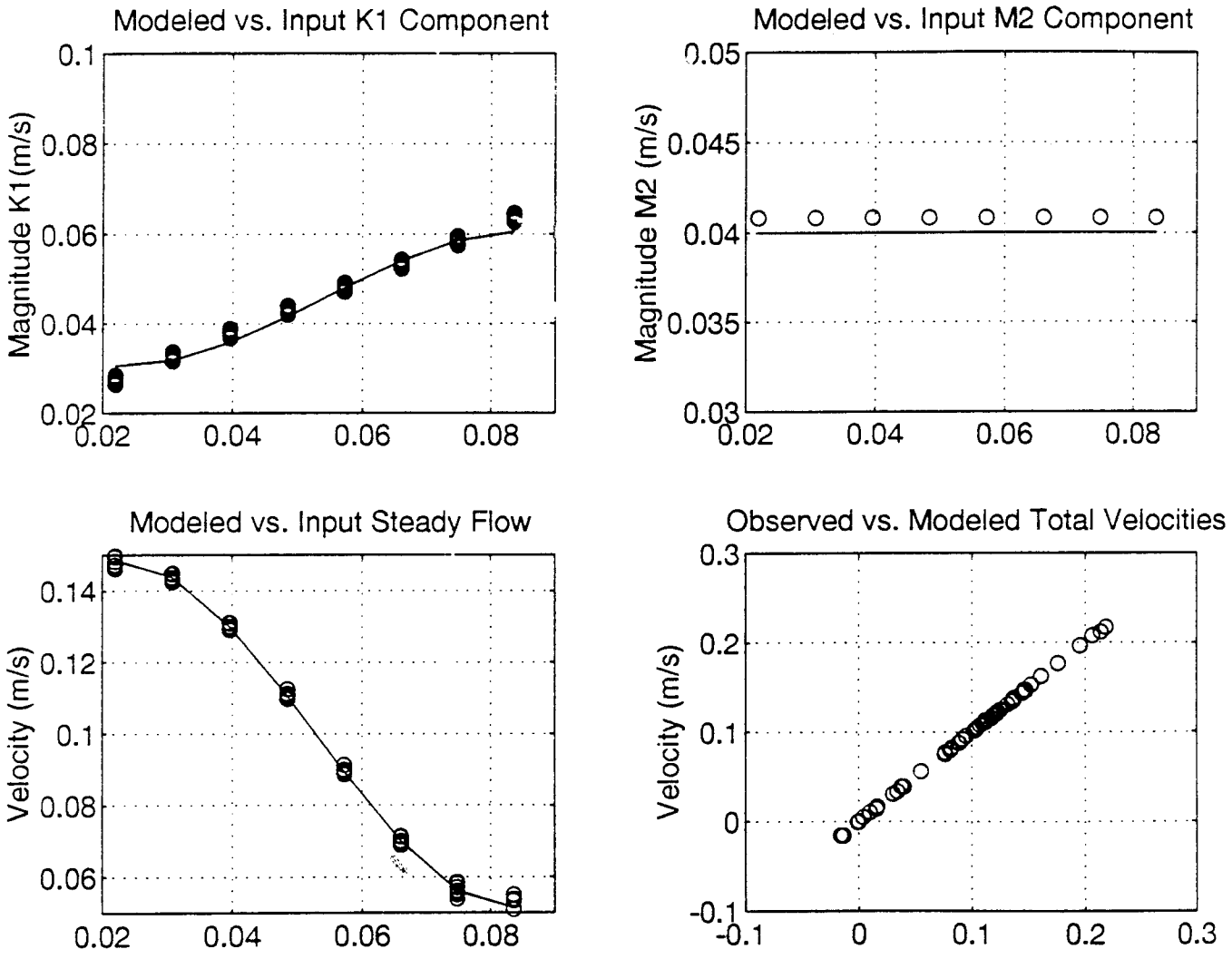

Figure 14. Correlation for specified fit (pm=4, pt=0,1) to Case 4. (a) K1 magnitude. (b) M2 magnitude. (c) Steady flow. (d) Total flow field.

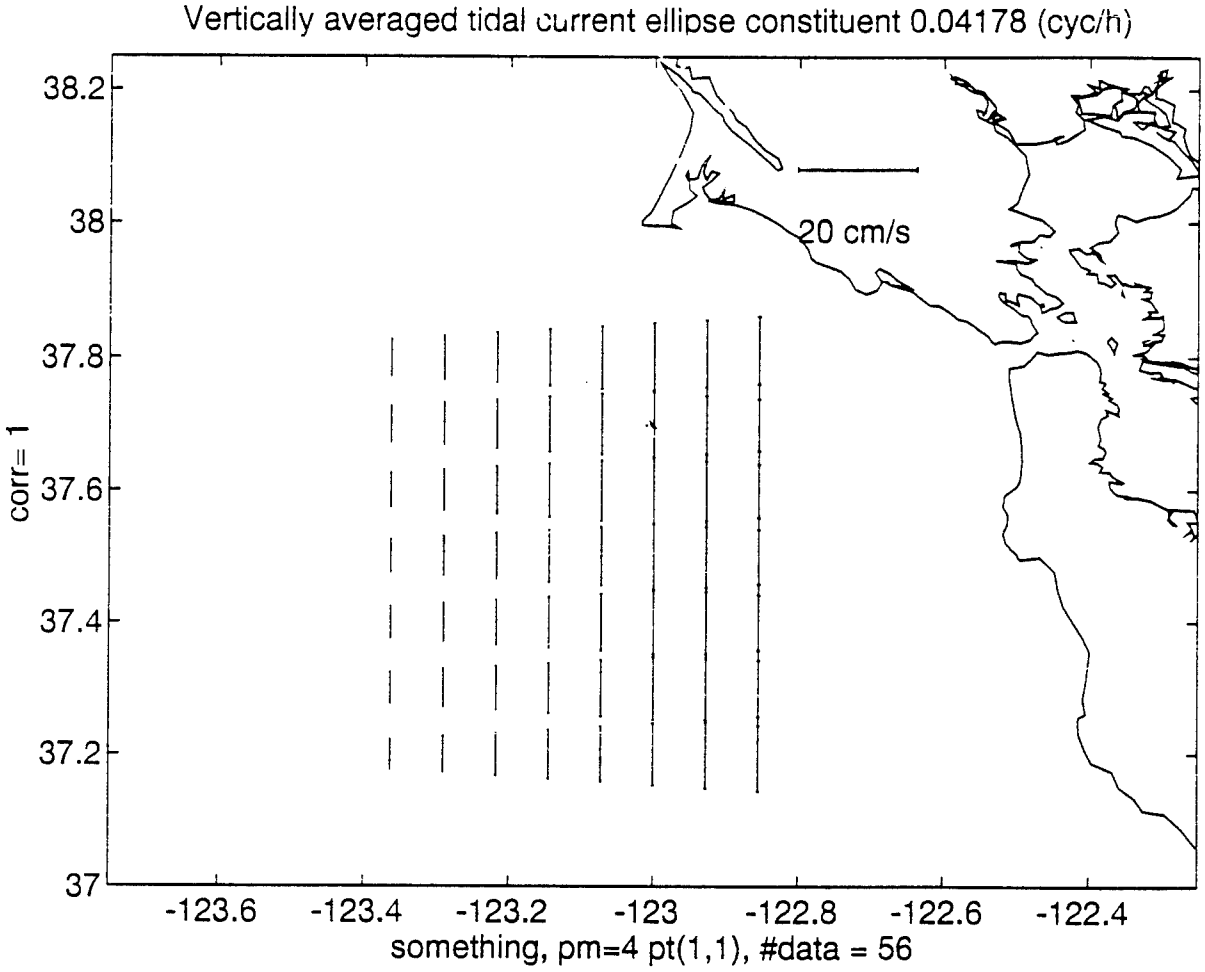

Figure 15a. K1 Tidal ellipse axes for specified polynomial fit (pm=4, pt=1,1) to Case 4.

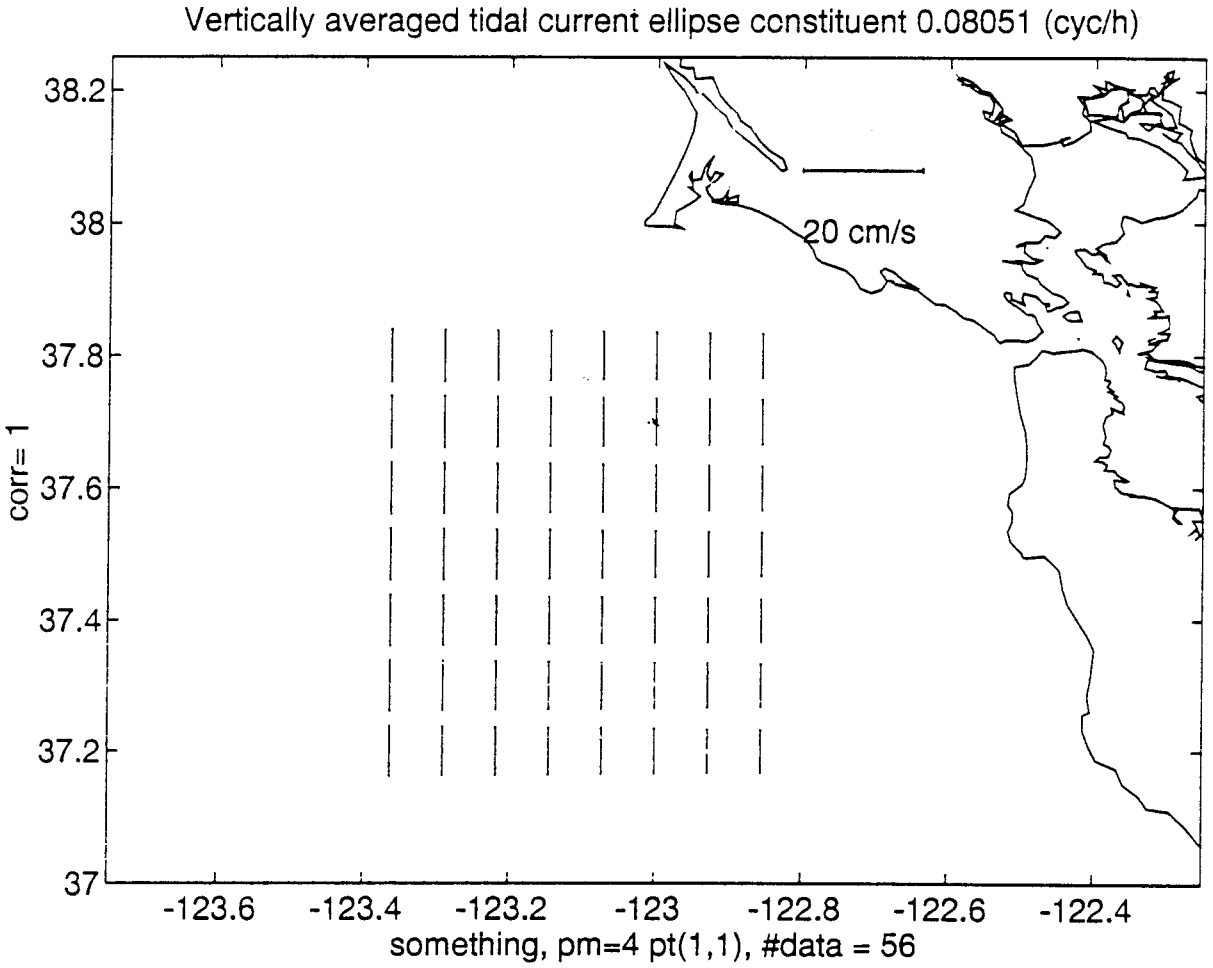

Figure 15b. M2 Tidal ellipse axes for specified polynomial fit (pm=4, pt=1,1) to Case 4.

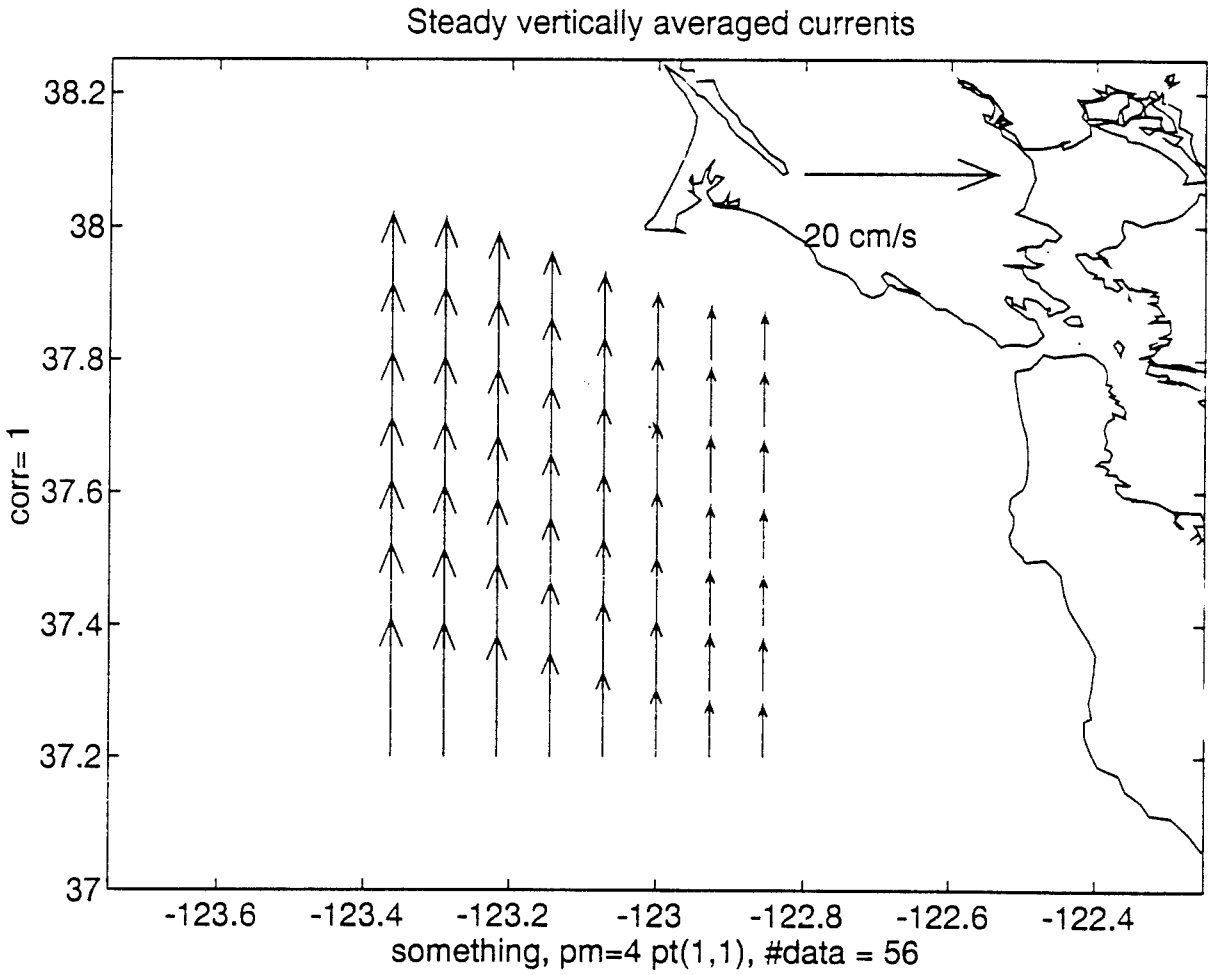

Figure 15c. Steady flow field for specified polynomial fit (pm=4, pt=1,1) to Case 4.

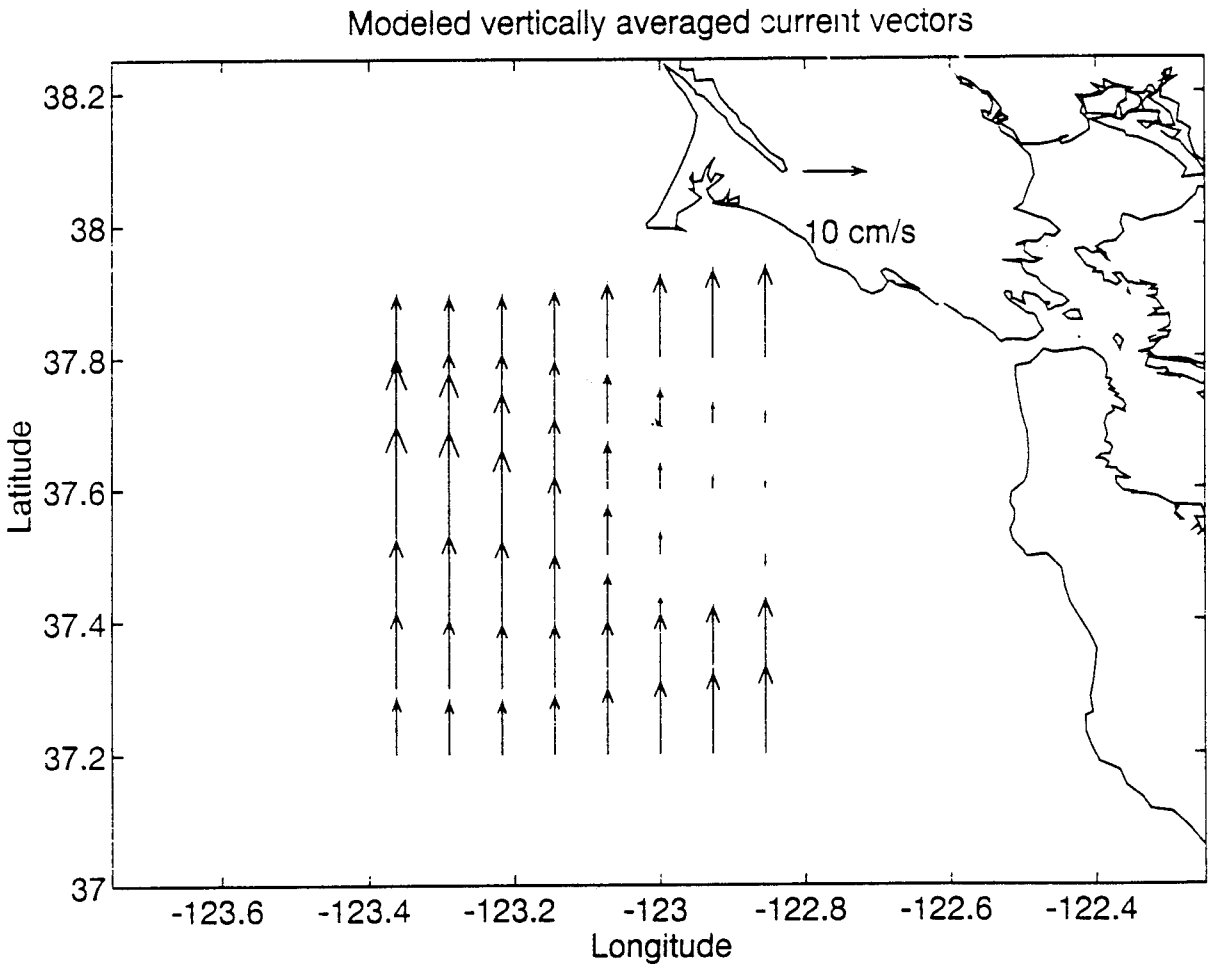

Figure 15d. Modeled total flow field for polynomial fit (pm=4,pt=1,1) to Case 4.

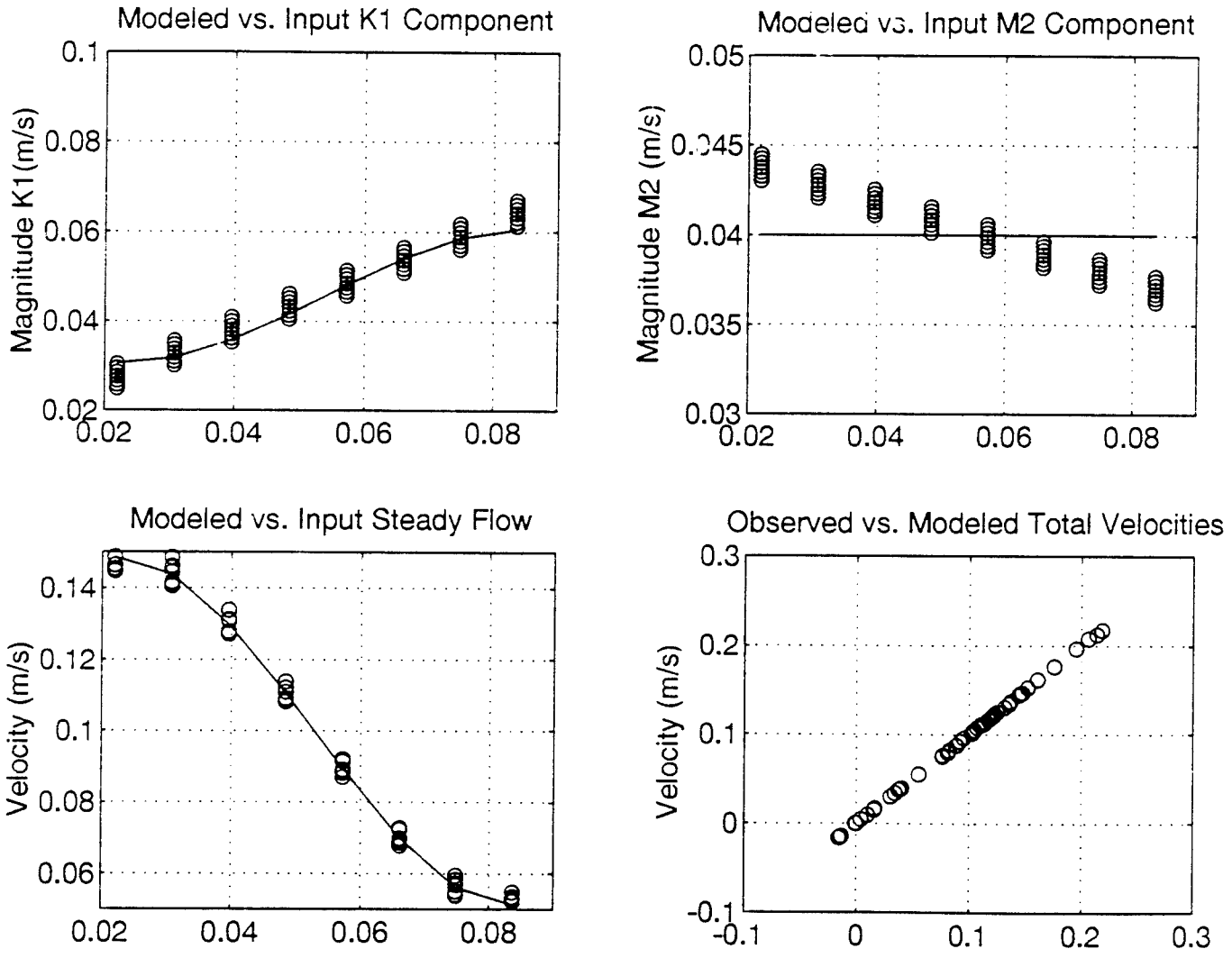

Figure 16. Correlation for specified fit (pm=4, pt=1,1) to Case 4. (a) K1 magnitude. (b) M2 magnitude. (c) Steady flow. (d) Total flow field.

IV. DATA OBSERVATIONS AND PROCESSING

Using the parameter choices determined in the analysis of synthetic data sets, polynomial fitting functions were applied to ADCP data sets from the 1991-92 Farallones study. These data were collected during shipboard cruises of approximately five days each during February, May, August, October/November 1991, and February 1992 .

A. ADCP OBSERVATIONS AND PROCESSING

ADCP data were collected continuously using the hull-mounted ADCP during all five of the cruises. This included five cross-shelf CTD sections and a designated ADCP inner grid labelled a-h (Figure 1). All segments were not run on all of the cruises due to time constraints. Each of the cruises' data were analyzed by 8 m bins and total velocity fields calculated. Along CTD transects, Ramp et al. (1992) noted some turning of the vectors at tidal time scales. This is consistent with the suggestion of spatial variability in current meter observations. Based on these observations, it was decided that a detiding method should be applied to the ADCP data.

1. Initial Processing

Raw ADCP data observations were processed to remove ship's speed and to determine the deepest reliable bin based on bottom depth or Percent Good Return. Each subset (approximately 21 hours of observations) was processed individually and a reference layer three bins wide was chosen. Additionally, these reference layer velocities were smoothed using a low-pass filter and final three-minute averages were obtained (Jessen et al., 1992). Typical good observations in calm seas reached as deep as 400 m over the continental slope.

2. Vertical Averages

The chosen detiding program requires input of net transports at given geographic locations. Spatial averages of 5 km were applied to the previously calculated three-minute

vectors. These vectors were then vertically summed at discrete geographical locations to create an instantaneous transport calculation. Observations collected during the transit to and from the study region were omitted to create a more uniform sample. This yielded approximately 500 observations for each cruises' data record.

B. OTHER OBSERVATIONS

1. CTD Analysis

The dynamic height method was applied to hydrographic data for all cruises. Resulting geopotential height and inferred geostrophic velocities can be used for comparison to velocity fields calculated using the Candela ADCP method. These fields are calculated from 0-200 dbar and 200-500 dbar (Ramp et al., 1992). A comparison to these geostrophic fields can be a useful tool to check the results of the detiding process.

2. Meteorological Observations

Winds are important in the forcing of the upper ocean and were observed at four NDBC buoys throughout the study. Additionally, hourly averaged winds observed from the ***R/V Point Sur*** are presented (Jessen et al., 1992a-d; Rago et al., 1992). Northwesterly winds prevail throughout much of the year.

Shipboard-observed winds varied greatly between each cruise. One of the most notable differences is between the February 1991 and February 1992. During the former cruise, winds were from the northwest (Jessen et al., 1992a) while they were southeasterly during the latter (Jessen et al., 1992d). Winds were generally lighter and more variable during the August and October cruises with speeds often less than 5 m s^{-1}, although the northwesterly component was quite apparent during both periods. (Rago et al., 1992; Jessen et al., 1992c). There were also some observations of onshore winds near the center of the Gulf which is consistent with data from NDBC buoy 46026 (Ramp et al., 1992).

3. Satellite Imagery

Satellite imagery is useful to illustrate some of the features such as eddies, filaments, and the transport of cool upwelled water. Coolest surface temperatures occurred during the May cruise with strong upwelling during that season (Ramp et al., 1992) Some cold filaments are also visible to the north of the Gulf in the vicinity of the persistent upwelling center near Point Reyes. These pictures reaffirm the small scale variability in SST, water masses, and associated current variability in the Gulf.

V. RESULTS

Each of the ADCP data records were processed with the detiding model using linear first-order polynomial functions for the major tidal constituents (M2 and K1) and linear and fourth-order polynomials for the total flow. Tidal results were generally larger in magnitude than representative current meter data, however the ADCP records are much shorter and can only be compared subjectively. Residual flow patterns were reasonably consistent with the expected seasonal variations. Each cruise is represented with the raw, undetided ADCP observations and the model output sub-tidal flow fields.

A. FEBRUARY 1991

Currents appear to be directed mostly poleward along the shelf and are aligned with the bathymetry to a significant degree. Shelf observations are variable in direction with some onshore component on the inner part of the shelf. The undetided, barotropic velocities are given in Figure 17a. Calculated non-tidal flow illustrates two distinct regimes separated by the shelf break. Both the linear (Figure 17b) and higher-order fits (Figure 17c) agree with the general flow pattern but differ in magnitude. Poleward flow on the slope is representative of a combination of the CUC and Davidson currents (Hickey, 1979). The shelf regime is consistent with shipboard winds that were predominantly northwesterly and strong (about 10 - 20 cm s^{-1}) throughout the entire period.

B. MAY 1991

This cruise is representative of the prime upwelling season in and around the Gulf. Observations were more variable making the fitting of the observed undetided field more difficult (Figure 18a). Higher polynomial fits resulted in exaggerated tidal amplitudes and

resultant non-tidal flow. Wind-driven shelf circulation is apparent with a significant offshore transport component including near the northerly part of the region (Figure 18b) when modeled with a first-order fit. Fourth-order choice for the mean flow (Figure 18c) yields a noisier residual field with stronger velocities on the shelf than the lower-order fit. Flow is predominantly poleward over much of the slope. The decreasing magnitude in the northwestern quadrant is at least partially due to the choice of polynomial weighted by the inshore observations with equatorward components.

C. AUGUST 1991

Strongest poleward flow was apparent in these data (Figures 19a,b). Winds were less upwelling-favorable than during the previous May cruise and shelf velocities were weak and mixed in direction. The use of the fourth-order for this case is advantageous over a simple linear fit since the strong poleward values would give an unrepresentative strong poleward component to the weak shelf currents (Figure 19c). This cyclonic turning of the shelf flow field is similar to results from August 1990 (Gezgin, 1991) using interpolated current meter data to detide ADCP observations.

D. OCTOBER 1991

The greatest variability in observations and modeled values were observed for this cruises data. The correlation between the observed ADCP field and modeled undetided field was poor leading to a lack of confidence in the model's handing of this data set. Total field (Figure 20a), and residual flows (Figure 20b,c) have overall weak correlation. This is likely due to the interaction from an offshore eddy (Ramp et al., 1992) that is not resolved well by the use of these simple polynomials.

E. FEBRUARY 1992

This was a cruise marked by strong winds associated with passing cyclones. Nearly all shelf and slope observations contain a poleward component. Observations are given in Figure 21a with the associated modeled sub-tidal currents in Figure 21b,c. Slope flow is consistent with previous assumptions about the CUC and Davidson current with the shelf flow largely wind-driven. There is slightly more spatial variability of the mean current implied by the higher-order polynomial.

F. DISCUSSION

Variability between each of the cruises agrees with the presumption of seasonal dependence of the non-tidal velocity field. The overall best fit, measured by the correlation of the observed versus modeled total flow (corr), occurs when the direction of flow is uniform or slowly spatially varying. Confidence in the representation of more complex flow regimes such as May (upwelling) and October (presence of an offshore eddy) is somewhat decreased. A better measure of the performance of the model would help to quantify the confidence level. Additionally, the best choice of polynomial fitting function will not necessarily be the same for each cruise.

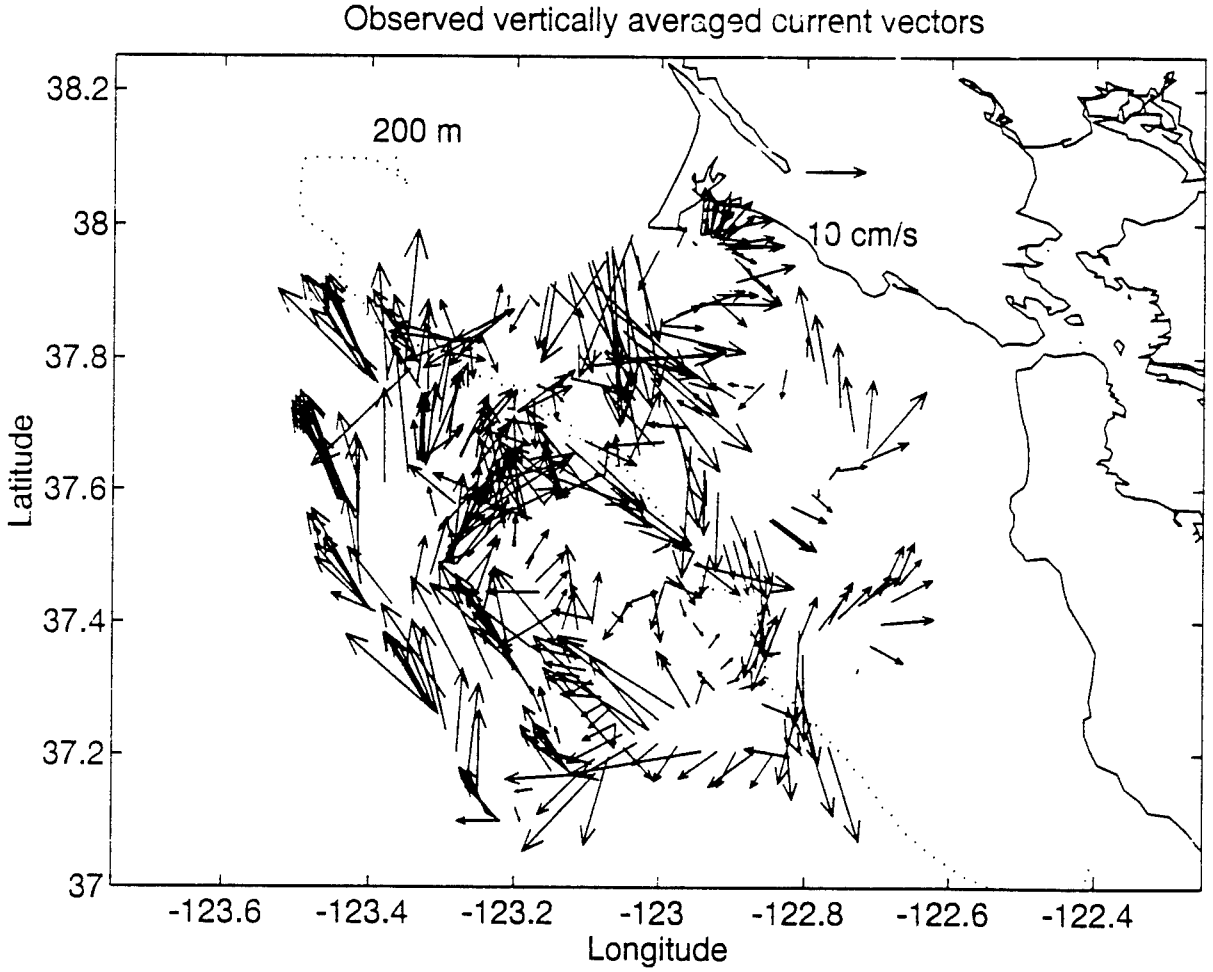

Figure 17a. Observed ADCP velocities collected during February 1991 cruise.

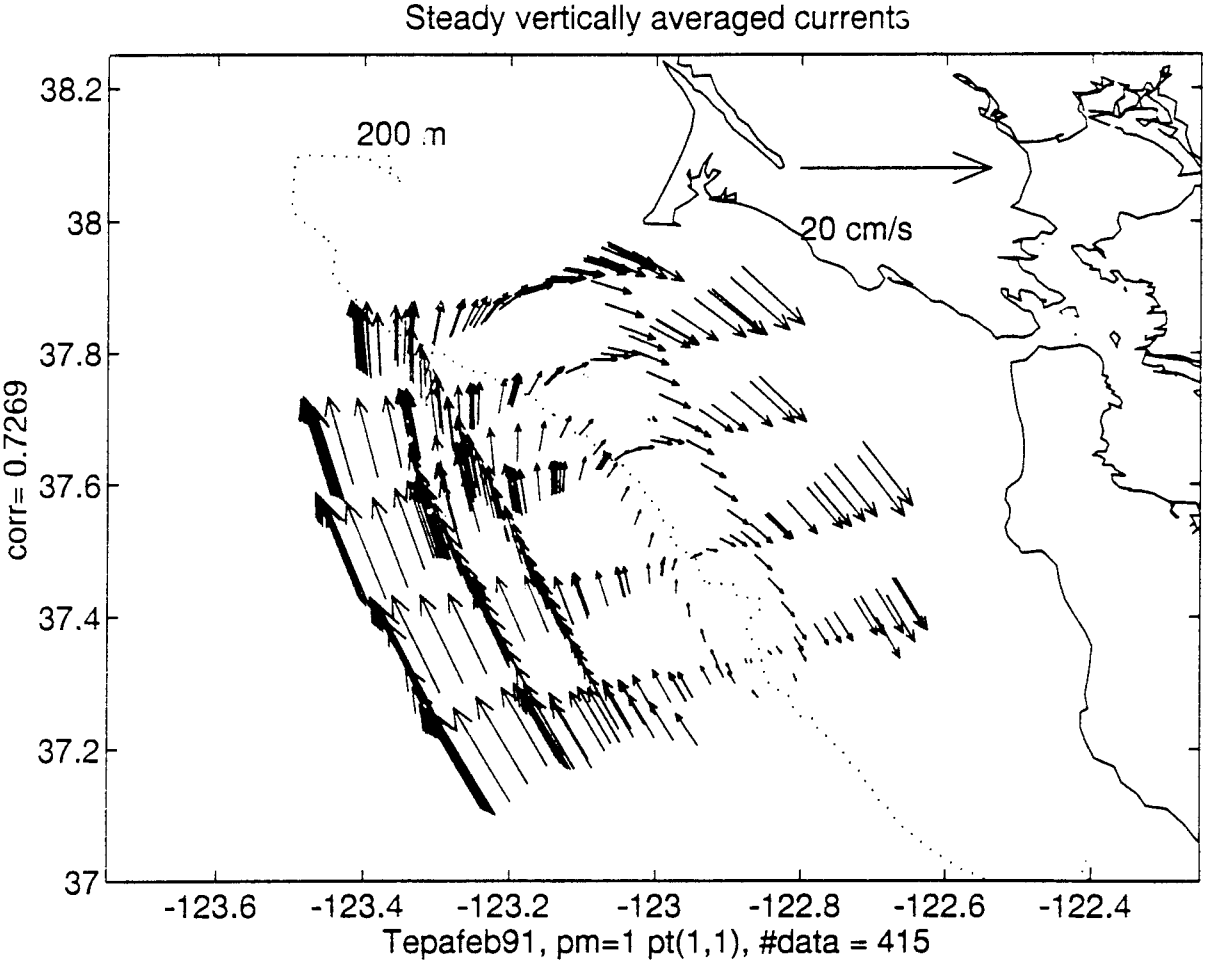

Figure 17b. Steady flow field for February 1991 cruise using a first-order polynomial to fit the mean flow (pm=1) and first-order polynomials to fit the M2 and K1 tidal constituents (pt=1,1).

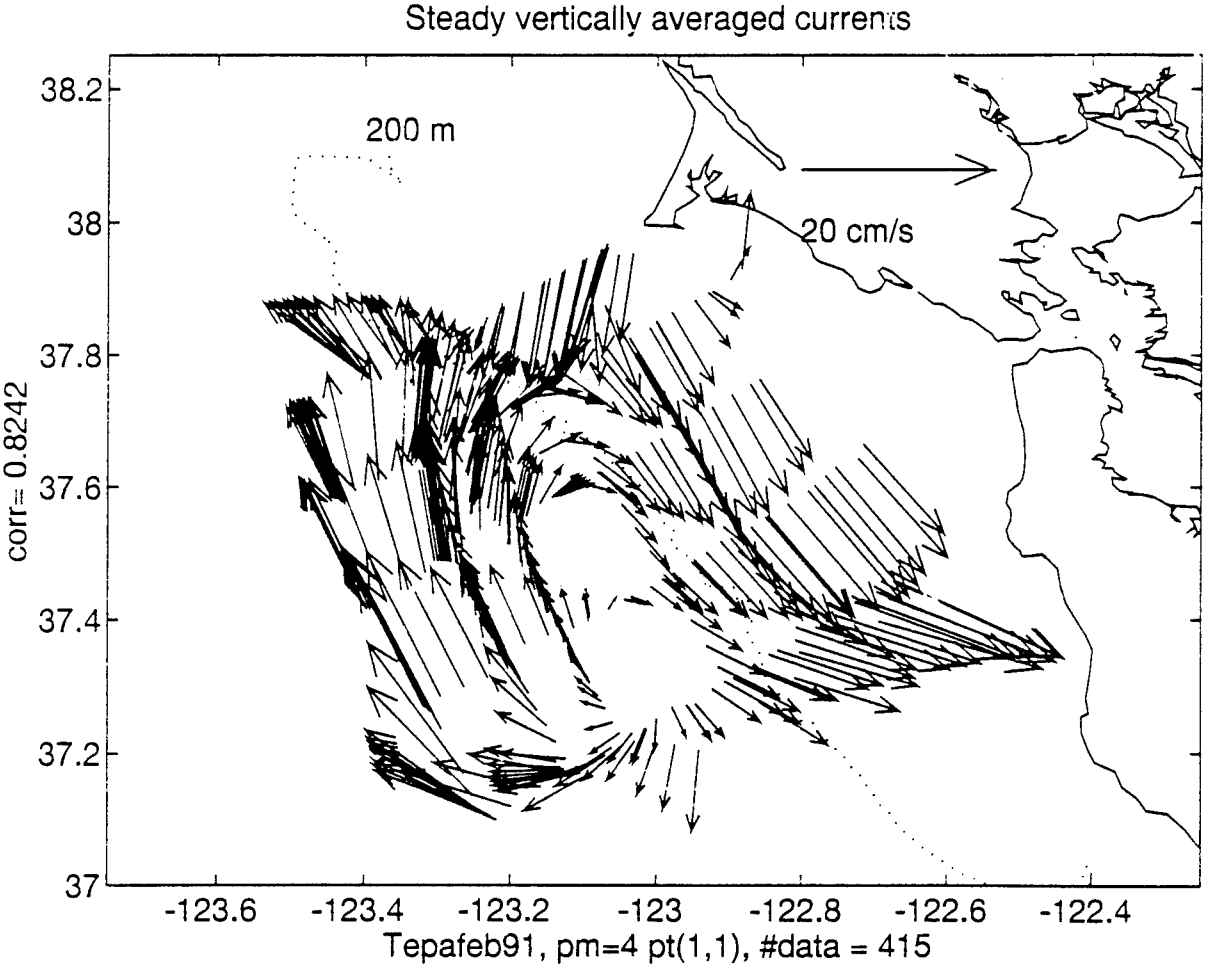

Figure 17c. Steady flow field for February 1991 cruise using a fourth-order polynomial to fit the mean flow (pm=4) and first-order polynomials to fit the M2 and K1 tidal constituents (pt=1,1).

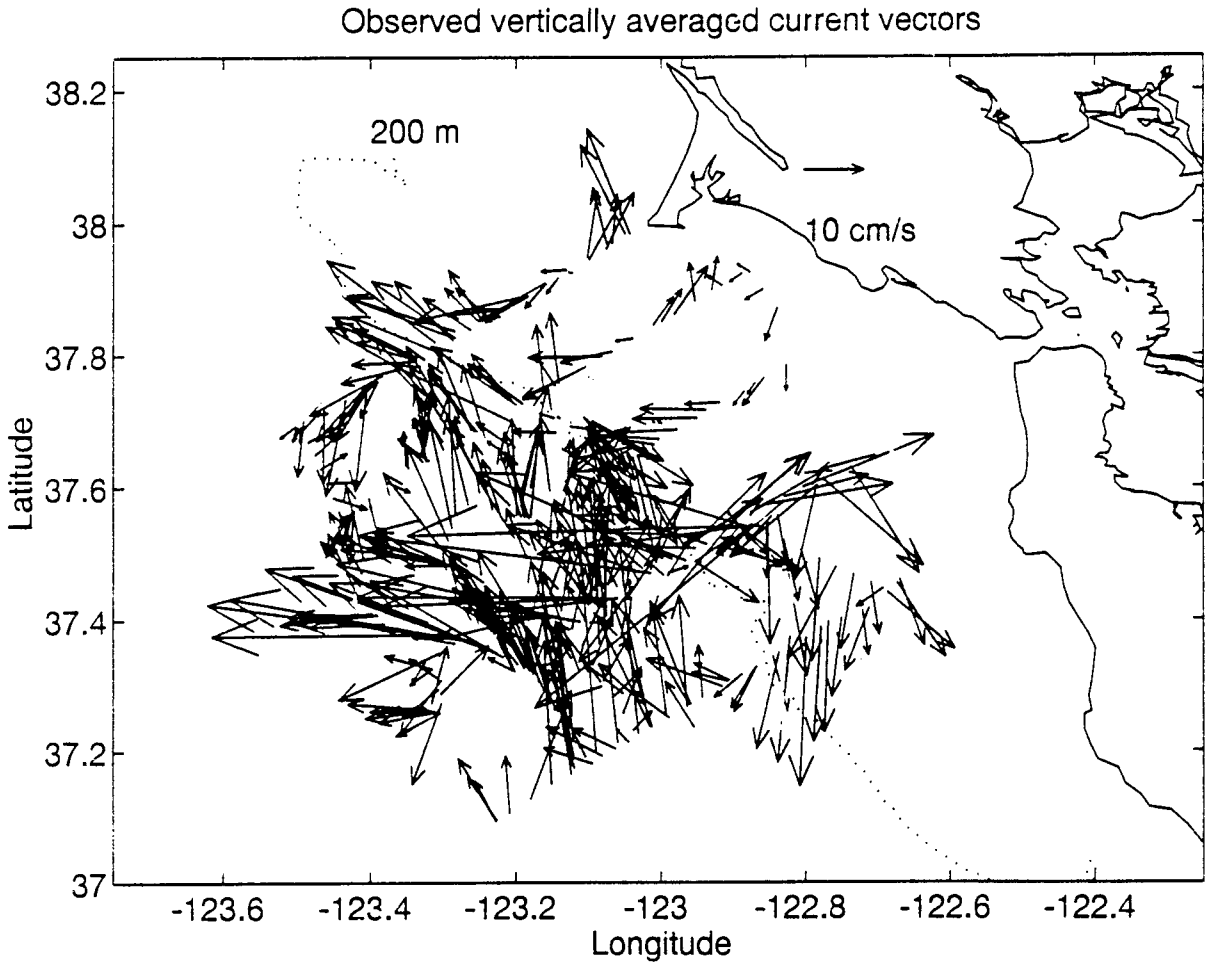

Figure 18a. Observed ADCP velocities collected during May 1991 cruise.

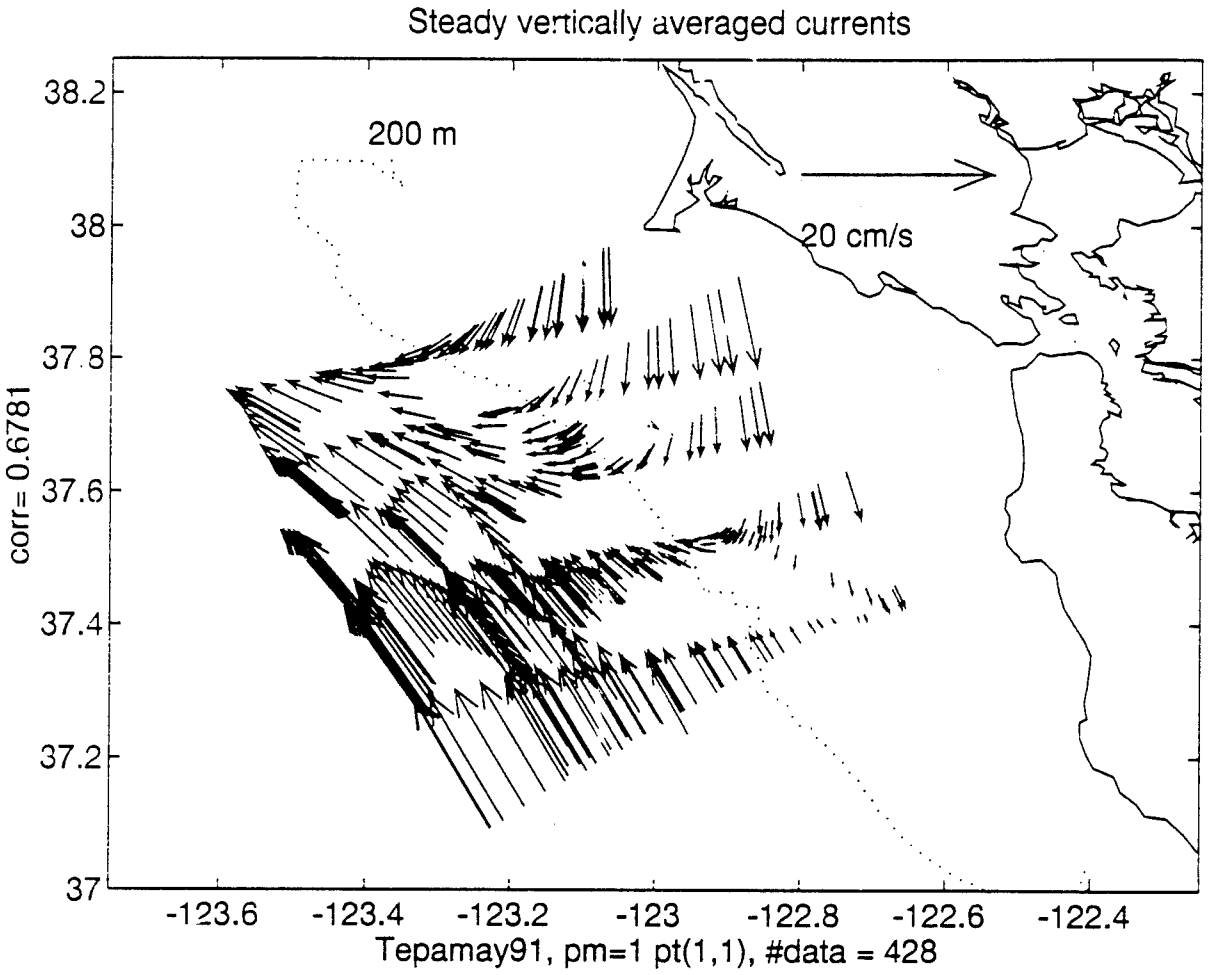

Figure 18b. Steady flow field for May 1991 cruise using a first-order polynomial to fit the mean flow (pm=1) and first-order polynomials to fit the M2 and K1 tidal constituents (pt=1,1).

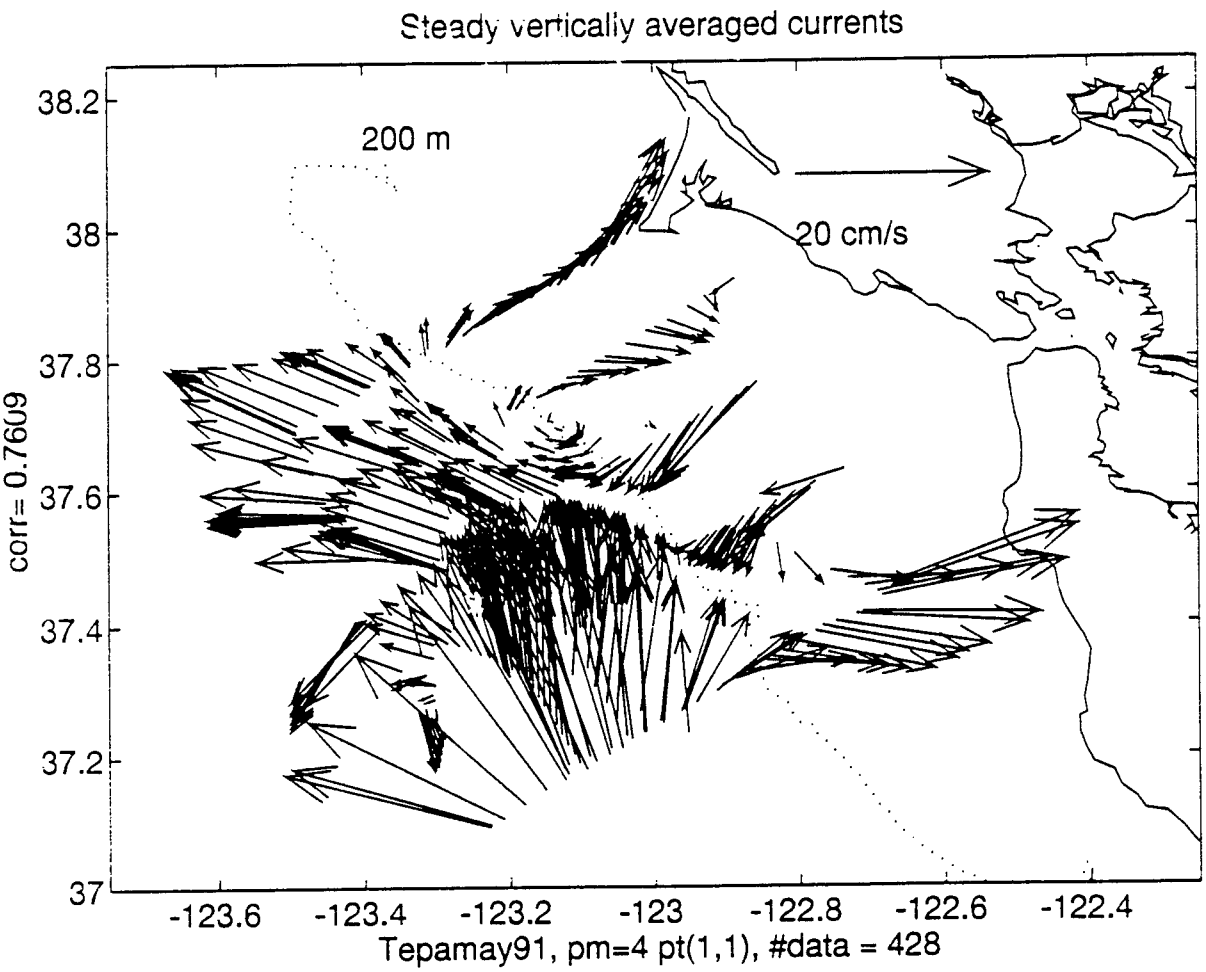

Figure 18c. Steady flow field for May1991 cruise using a fourth-order polynomial to fit the mean flow (pm=4) and first-order polynomials to fit the M2 and K1 tidal constituents (pt=1,1).

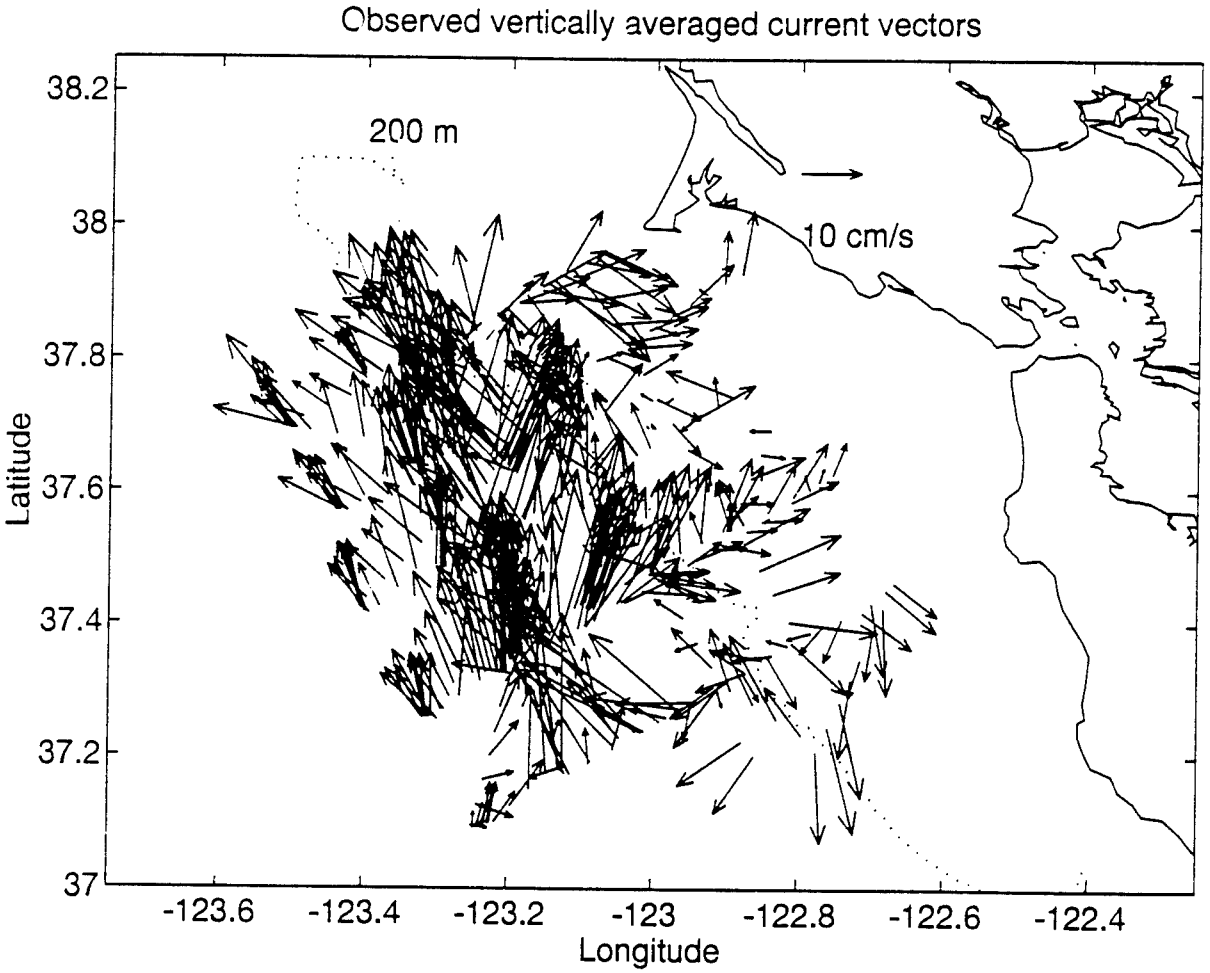

Figure 19a. Observed ADCP velocities collected during August 1991 cruise.

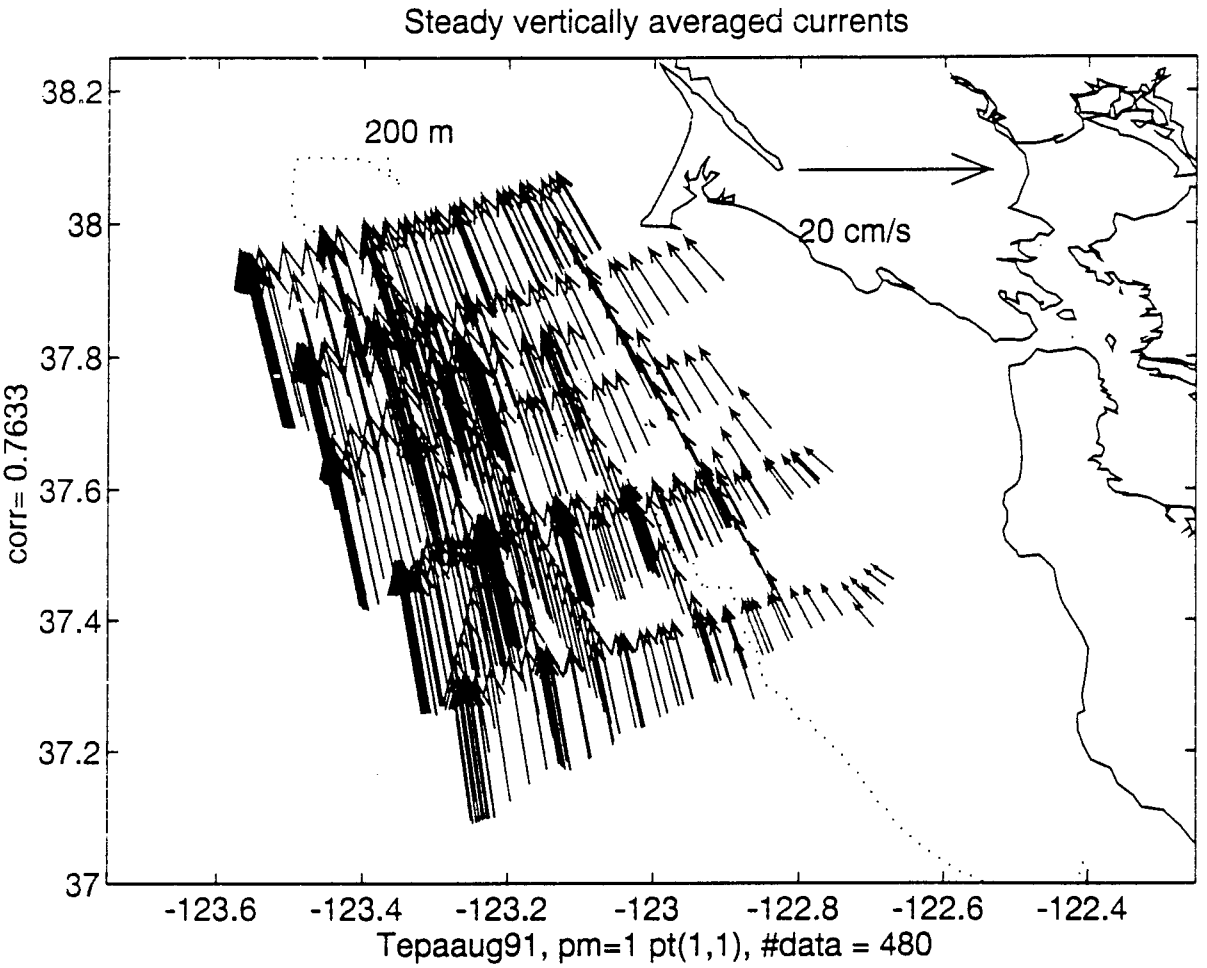

Figure 19b. Steady flow field for August 1991 cruise using a first-order polynomial to fit the mean flow (pm=1) and first-order polynomials to fit the M2 and K1 tidal constituents (pt=1,1).

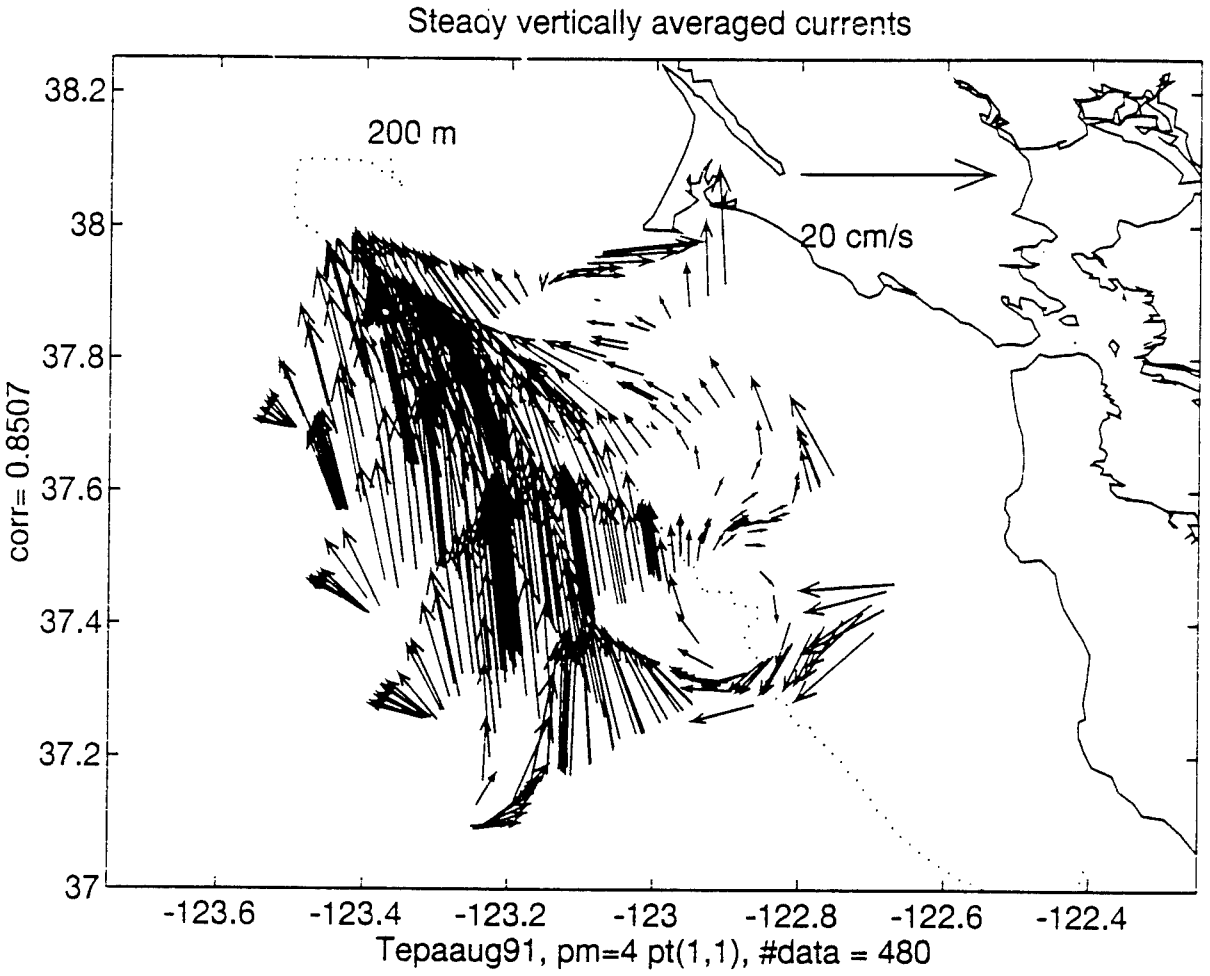

Figure 19c. Steady flow field for August 1991 cruise using a fourth-order polynomial to fit the mean flow (pm=4) and first-order polynomials to fit the M2 and K1 tidal constituents (pt=1,1).

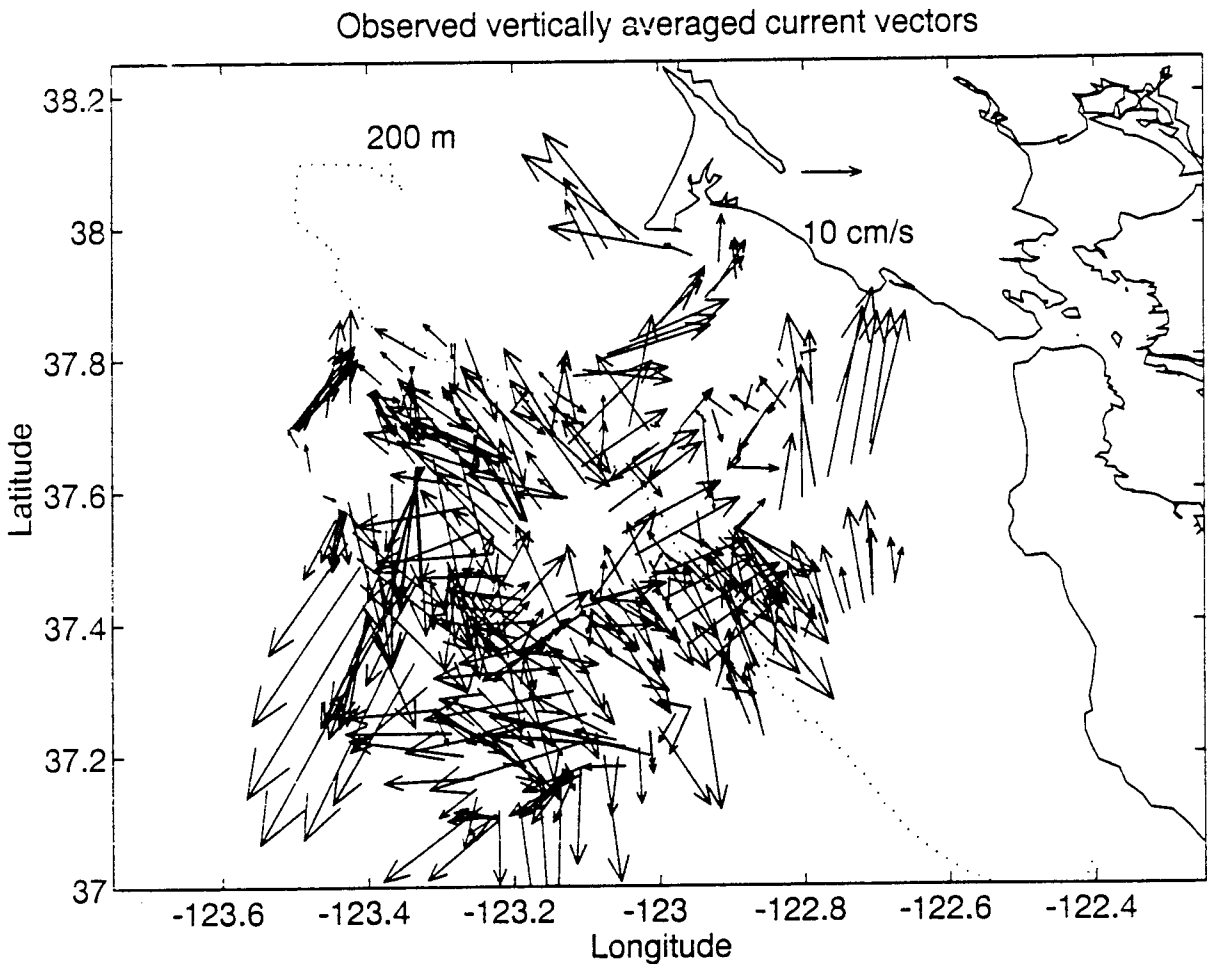

Figure 20a. Observed ADCP velocities collected during October 1991 cruise.

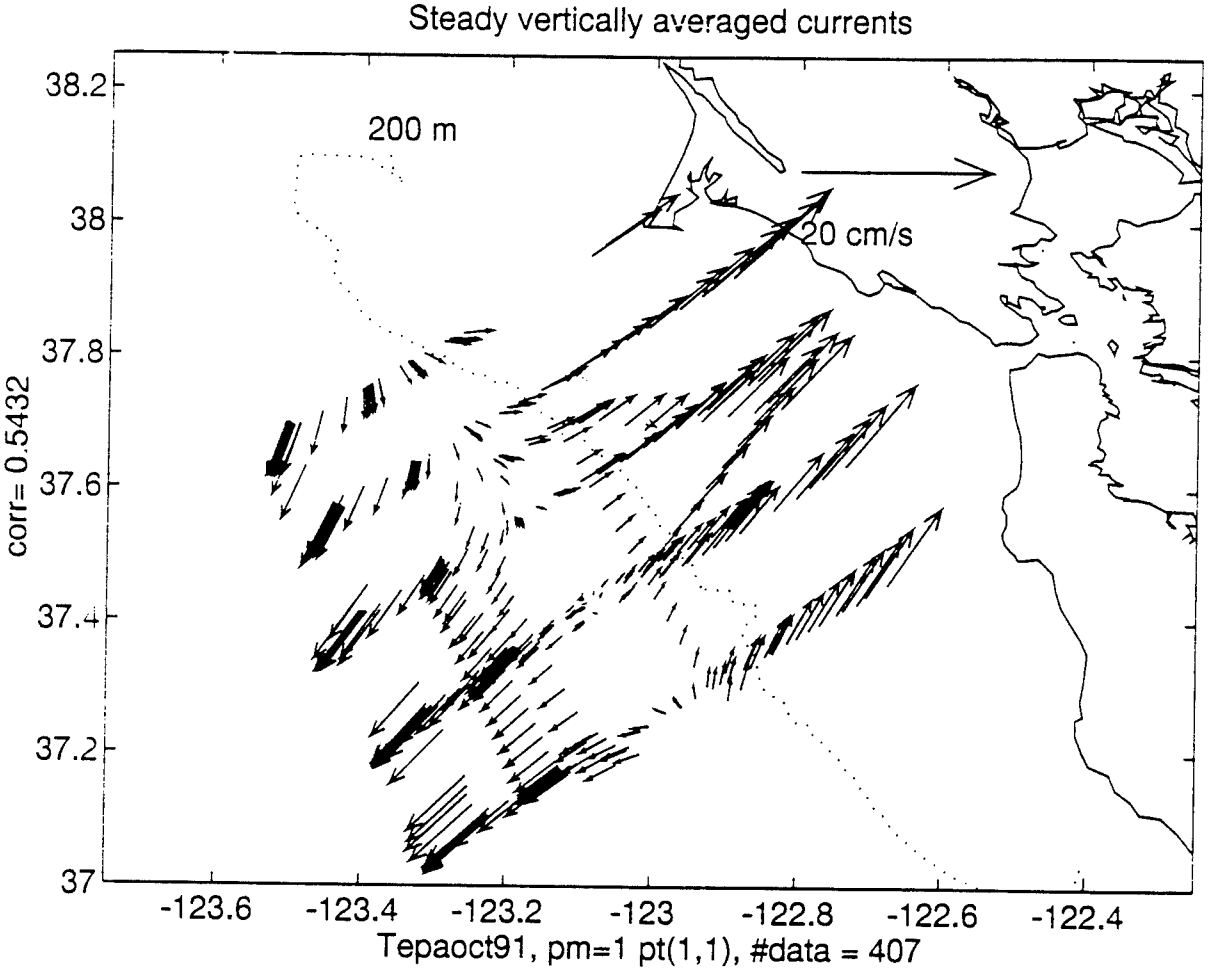

Figure 20b. Steady flow field for October 1991 cruise using a first-order polynomial to fit the mean flow (pm=1) and first-order polynomials to fit the M2 and K1 tidal constituents (pt=1,1).

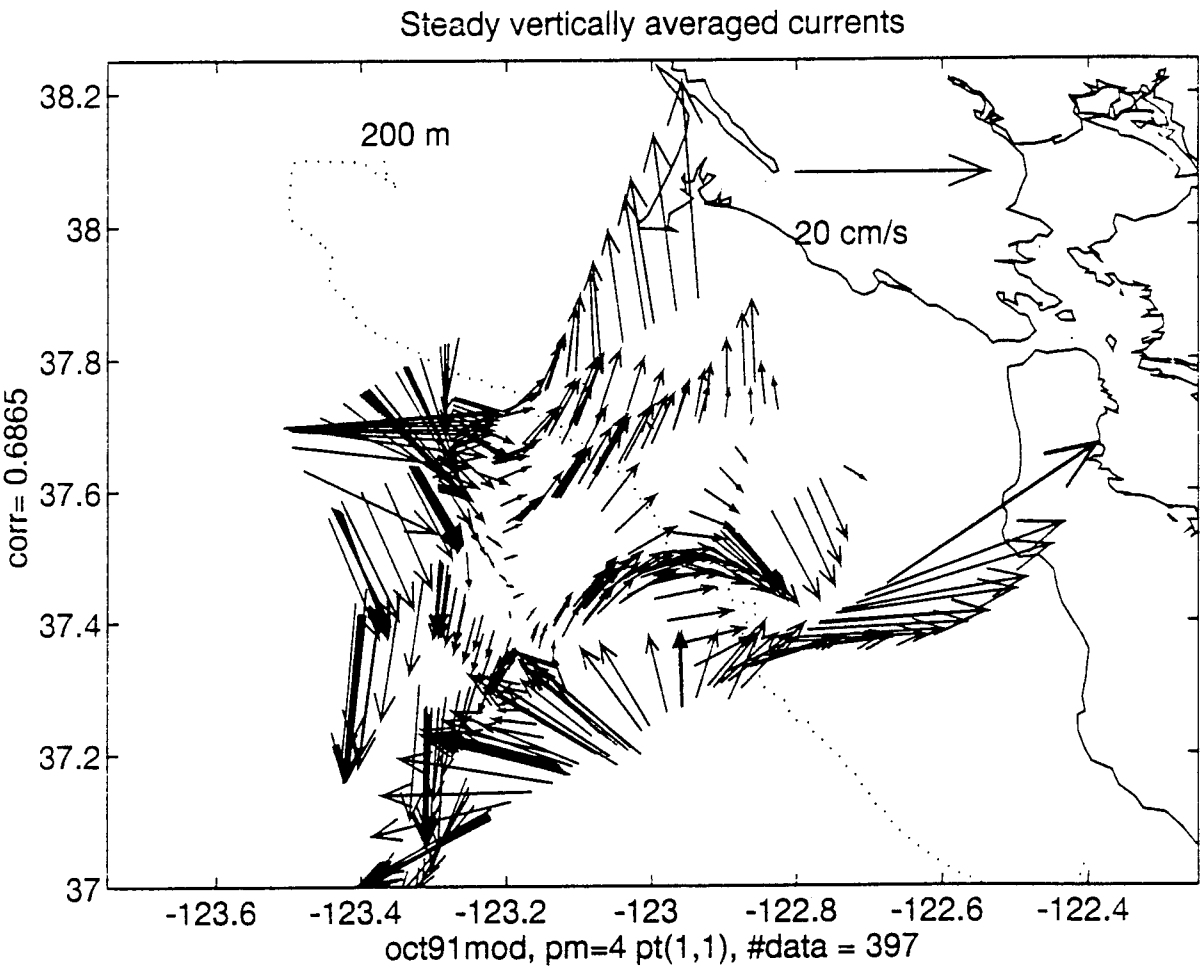

Figure 20c. Steady flow field for October 1991 cruise using a fourth-order polynomial to fit the mean flow (pm=4) and first-order polynomials to fit the M2 and K1 tidal constituents (pt=1,1).

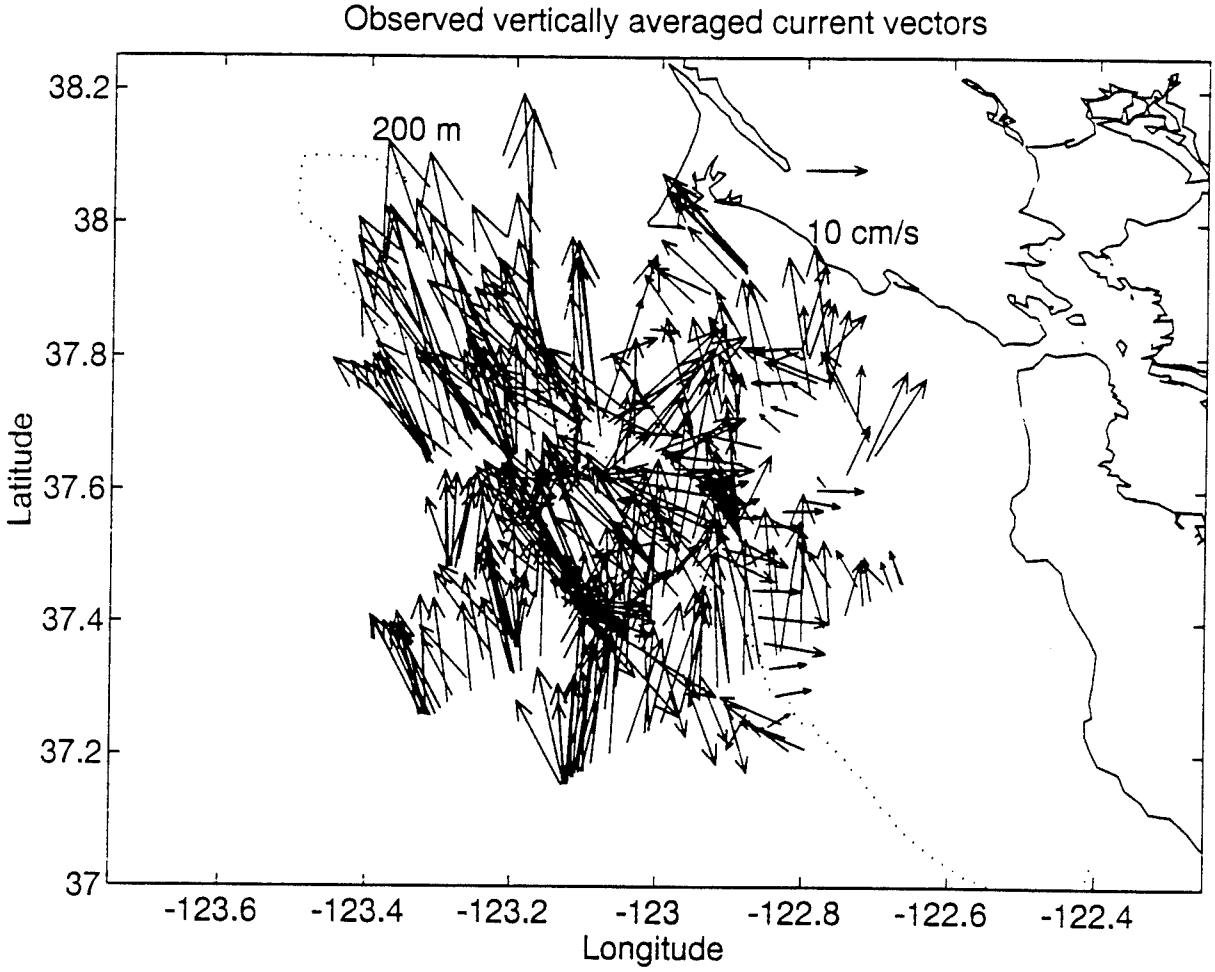

Figure 21a. Observed ADCP velocities collected during February 1992 cruise.

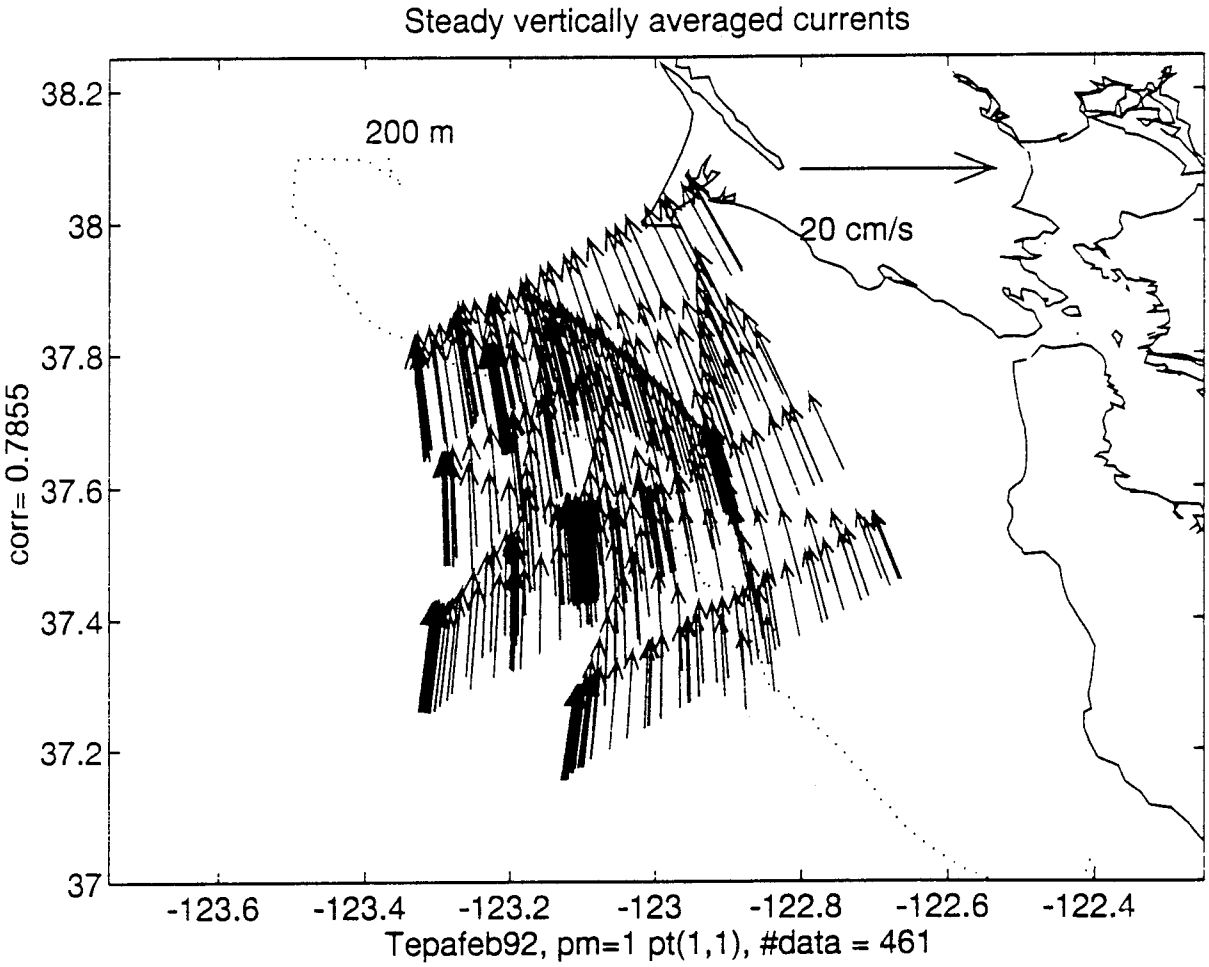

Figure 21b. Steady flow field for February 1992 cruise using a first-order polynomial to fit the mean flow (pm=1) and first-order polynomials to fit the M2 and K1 tidal constituents (pt=1,1).

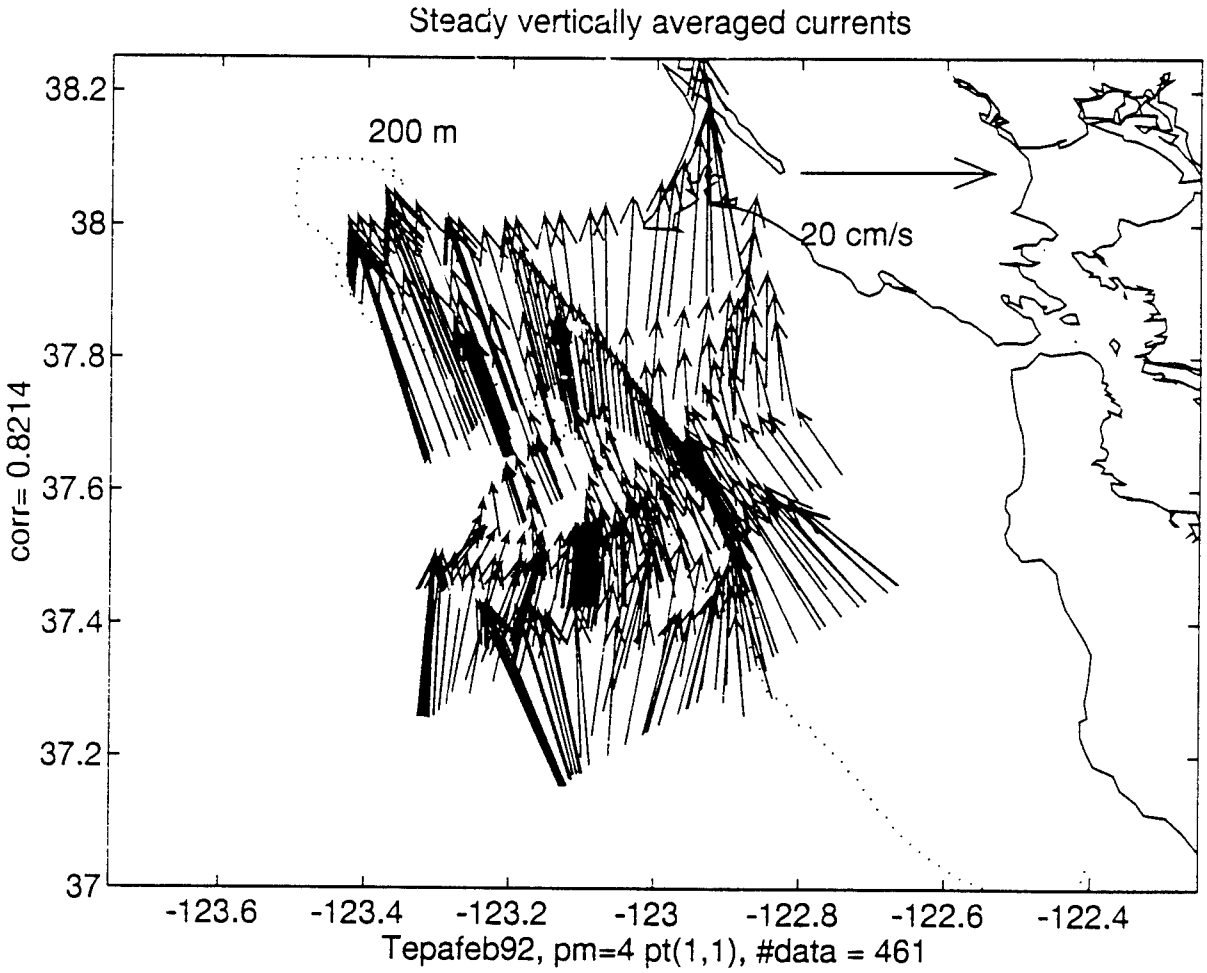

Figure 21c. Steady flow field for February 1992 cruise using a fourth-order polynomial to fit the mean flow (pm=4) and first-order polynomials to fit the M2 and K1 tidal constituents (pt=1,1).

VI. CONCLUSIONS

A. SUMMARY

The Gulf of the Farallones is a region over the upper continental slope and shelf where the tidal and non-tidal current fields vary considerably both spatially and temporally. To better understand this variability, ADCP data from five cruises throughout a year were examined. Assuming a barotropic flow by vertically averaging these data, a spatial interpolation scheme using simple polynomials was investigated by using synthetic data designed to represent the presumed spatial variability of the flow in the region. The method was then applied to the data from each of the cruises to produce a representation of the non-tidal flow field.

Choosing a scheme to represent components of a velocity field which has significant spatial variation can be a difficult proposition. Polynomials specified in the detiding method should not be arbitrarily specified but chosen based on knowledge of the spatial structure of the surveyed region's tidal and non-tidal circulation. Specifically, selecting too high of a polynomial fit in any model component leads to overfitting of the tides and mean flow characterized by misallocation of energy into other components. This is particularly critical in the tidal constituents. For the Gulf of the Farallones, it is best to use a least squares fit to a linear function because a larger order polynomial may yield unrealistic representations of the magnitude of the constituent. There is not a single best choice of fitting function for steady flows but higher order choices tend to better represent the observations. The best solution appears to be to choose linear polynomials for each of the tidal constituents and increase the order of the fit to the steady flow.

This is a detiding method, not a tidal prediction model, for this region with the current model configuration. To arrive at a reasonable physical fit of the circulation, a realistic estimate of tidal constituent amplitudes should be achieved. Additionally, high correlation between the observed and modelled total flow as well as individual model

components is necessary. The detiding method does not have a quantifiable confidence estimate nor error estimation built in to indicate to the user the skill level at which the model is performing. When analyzing the model output, the magnitude and direction of the tides may provide a qualitative estimate of performance, in comparison to moored results, but most tidal records are much longer than survey data sets. Significant modulation of the amplitude and phase of the tidal constituents could be present given the length of the records. Furthermore, tidal records at single moored stations show nothing about spatial variability, making it more difficult to make the proper choice of the tides. Output tidal information should be treated as noise in representative frequency bands.

The most important result of this process is the production of an estimation of the non-tidal or steady flow. However, it is only an instantaneous representation of the non-tidal flow and temporal variability can be expected on synoptic through interannual time scales. Results from the various cruises examined show some agreement with the expected seasonal variation of this field.

B. RECOMMENDATIONS

Confidence in the use of this method must be improved to make it more easily applicable to data sets in the Gulf and elsewhere. Some steps that can be taken to validate it include computation of volume and salt budgets using the calculated non-tidal flows from each of the cruises. Second, current meter observations may be integrated into the ADCP record to create a larger sample size which may improve the overall representation of the tides and the non-tidal flow.

This method should not be uniformly applied to ADCP data sets without some prior knowledge of the surveyed area such as hydrography, current meters, satellite imagery, and/or surface and sub-surface drifting buoys. If there is reasonable confidence that the individual components of the flow field can be represented by polynomials, a good estimate of the velocity or transport fields should result.

Future work should include a direct comparison of techniques using common data sets (Gezgin, Steiner). Ideally, the technique would be used in conjunction with a numerical tidal model to aid in the prediction of each of the components. This technique has the potential to be applicable in many coastal regions if some knowledge of the area is available along with some method of quantitatively demonstrating confidence in the solutions of the model.

LIST OF REFERENCES

Candela, J., Beardsley, R.C., and Limeburner, R., "Removing Tides from Ship-Mounted ADCP Data, with Application to the Yellow Sea," *IEEE Fourth Conference on Current Measurements,* pp. 258-266, 1990.

Candela, J., Beardsley, R.C., and Limeburner, R., "Separartion of Tidal and Subtidal Currents in Ship-Mounted Acoustic Doppler Current Profiler Observations," *J. Geophys. Res.,* v.97, no. C1, pp. 769-788, 1992.

Chelton, D.B., "Seasonal Variability of Alongshore Geostrophic Velocity Off Central California," *J. Geophys. Res.,* v. 89, no. C3, pp. 3473-3486, 20 May 1984.

Chelton, D.B., Bratkovich, A.W., Bernstein, R.L., and Kosro, P.M., "Poleward Flow off Central California During the Spring and Summer of 1981 and 1984," *J. Geophys. Res.,* v. 93, no.C9, pp. 10604-10620, 15 September 1988.

Foreman, M.G.G., *Manual for Tidal Heights Analysis and Prediction*, Institute of Ocean Sciences, Victoria, BC, 1978.

Foreman, M.G.G., and Freeland, H.J., "A Comparison of Techniques for Tide Removal from Ship-Mounted Acoustic Doppler Measurements along the Southwest Coast of Vancouver Island," *J. Geophys. Res.,* v. 96, pp. 17,007-17,021, 1991.

Gezgin, E., "A Study on Hydrographic Conditions and Salt Budget for the Gulf of the Farallones with the Data Collected in August 1990," Master's Thesis, Naval Postgraduate School, Monterey, California, March 1991.

Hickey, B.M., "The California Current System - Hypotheses and Facts," *Progress in Oceanography*, v.8, pp. 191-279, 1979.

Huyer, A., "Coastal Upwelling in the California Current System," *Prog. Oceanog.,* v.12, pp. 259-284, 1983.

Jessen, P.F., Ramp, S.R., Collins, C.A., Garfield, N., Rosenfeld, L.K., and Schwing, F.B., "Hydrographic and Acoustic Doppler Current Profiler (ADCP) Data from the Gulf of the Farallones Shelf and Slope Study 13-18 February 1991," Naval Postgraduate School Technical Report NPS-OC-92-003, Monterey, CA, 1992a.

Jessen, P.F., Ramp, S.R., Collins, C.A., Garfield, N., Rosenfeld, L.K., and Schwing, F.B., "Hydrographic and Acoustic Doppler Current Profiler (ADCP) Data from the Gulf of the Farallones Shelf and Slope Study 16-21 May 1991," Naval Postgraduate School Technical Report NPS-OC-92-004, Monterey, CA, 1992b.

Jessen, P.F., Ramp, S.R., Collins, C.A., Garfield, N., Rosenfeld, L.K., and Schwing, F.B., "Hydrographic and Acoustic Doppler Current Profiler (ADCP) Data from the Gulf of the Farallones Shelf and Slope Study 29 October-3 November 1991," Naval Postgraduate School Technical Report NPS-OC-92-007, Monterey, CA, 1992c.

Jessen, P.F., Ramp, S.R., Collins, C.A., Garfield, N., Rosenfeld, L.K., and Schwing, F.B., "Hydrographic and Acoustic Doppler Current Profiler (ADCP) Data from the Gulf of the Farallones Shelf and Slope Study 7-17 February 1992," Naval Postgraduate School Technical Report NPS-OC-92-005, Monterey, CA, 1992d.

Kinoshita, K., Noble, M., and Ramp S.R., "The Farallones Moored Array Data Report," U.S. Geological Survey, Menlo Park, CA, 1992.

Munchow, A., R.W. Garvine, and T.F. Pfeiffer, "Subtidal Currents from a Shipboard Acoustic Doppler Current Profiler in Tidally Dominated Waters," *Continental Shelf Research,* v.12, pp. 499-515, 1992.

Noble, M. and Gelfenbaum, G., "A Pilot Study of Currents and Suspended Sediment in the Gulf of the Farallones," U.S. Geological Survey Open-File Report 90-471, U.S. Geological Survey, Menlo Park, CA, 1990.

Noble, M., Personal communication, U.S. Geological Survey, Menlo Park, CA, 1994.

Officer, C.B., *Phsical Oceanography of Estuaries (and Associated Coastal Waters),* John Wiley and Sons, 1976.

Pond, S. and G.L. Pickard, *Introductory Dynamical Oceanography,* second edition, Pergamon Press, 1983.

Rago, T.A., Rosenfeld, L.K., Jessen, P.F., Ramp, S.R., Collins, C.A., Garfield, N., and Schwing, F.B., "Hydrographic and Acoustic Doppler Current Profiler (ADCP) Data from the Gulf of the Farallones Shelf and Slope Study 12-18 August 1991," Naval Postgraduate School Technical Report NPS-OC-92-006, Monterey, CA, 1992.

Ramp, S.R., Garfield, N., Collins, C.A., Rosenfeld, L.K., and Schwing F.B., "Circulation Studies Over the Continental Shelf and Slope Near the Farallon Islands, CA: Executive Summary," Naval Postgraduate School, Monterey, CA, 1992.

Sandwell, D.T., "Biharmonic Spline Interpolation of Geos-3 and Seasat Altimeter Data," *Geophys. Res. Lett.,* v.14 pp. 139-142, 1987.

Schwing, F.B., Husby, D.M., Garfield, N., and Tracy, D.E., "Mesoscale Oceanic Response to Wind Events off Central California in Spring 1989: CTD Surveys and AVHRR Imagery, " *CalCOFI Rep.*, v.32, 1991.

Strub, P.T., Allen, J.S., Huyer, A., Smith, R.L., and Beardsley, R.C., " Seasonal Cycles of Currents, Temperatures, Winds, and Sea Level over the Northwest Pacific Continental Shelf 35° N to 48° N," *J. Geophys. Res.,* v. 92, pp. 1507-1526, 1987.

INITIAL DISTRIBUTION LIST

		No. Copies
1.	Defense Technical Information Center Cameron Station Alexandria, VA 22304-6145	2
2.	Library, Code 52 Naval Postgraduate School Monterey, CA 93943-5101	2
3.	Dr. Robert H. Bourke (Code OC/BO) Department of Oceanography Naval Postgraduate School Monterey, CA 93943-5000	1
4.	Dr. Newell Garfield (Code OC/Gf) Department of Oceanography Naval Postgraduate School Monterey, CA 93943-5000	1
5.	Dr. Leslie Rosenfeld (Code OC/Ro) Department of Oceanography Naval Postgraduate School Monterey, CA 93943-5000	1
6.	Dr. Franklin B. Schwing Pacific Fisheries Environmental Group P. O. Box 831 Monterey, CA 93942	1
7.	LT Marc T. Steiner Naval Atlantic Meteorology and Oceanography Center Norfolk, VA 23511-2394	1
8.	Dr. Steven R. Ramp Phy. Oceanography Prog. ONR Code 322PO Office of NAVRES 800 N. Quincy St. Arlington, VA 22217-5660	1

9.	Dr. Marlene Noble U.S. Geological Survey 345 Middlefield Road Menlo Park, CA 93025	1
10.	Director Naval Oceanography Division Naval Observatory 34th and Massachusetts Avenue NW Washington, DC 20390	1
11.	Commander Naval Meteorology and Oceanography Command Stennis Space Ctr, MS 39529-5000	1
12.	Commanding Officer Naval Oceanographic Office Stennis Space Ctr Bay St. Louis, MS 39522-5001	1